Polymer 53 (2012) 4879–4921

Contents lists available at SciVerse ScienceDirect

Polymer

journal homepage: www.elsevier.com/locate/polymer

Feature article

Transition metal-containing macromolecules: En route to new functional materials

Alaa S. Abd-El-Aziz [a,b,*], Elizabeth A. Strohm [b]

[a] Department of Chemistry, University of Prince Edward Island, 550 University Avenue, Charlottetown, Prince Edward Island C1A 4P3, Canada
[b] Department of Chemistry, University of British Columbia, Okanagan Campus, 3333 University Way, Kelowna, British Columbia V1V 1V7, Canada

ARTICLE INFO

Article history:
Received 28 May 2012
Received in revised form
4 August 2012
Accepted 10 August 2012
Available online 31 August 2012

Keywords:
Organometallic polymers
Coordination polymers
Metallocene-based systems

ABSTRACT

Recent development in the field of organometallic and coordination polymers based on transition metals, particularly the methods and degree of polymerization, the nature of bonding present, and the type of metal moiety, has become an area of ever-growing interest. Metal-containing polymers have catalytic, magnetic, optical, electrical, and electrochemical properties which allow for a variety of applications. This review will mainly shed light on the past five years of research in organometallic and coordination polymers containing transition metals, focusing on the synthetic methodologies, structural properties, and applications.

1. Introduction

A vast array of research pertaining to the field of metal-containing polymers has advanced substantially and thus a number of reviews have been published in this area of chemistry [1–32]. These macromolecular materials possess unique chemical and physical properties [22] that lead to their potential application in an assortment of areas such as organometallic, coordination, and medicinal chemistry, as well as biotechnology. Due to the nature and incorporation of the metal center, metal-containing polymers can adopt various coordination numbers, oxidation states, geometries, types of bonding, and degrees of polymerization, all of which can impact the properties of this class of polymers. Furthermore, these macromolecules may have catalytic, electrochemical, optical, and/or magnetic properties that contribute to the applications of metal-containing macromolecules. Generally, the metal moiety can be incorporated into the polymer backbone by either covalently bonding directly to the main chain or coordinating to ligands within the backbone. The metal moiety could also be pendant or attached to the side chain of the polymer.

Although many reviews have been dedicated to the area of coordination and organometallic polymers, this feature article will highlight some recent developments in transition metal-containing macromolecules within approximately the last five years. Although many of the macromolecules may be suitable for multiple sections, this review is organized according to the structure of the macromolecules, including metal moieties embedded within the polymer backbone (polymetallaynes, metallocene-based systems), polymers containing metalmetal bonds, coordination polymers, polymers containing metals in the side chains, and dendrimers and star polymers.

2. Polymetallaynes

A very intriguing subclass of metal-containing polymers and one that has been studied at length is polymers that have metal-carbon σ-bonds embedded in their main chain, known as polymetallaynes [7,27,33,34]. Due to the rigid-rod M–$(C{\equiv}C)_n$– geometry, these particular metallopolymers can exhibit optical nonlinearity [35], luminescence, and photovoltaic and liquid crystallinity behaviour [33,36].

Optical power limiters, used to protect sensitive optical sensors from pulsed laser radiation, function optimally if they have high optical transparencies, good optical nonlinearity, excellent solubility, and a quick response speed [37]. Metalloporphyrins, metallophthalocyanins, fullerenes, and polyynes are a few examples of molecules that can be used for optical power limiting (OPL). However, many of these compounds will have sufficient OPL, but cannot attain high transparency. In 2007, Zhou et al. reported the

* Corresponding author. Department of Chemistry, University of Prince Edward Island, 550 University Avenue, Charlottetown, Prince Edward Island C1A 4P3, Canada.
E-mail address: abdelaziz@upei.ca (A.S. Abd-El-Aziz).

0032-3861 © 2012 Elsevier Ltd. Open access under CC BY-NC-ND license.
http://dx.doi.org/10.1016/j.polymer.2012.08.024

synthesis and characterization of Pd(II), Pt(II), Hg(II), and Au(I) polyynes that are solution-processable and for the most part exhibit excellent OPL and optical transparencies [37]. Oxidative self-coupling was employed for the synthesis of polymers using a catalytic mixture of CuCl and O_2. Polymers **1** and **2** are shown as example polyynes (Fig. 1). It was found that all of the polyynes had excellent solubility for aprotic organic solvents and showed sufficient film-forming properties. Gel permeation chromatography (GPC) was used to determine the weight average molecular weights, M_w, (~4520–67,700) of the polymers, number average molecular weights (M_n), and polydispersion index, PDI, (~1.12 and 2.23). Furthermore, thermogravimetric analysis (TGA) revealed that onset decomposition temperatures (T_d) occurred between 338 and 406 °C, thus indicating relatively good thermal stability. The authors also discovered that the different metal centers within the polymers varied in their ability to enhance the OPL and found that platinum exhibited the highest contribution. Additionally, the results for the transition metal polyynes revealed that at 92% linear transmittance, the optical-limiting thresholds went down to 0.07 J cm^{-2}. As a result, novel polymetallynes that have the potential to be employed as efficient OPL devices were prepared.

Derivatives of triphenylamine comprised of a central nitrogen atom are chromophores that can be used to functionalize various polymers and enhance polymeric properties [38]. Such macromolecules can be used for applications in photonics and optoelectronics [38]. Recently, Wong's group prepared a platinum(II) polyyne branched polymer functionalized with a tris(*p*-ethynylphenyl)amine bridging unit (**3**) (Fig. 2) [38]. The metallopolyyne **3** was synthesized using a palladium catalyst coupled with copper iodide. Photophysical studies reveal an absorption maximum at 393 nm and a fluorescence emission at 446 nm, along with a fluorescence quantum yield of 1.89%.

Electron donor and acceptor systems can be very useful for designing narrow-band gap macromolecules used for applications such as optoelectronics [39]. Wong and coworkers have synthesized a donor-acceptor polyplatinayne containing a silole ring (**4**) (Fig. 3) that acts as an electron-acceptor [39]. The σ*–π* conjugation in the silole ring contributes to its low-lying LUMO level, which contributes to a new distinctive donor-acceptor system for platinum polyynes.

Mei et al. have reported the synthesis and characterization of platinum acetylide-containing polymers that may be used to develop organic photovoltaic devices (OPVs) [40]. The

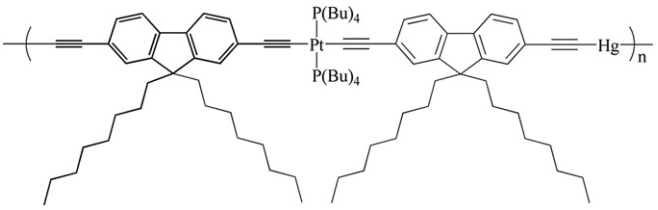

1

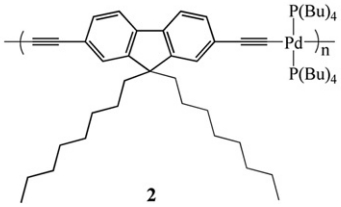

2

Fig. 1. Platinum and palladium polyynes, **1** and **2**, respectively, which exhibit optimal OPL [37].

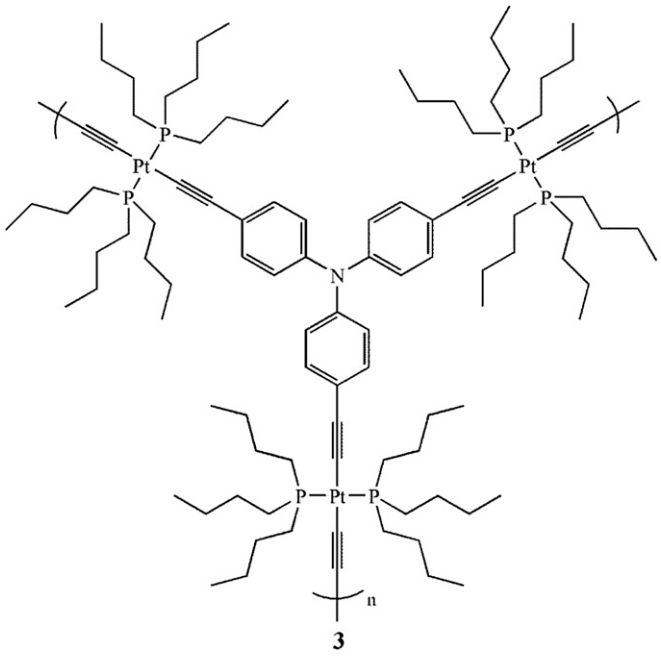

3

Fig. 2. Structure of a platinum(II) polyyne branched polymer containing a tris(*p*-ethynylphenyl)amine bridging unit (**3**) [38].

metallopolymers (**5**, **6**) (Fig. 4) are functionalized with low-band gap donor–acceptor π-conjugated chromophores. Specifically, 2,1,3-benzothiadiazole was used as the acceptor unit and either 2,5-thienyl groups or (3,4-ethylenedioxy)-2,5-thienyl moieties were used as the donor units. Number–average molecular weights (M_n) of 33 and 22 kDa for polymers **5** and **6**, respectively, were determined using GPC. The photophysical studies show that (ethylenedioxy)thiophene-containing Pt(II) polymer **5** and its corresponding monomer **7** (Fig. 4) exhibit a lower band gap and have higher light-harvesting efficiency at longer wavelengths compared to thiophene-containing Pt(II) polymer **6** and its corresponding monomer **8** (Fig. 4). As a result of the lower band gap, the wavelength absorption maxima of monomer **7** and polymer **5** are significantly red-shifted compared to that of monomer **8** and polymer **6** (Fig. 5). The authors suggest that these results are attributed to the stronger electron-donating ability of the (ethylenedioxy)thiophene moiety compared to the thiophene unit.

A number of platinum-based semiconducting donor–acceptor polymers and copolymers were synthesized via Sonogashira-type coupling polymerization and characterized by Wu et al. [41]. For example, this polymerization method was used to isolate thermally stable Pt-bridged poly(aryleneethynylene) polymer **9** (T_d = 331 °C) and copolymer **10** (T_d = 287 °C) with weight average

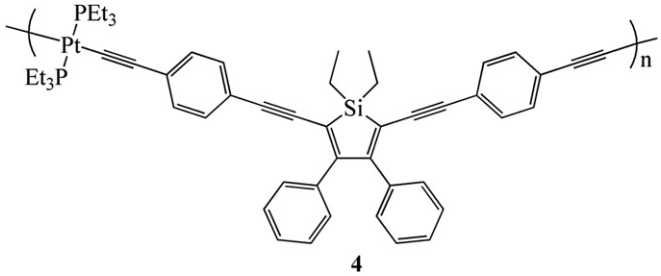

4

Fig. 3. Structure of a polyplatinayne containing a silole ring (**4**) [39].

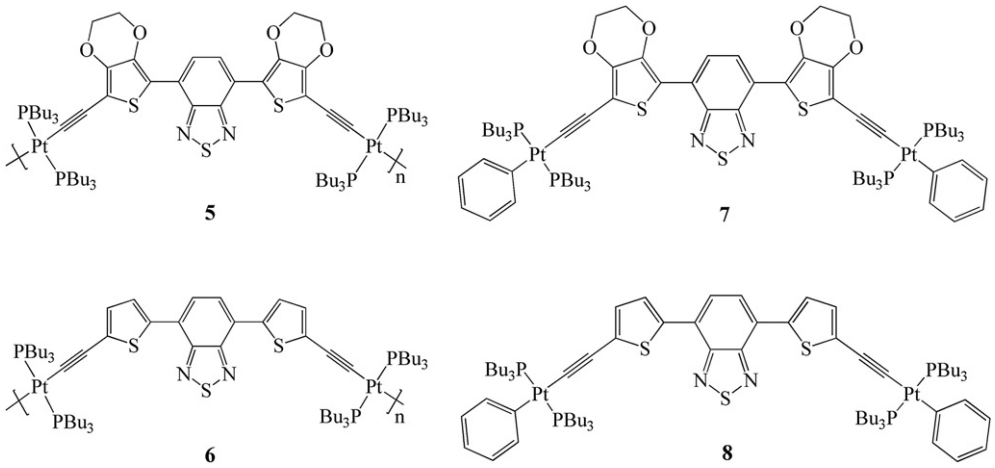

Fig. 4. Structures of platinum acetylide-containing polymers (**5**,**6**) that may be used to develop organic photovoltaic devices and their corresponding monomers (**7**,**8**) [40].

molecular weights of 58,200 and 20,900, respectively (Fig. 6). The optical absorption spectra of polymers **9** and **10** in solution reveal low energy bands at wavelength maxima (λ_{max}) 376 and 378 nm, respectively (Fig. 7), and intramolecular charge transfer bands at λ_{max} = 532 nm for polymer **9** and λ_{max} = 532 and 632 nm for copolymer **10**. Furthermore, optical band gaps of 1.97 and 1.55 eV were also observed for **9** and **10**, respectively. Polymer blends with [6,6]phenyl-C_{71}-butyric acid methyl ester allowed for high photovoltaic power conversion efficiencies such as 0.68% for polymer **9**.

A novel water-soluble conjugated platinum polyelectrolyte was prepared by Qin et al. [42]. The Pt acetylide-based polymer exhibits both fluorescent and phosphorescent properties. Furthermore, Wong and coworkers designed a new colorimetric silver ion sensor derived from **11** (Fig. 8). The sensor demonstrated excellent selectivity and sensitivity for silver(I) ions in a buffered water solution as a result of the silver ion-induced intersystem crossing from the singlet to triplet states. Photophysical studies of **11** show a wavelength maximum absorption peak at 390 nm as a result of the $\pi-\pi^*$ transition of the platinum acetylide backbone in aqueous solution.

The authors also investigated the response of polymer **11** to various metal ions in excess concentration using UV–vis absorption spectroscopy (Fig. 9). The spectral results indicated only a minor decrease in intensity of the absorption wavelength maxima at 390 nm when the metal ions were introduced, with the exception of Hg^{2+} and Ag^{+}. When Hg^{2+} was introduced, the absorption peak was blue-shifted (12 nm) and a substantial decrease in absorption intensity was observed. However, upon the addition of Ag^{+}, the absorption peak was red-shifted (25 nm) and the intensity of the absorption peak was significantly decreased. Furthermore, upon the exposure to excess Ag^{+} ions, a visible colour change from colourless to yellow was displayed. On the contrary, when polymer **11** was exposed to the other metal ions in excess, no colour change was observed (Fig. 10). The study indicated a limit of detection as low as 0.5 μM, with concentrations in the parts per billion. As a result of its ability to both fluoresce and phosphoresce, the Pt polyelectrolyte makes an excellent candidate for chemosensing applications.

Very recently, the research groups of Manners, Tang, and Wong designed and examined the properties of an iron- and platinum-containing polymer (**12**), as seen in Fig. 11 [43]. Face-centered tetragonal phase (also known as $L1_0$ phase) iron-platinum-containing nanoparticles were prepared via the pyrolysis of polymer **12**. This method of synthesis allows for nanoparticle formation (average size of 4.6 nm) without the need of any post-annealing step. Furthermore, the authors report the use of soft nanoimprint lithography as a practical single-source precursor to afford the high-throughput patterning of $L1_0$ phase magnetic FePt nanoparticles.

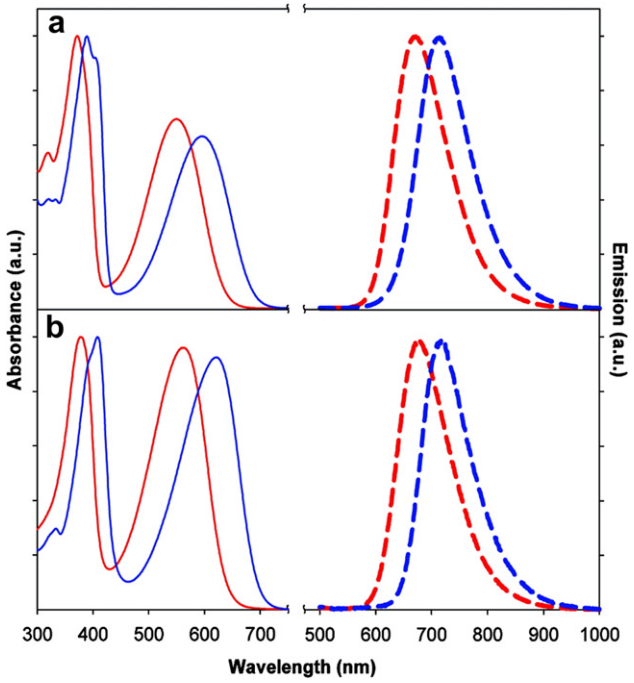

Fig. 5. Absorption (—) and emission (- - -) spectra of (a) polymer **6** (blue) and monomer **8** (red) and (b) polymer **5** (blue) and monomer **7** (red) [40]. Reprinted with permission from ACS Appl Mater Interfaces, 1, Mei J, Ogawa K, Kim Y-G, Heston NC, Arenas DJ, Nasrollahi Z, McCarley TD, Tanner DB, Reynolds JR, Schanze KS, "Low-band gap platinum acetylide polymers as active materials for organic solar cells", 150–161. Copyright (2009) American Chemical Society.

3. Metallocene-based systems

The synthesis of ferrocene-containing polymers was reported in the early 1960s by Korshak and Nesmeyanov and occurred via reacting ferrocene with *tert*-butyl hydroperoxide [44,45]. In 1966, Neuse and coworkers discovered that these polymers were

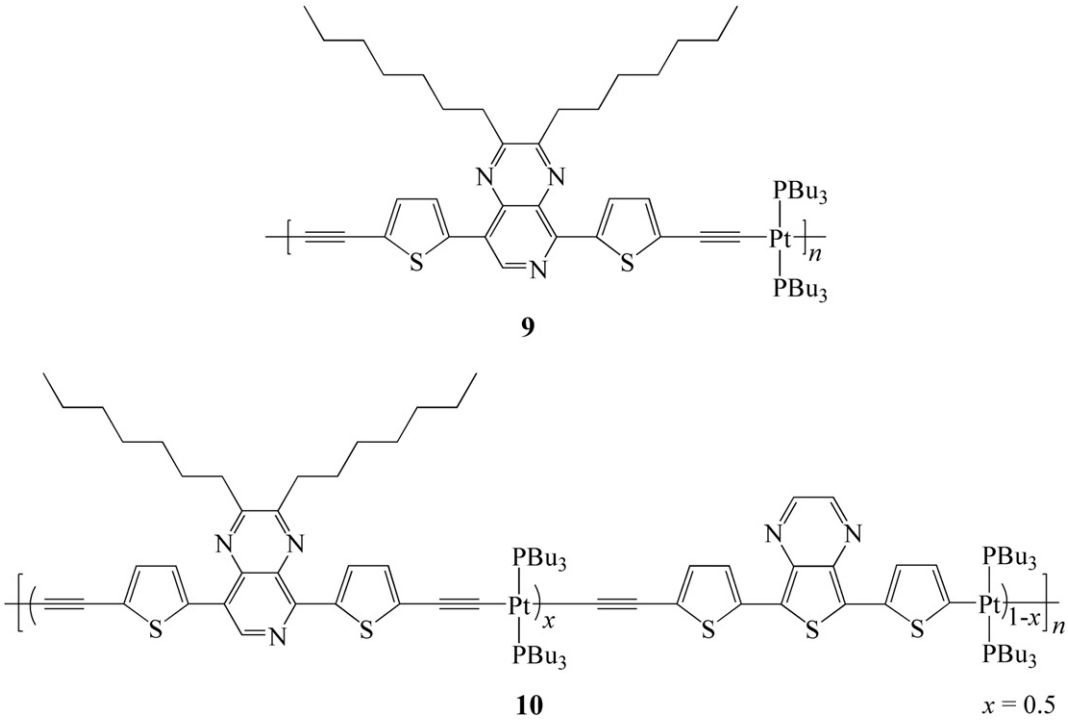

Fig. 6. Structures of Pt-bridged poly(aryleneethynylene) polymer **9** and copolymer **10**, respectively [41].

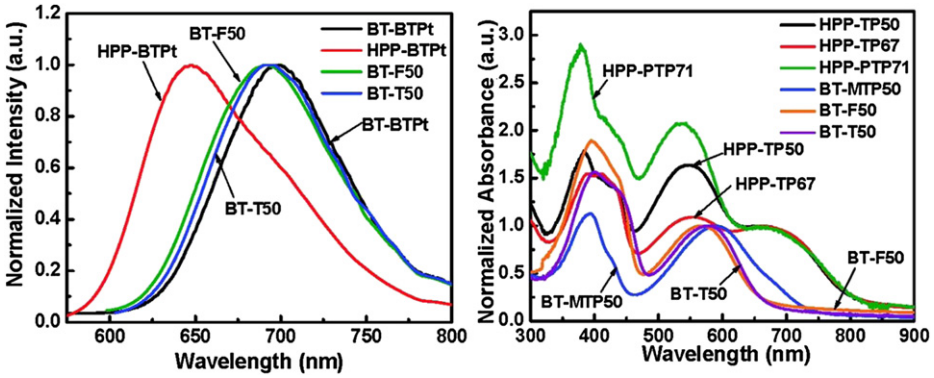

Fig. 7. Optical absorption spectra of organometallic polymers as thin films. Polymer **9** is represented as **HPP-BTPt** (left spectra). Polymer **10** is represented as **HPP-TP50** (right spectra) [41]. Adapted with permission from Macromolecules, 42, Wu P-T, Bull T, Kim FS, Luscombe CK, Jenekhe SA, "Organometallic donor–acceptor conjugated polymer semiconductors: tunable optical, electrochemical, charge transport, and photovoltaic properties", 671–681. Copyright (2009) American Chemical Society.

comprised of homo- and hetero-annular aliphatic ether-substituted moieties and had M_n < 7000 [46]. Polyferrocene derivatives are one of the most common polymetallocenes, although there are still many examples of other polymetallocenes without the inclusion of ferrocene. For example, the synthesis of hafnium-based polymetallocenes **13** and **14** (Fig. 12) was reported by Dzhardimalieva and coworkers [47]. Radical polymerization of acrylic or methacrylic acid with hafnocene dichloride in the presence of the radical initiator, 2,2′-azobis(2-methylpropionitrile) (AIBN), occurred to afford metallopolymers **13** and **14**, respectively. Thermolysis was investigated and observed for metallopolymers **13** and **14** when they were heated between 300 and 1000 °C. Based on the thermal analysis and X-ray diffraction studies, the authors indicate that thermolysis of the metallopolymers gives rise to the formation of metal-polymer nanocomposites.

Acrylic polymers containing cobalt arene moieties in the side chains (**15**, **16**) (Fig. 13) were reported by Ragogna and coworkers

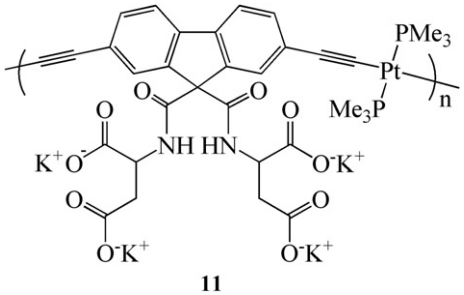

Fig. 8. Water-soluble platinum(II) acetylide-based conjugated polymer (**11**) used for chemosensing applications [42].

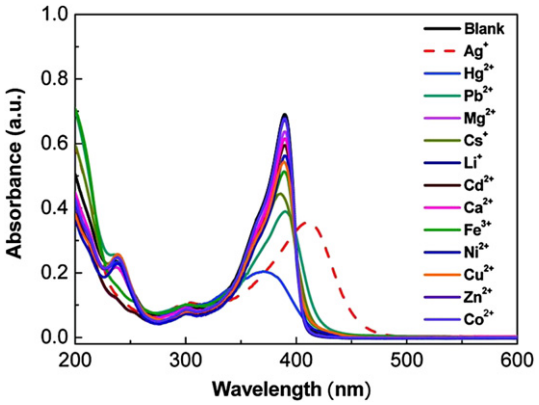

Fig. 9. Absorption spectra of polymer **11** in the presence of different metal ions in degassed water. The concentrations of polymer **11** and the metal ions are 5×10^{-6} M and 1×10^{-5} M, respectively [42]. Reprinted with permission from Macromolecules, 44, Qin C, Wong W-Y, Wang L, "A water-soluble organometallic conjugated polyelectrolyte for the direct colorimetric detection of silver ion in aqueous media with high selectivity and sensitivity", 483–489. Copyright (2011) American Chemical Society.

Fig. 10. Colour change of polymer **11** upon the addition of various metal ions in pure water. The numbered vials are labelled as follows, 0: blank, 1: Ag^{+}, 2: Hg^{2+}, 3: Pb^{2+}, 4: Mg^{2+}, 5: Cs^{+}, 6: Li^{+}, 7: Cd^{2+}, 8: Ca^{2+}, 9: Fe^{3+}, 10: Ni^{2+}, 11: Cu^{2+}, 12: Zn^{2+}, and 13: Co^{2+}. The concentrations of polymer **9** and the metal ions are 5×10^{-6} M and 1×10^{-5} M, respectively [42]. Reprinted with permission from Macromolecules, 44, Qin C, Wong W-Y, Wang L, "A water-soluble organometallic conjugated polyelectrolyte for the direct colorimetric detection of silver ion in aqueous media with high selectivity and sensitivity", 483–489. Copyright (2011) American Chemical Society.

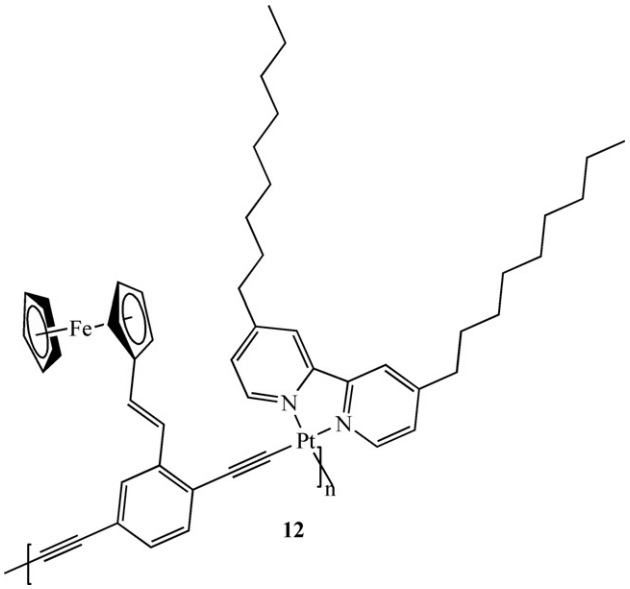

Fig. 11. Structure of a bimetallic iron- and platinum-containing polymer (**12**) [43].

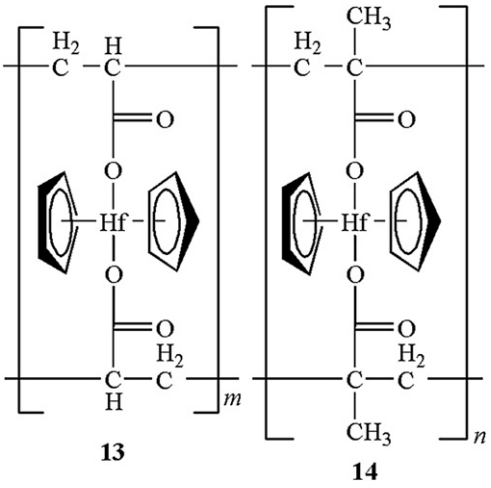

Fig. 12. Hafnium-based cross-linked polymetallocenes **13** and **14** [47].

[48]. The butadiene ring bound to the cobalt centers was functionalized with either methyl or phenyl substituents. The number average molecular weights were between 3600 and 30,500, depending on the reaction conditions for polymerization. Thermal studies were conducted using TGA and revealed decomposition starting at 360 °C for polymer **15** and 235 °C for polymer **16**. As a result, thermal analysis indicates that the phenyl-substituted polymetallocene has a higher thermal stability compared to the methyl-substituted polymetallocene.

One of the ways to alter the properties of metallocene-based polymers and their polymerization methods is the substitution of cyclopentadienyl rings for cycloheptatriene rings and modification

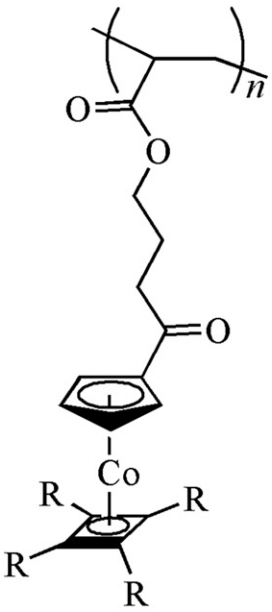

Fig. 13. Acrylic polymers containing cobalt arene moieties in the side chains (**15**, **16**) [48].

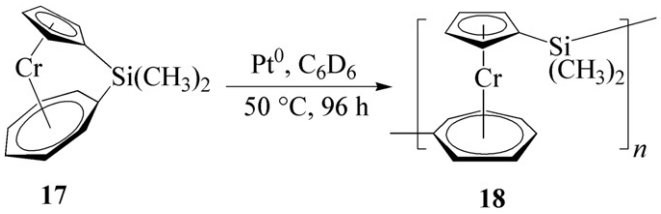

Scheme 1. Synthesis of silyl-containing chromium polymetallocene **18** [49].

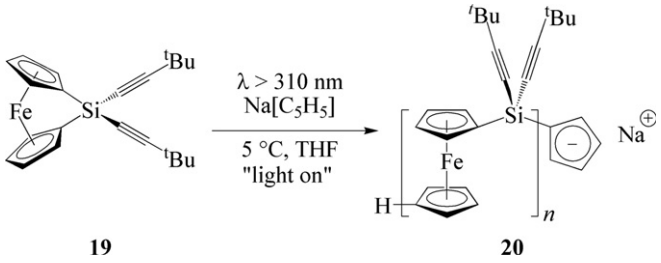

Scheme 2. Photocontrolled ROP of alkyne-substituted ferrocenylsilane monomer **19** [52].

of the metal center. For instance, polymerization of these metallocene-containing monomers can occur using a number of different methods such as anionic or thermal polymerization, or through transition metal catalysts [49]. Metallocenes containing bridging compounds between the lower and upper arenes are beneficial for ring opening polymerization (ROP) due to their increased strain. An example polymetallocene containing both cycloheptatriene and cyclopentadienyl rings in the metallocene units (**18**) was reported by Bartole-Scott and coworkers [49]. Karstedt's catalyst accompanied with deuterated benzene was used for the polymerization of monomer **17** to afford polymer **18** (Scheme 1). It was found that silyl-containing chromium polymetallocene **18** had a number average molecular weight of 6400 and weight–average molecular weight of 4000 (PDI = 1.6) using gel permeation chromatography.

A titanium analogue of polymetallocene **18** was similarly prepared by Tamm and coworkers [50]. The results indicated that the oligomers have low molecular weights, but high molecular weight distributions, according to MALDI-TOF-MS results. Braunschweig et al. reported a similar vanadium metallocene complex that was polymerized catalytically via ROP [51]. The authors found that the vanadium centers in the polymetallocene were spin-active and the M_w of the polymer was 28,000.

Ferrocenylsilane-containing polymers have been thoroughly investigated by Manners and coworkers [2]. In 2007, an alkyne-

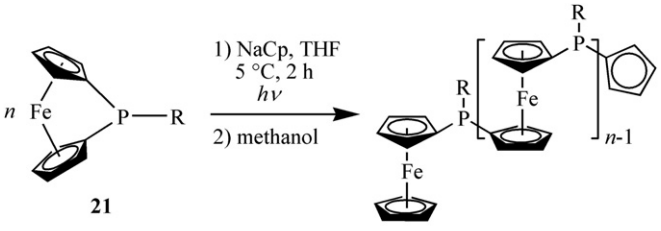

22: R = $C(CH_3)_3$
23: R = $CH_2C(CH_3)_3$
24: R = $CH_2Si(CH_3)_3$

Scheme 3. Synthesis of phosphorus-bridged ferrocenophanes **22**–**24** [53].

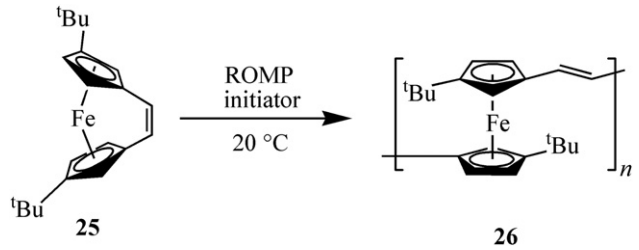

Scheme 4. ROMP of alkene-bridged ferrocenophane (**25**) containing *tert*-butyl substituents on the arene rings [56].

substituted ferrocenylsilane monomer (**19**) was prepared and polymerized via photocontrolled ring opening polymerization to afford poly(ferrocenylsilane) **20** (Scheme 2) [52]. Anionic and thermal ROP along with transition metal-mediated ROP using Karstedt's catalyst were attempted, but did not result in the formation of any polymers. The authors attributed the lack of polymerization with Karstedt's catalyst because of its ability to react with –C≡C– on the alkyne monomer.

Comparable to the silicon-bridged ferrocenophanes mentioned previously, Patra and coworkers recently reported the synthesis and characterization of phosphorus-bridged ferrocenophanes [53]. These monomeric ferrocenophanes (**21**) were polymerized via photolytic living anionic ROP to afford high molecular weight polymers **22**–**24** (M_n = 11,850–56,150) with narrow polydispersity indices between 1.05 and 1.23 (Scheme 3). Due to the monomer-to-initiator ratio, the molecular weights could be controlled without difficulty.

Besides silicon- and phosphorus-containing ferrocenophanes, there are additional bridges that induce strain including aliphatic, alkene, and germanium bridges [54,55]. For instance, germanium-bridged polyferrocenophane homopolymers and block copolymers were prepared at room temperature via anionic ROP in the presence of either *n*-butyl lithium or *sec*-butyl lithium, respectively [54]. The results showed that the number average molecular weights of the homopolymers ranged from 18,800 to 33,700 (PDI = 1.02–1.05). An alkene-bridged polyferrocenophane containing *tert*-butyl substituents on the arene rings (**26**) was synthesized by Manners and coworkers [56]. Ferrocenophane monomer **25** was polymerized via ring opening metathesis polymerization (ROMP) in the presence of either molybdenum or ruthenium catalysts at room temperature to afford polyferrocenophane **26** (Scheme 4). By incorporating the bulky *tert*-

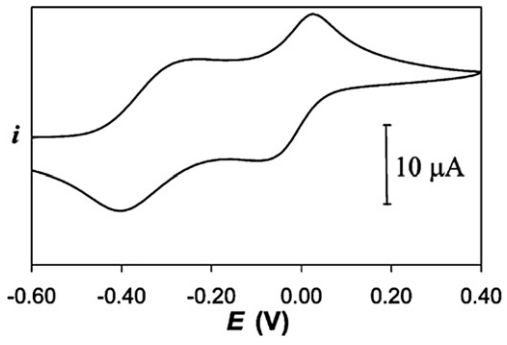

Fig. 14. Cyclic voltammogram of polymer **26** in methylene chloride vs. ferrocene/ferrocenium ion couple at a scan rate of 100 mV/s [56]. Adapted with permission from Macromolecules, 41, Masson G, Lough AJ, Manners I. "Soluble poly(-ferrocenylenevinylene) with *t*-butyl substituents on the cyclopentadienyl ligands via ring opening metathesis polymerization", 539–547. Copyright (2008) American Chemical Society.

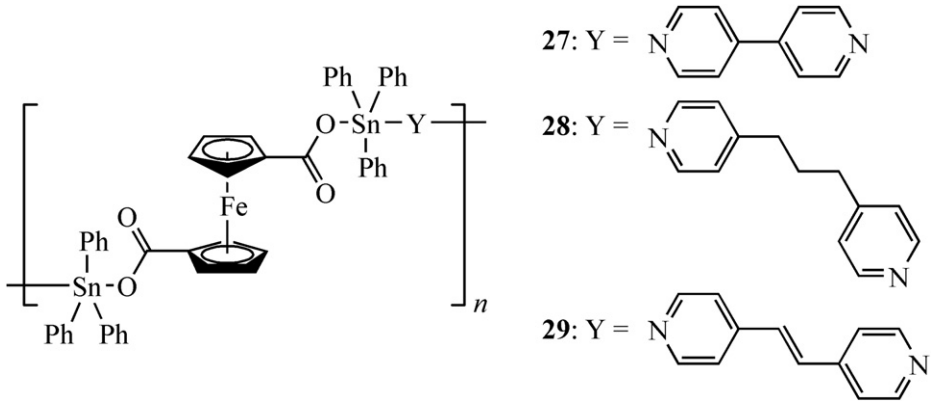

Fig. 15. Structures of polyferrocene-based tin coordination polymers (**27**–**29**) prepared via condensation polymerization [57].

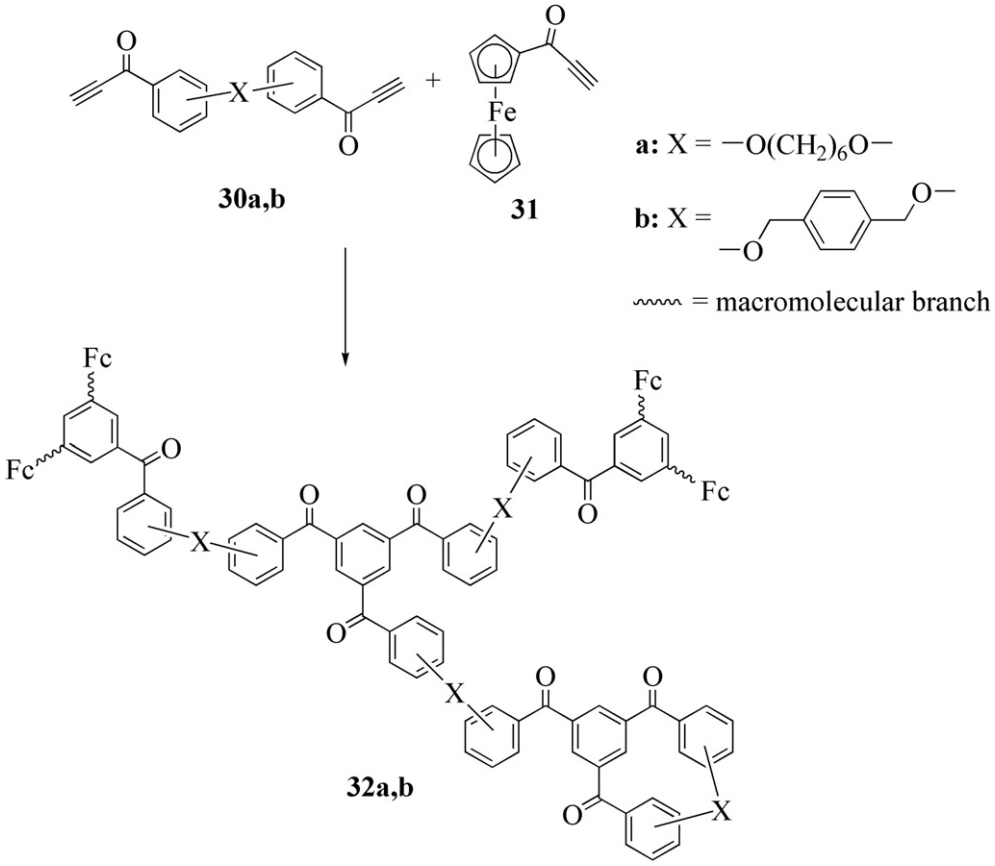

Scheme 5. Copolymerization of bis(aroylacetylenes) **30** with ferrocene monomer **31** to give ferrocene-containing hyperbranched polymers **32a,b** [58].

butyl groups on the arene rings, polymer **26** exhibited high solubility and a negative shift in the first oxidation potential (Fig. 14) compared to that of ferrocene. The authors conclude that the negative shift in oxidation potential is a result of the electron-donating ability of the *tert*-butyl groups towards the ferrocene moiety.

Carbon-bridged strained dicarba[2]ferrocenophanes also reported by Manners and coworkers, were polymerized via photo-controlled ROP to afford high molecular weight poly(ferrocenylethylenes) [55]. The study revealed that monomers with increased substitution along the alkyl chain could achieve higher molecular weights, which the authors accredit to the increased solubility of the propagating chain.

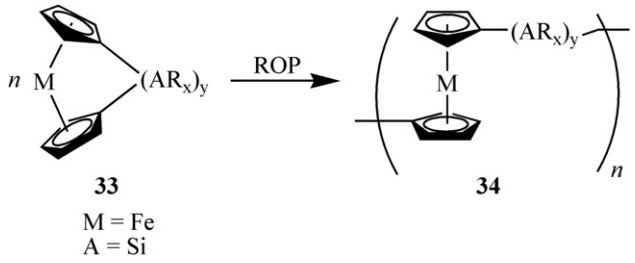

Scheme 6. Synthesis of polymetallocenes (**34**) via ROP [66,69].

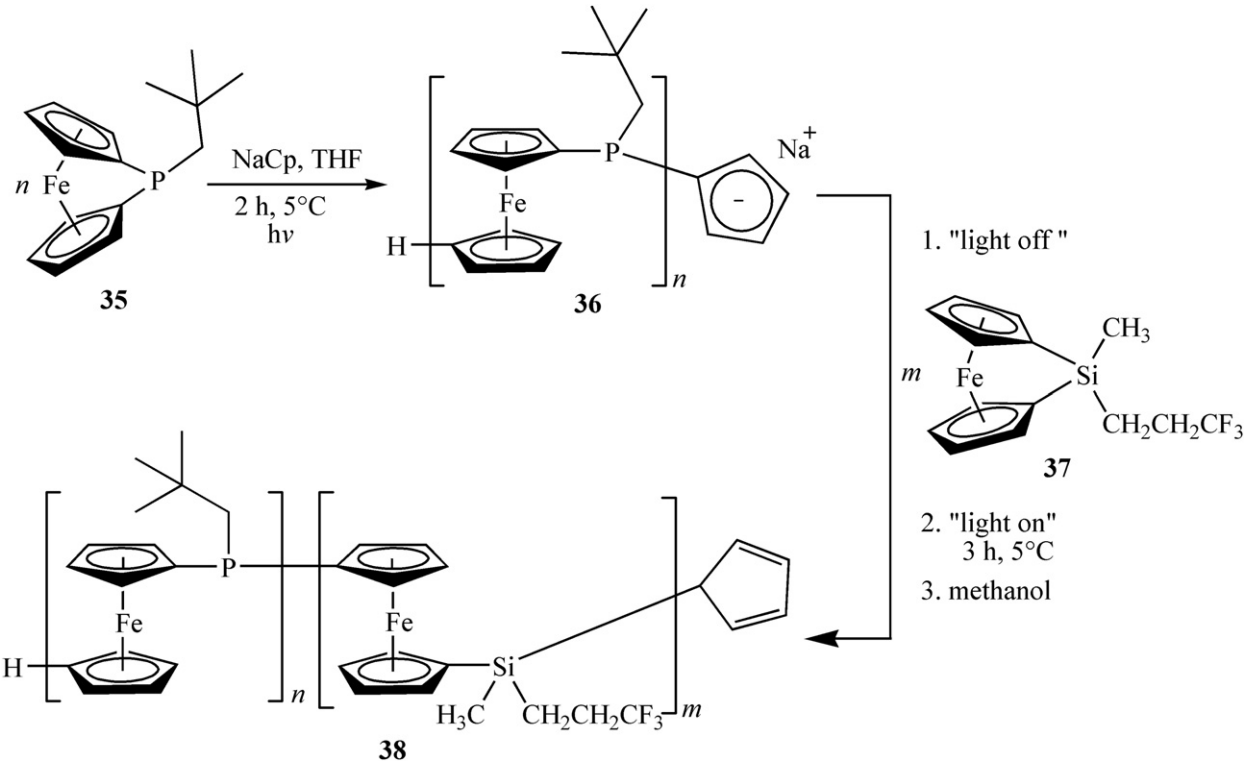

Scheme 7. Synthesis of poly(ferrocenylphosphine)- and poly(ferrocenylsilane)-containing diblock copolymer **38** via sequential photocontrolled living ROP [53].

Rather than using ROP to generate polymetallocenes, condensation polymerization can be employed as an alternative method of polymerization. For instance, Chandrasekhar et al. used disubstituted ferrocenes containing carboxylic acid moieties to react with tin complexes to afford various polyferrocene-based tin coordination polymers [57]. The studies showed that when *n*-butyl or methyl substituents were bound to the tin center, two-dimensional metallocene-based coordination polymers were formed. On the contrary, when phenyl groups were bound to the tin center, an open coordination site resulted and thus polymerization was unsuccessful. Interestingly, reacting dicarboxylic acid ferrocene and bis(triphenyltin) oxide in the presence of nitrogen-containing ditopic ligands resulted in the formation of one-dimensional polyferrocene-based tin coordination polymers **27**–**29** (Fig. 15) [57].

Tang's research group reported the synthesis and characterization of various ferrocene-containing hyperbranched polymers [58]. Ferrocenylcarbonyl acetylene (**31**) was copolymerized with bis(aroylacetylenes) **30** to afford hyperbranched polymers **32a,b** (Scheme 5) with M_w between 7600 and 23,000. Additionally, low molecular weight polymers resulted when the concentration of ferrocene monomer **31** was increased. It was suggested that the ferrocene moiety functions as a capping agent in polymerization, thus contributing to the lower molecular weight polymers. Thermogravimetric analysis confirmed that these polymers exhibit good thermal stability with structural degradation beginning from 340 to 380 °C.

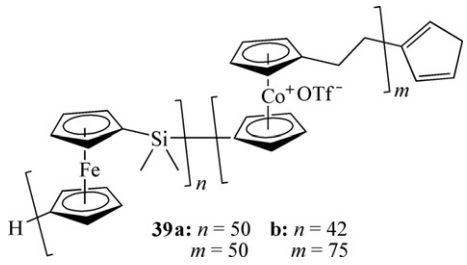

Fig. 16. Diblock copolymers containing both cobaltocenium and ferrocene moieties in the main-chain (**39**) [81].

A number of effective synthetic methods have been designed for the formation of metal-containing polymers such as living, ionic, and controlled radical polymerization [59–61], polycondensation [62–65], electropolymerization [66], and ring opening polymerization [67,68]. For instance, polymerization of strained organometallic arenes such as silicon-bridged ferrocenophanes (**33**) via ROP (Scheme 6) has provided a versatile synthetic route to polymetallocenes with high molecular weights (i.e. $M_n > 100{,}000$) such as polyferrocenylsilanes (**34**) [66,69]. Polymerization via ROP has also been applied to a variety of similar strained monomers with other single-atom linkers (where A = Sn, S, etc.), two-atom linkers (where A = CeC, CeP, etc.), transition metals (where M = Ti, V, Cr, Ru, Co, etc.), and various cyclic *para*-hydrocarbon rings such as cycloheptatrienyl ligands and arenes [50,70–80].

Recently, a number of ferrocene-containing homo- and copolymers have been reported by Patra and coworkers [53]. For example, a poly(ferrocenylphosphine) (**36**) bound with neopentyl substituents on the phosphorous atoms was prepared via photocontrolled living ROP of ferrocenylphosphine **35** (Scheme 7). Subsequently, poly(ferrocenylphosphine) **36** and ferrocenylsilane **37** were polymerized via photocontrolled living ROP to afford poly(ferrocenylphosphine)- and poly(ferrocenylsilane)-containing diblock copolymer **38** (Scheme 7) [53]. The polymers possessed high molecular weights and narrow molecular weight distribution. Furthermore, the study also indicated that block copolymer **38** undergoes microphase separation in thin films.

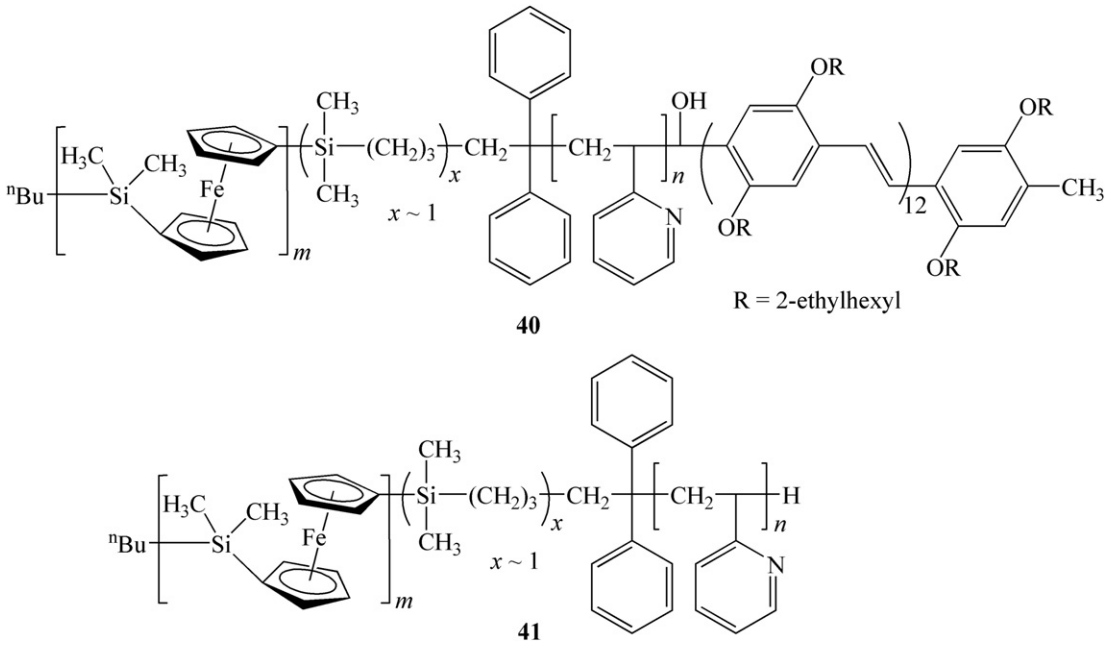

Fig. 17. Structures of triblock copolymer **40** and diblock copolymer **41** [82].

Diblock copolymers (**39**) containing both cobaltocenium and ferrocene moieties in the polymer backbone (Fig. 16) have been synthesized via living photocontrolled ROP and investigated by Manners and coworkers [81]. The study demonstrated the self-assembly of the copolymers, providing a new example for the preparation of polymers with heterobimetallic block co-micelle architectures via living self-assembly. Furthermore, due to the cobaltocenium and ferrocene moieties, unique redox properties were revealed by the electrochemical studies, which showed a 1.5 V separation between the oxidation and reduction waves.

The self-assembly of di- and tri-block copolymers **40** and **41**, respectively, (Fig. 17) was reported by Manners' group and resulted in the formation of multiblock co-micelles with interesting optical properties [53]. The fluorescent triblock copolymer **40** and diblock copolymer **41** were added to micelle fragments generated by sonication in a solution of tetrahydrofuran to form elongated uniform cylindrical structures. Furthermore, these multi-block micelles contained alternating fluorescent copolymer and nonfluorescent copolymer segments, which were observable by laser confocal fluorescence microscopy (LCFM) in 2-propanol (Fig. 18).

Very recently, Manners and coworkers have prepared redox-active polyferrocenylsilanes-based diblock copolymers **42** with ionically complexed azo dyes (Fig. 19) [83]. These organometallic diblock copolymers form surface-relief gratings when irradiated with light. Furthermore, the polymers have superior etch resistivity and have improved modulation depth as a result of the redox-active polyferrocenylsilane polymer backbone. As a result, there are a number of ways to undergo post-modification of these surface-relief gratings without altering their periodic structures. These supramolecular systems are excellent candidates for the use in applications such as non-reversible holographic data storage, templating, and simple read-only identification tags [83].

Polymers that contain neutral iron moieties in the backbone and cationic iron moieties in the side chain have been prepared via nucleophilic aromatic substitution of organoiron complexes **43a,b** with 4,4′-thiobisbenzenethiol (**44**) (Scheme 8) [84]. Photolysis of

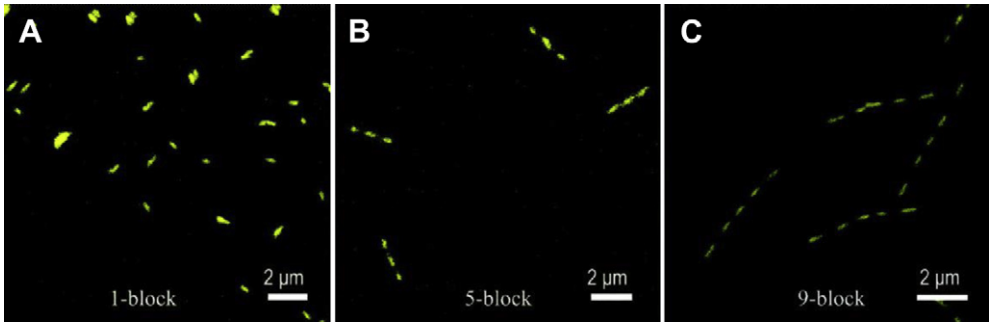

Fig. 18. Laser confocal fluorescence microscopy images of (A) the initial **40** (1-block) micelles, (B) 5-block and (C) 9-block co-micelles. These images were obtained from thin (0.1 mm) solutions in 2-propanol [82]. Reprinted with permission from J Am Chem Soc, 133, He F, Gädt T, Manners I, Winnik MA, "Fluorescent "barcode" multiblock co-micelles via the living self-assembly of di- and tri-block copolymers with a crystalline core-forming metalloblock", 9095–9103. Copyright (2011) American Chemical Society.

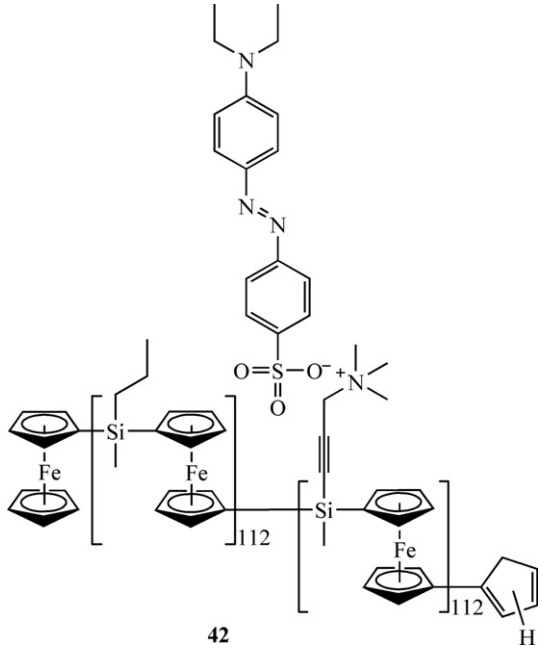

42

Fig. 19. Structure of polyferrocenylsilane-based diblock copolymer with ionically complexed azo dyes (**42**) [83].

polymers **45a,b** resulted in the cleavage of the cationic iron moieties and to afford neutral organoiron-containing polymers (**46a,b**). According to GPC results, the weight average molecular weights of polymers **46a,b** occurred between 8700 and 13,500 (PDI = 1.1–1.3). Additionally, thermal analysis revealed higher thermal stability for the mixed-charge organoiron polymers (**45a,b**) (T_g = 117–161 °C) compared to the neutral ferrocenyl-containing polymers (**46a,b**) (T_g = 55–92 °C).

4. Organometallic polymers with metallic moieties either in the backbone or the side chain

Over the past decade there has been an exponential increase in the number of organometallic polymers developed including polymers with metals directly attached to organic spacers via σ- or π-bonding, or polymers containing metal–metal bonds. Polymers containing metal–metal (M–M) bonds represent a very unique subclass of metal-containing polymers. The metal–metal bonds behave as chromophores and thus produce characteristic absorption bands. Due to the ease of breaking M–M bonds using visible light, these photolytically degradable polymers can be used as photosensitive materials [85]. Additionally, some polymers containing Fe–Fe bonds may have potential use as conductive or lithographic materials [85,86]. Methods of polymerization must be strategically designed to prevent M–M bond cleavage. Manners and coworkers have thoroughly studied polymers that are highly metallized, including poly(ferrocenylsilane)s containing metal–metal bonds of cobalt (**48**), nickel (**49**), and molybdenum (**50**) [87]. The poly(ferrocenylsilane)s (**47**) were prepared first and subsequently reacted with a –C≡C– bond to a metal cluster to afford polymers with M–M bonds (Scheme 9). The synthesis of the nickel-containing polymer **49** required the presence of UV light as opposed to the cobalt- and molybdenum-containing polymers **48** and **50**, respectively, which required the presence of heat. The study revealed that a thin film of molybdenum polymer **50** on a silicon substrate exhibits sharp micron-sized features when exposed to UV light through a chrome contact mask (Fig. 20). Additionally, any of the unexposed polymer was removed completely during UV exposure. As a result, these polymers may be used in UV-photolithography as good negative-tone photoresists.

Heterometallic organoiron and organocobalt-containing polymers **57** and **62a,b** have been prepared via ROMP (Schemes 10 and 11) [88]. As illustrated in Schemes 10 and 11, a stepwise synthesis of polymers **57** and **62a,b** occurred in which organoiron-

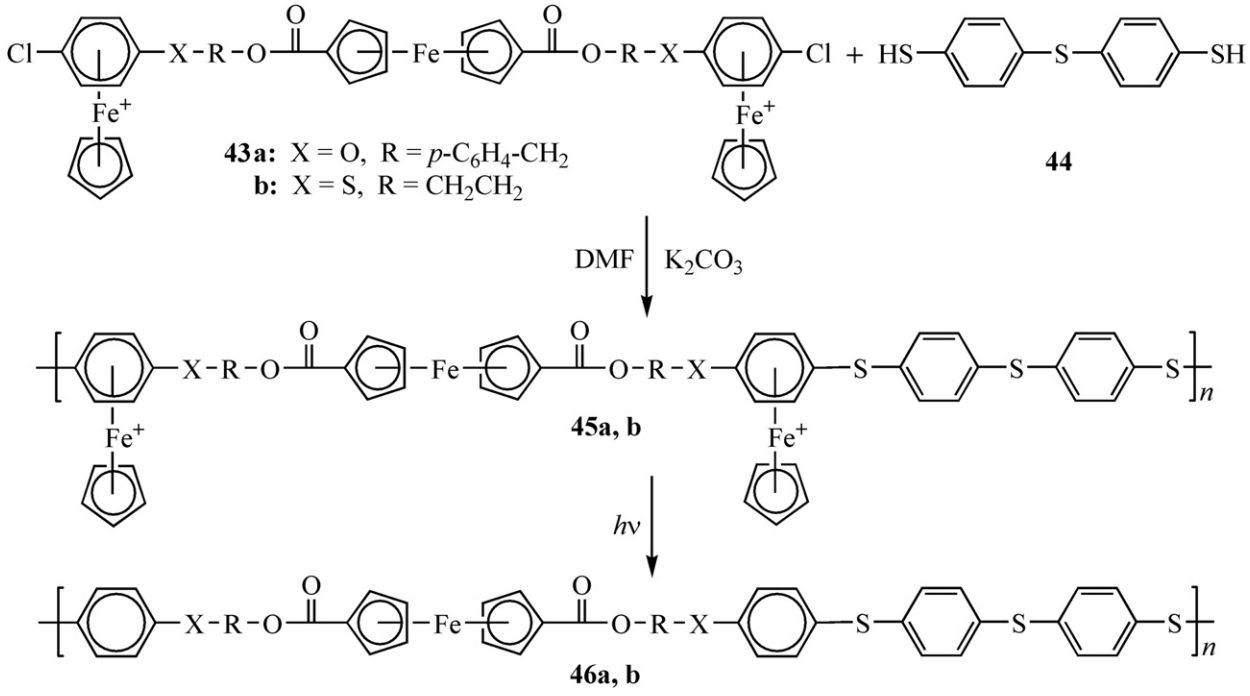

Scheme 8. Preparation of organoiron-containing polymers (**45a,b**) and their corresponding ferrocene analogues (**46a,b**) [84].

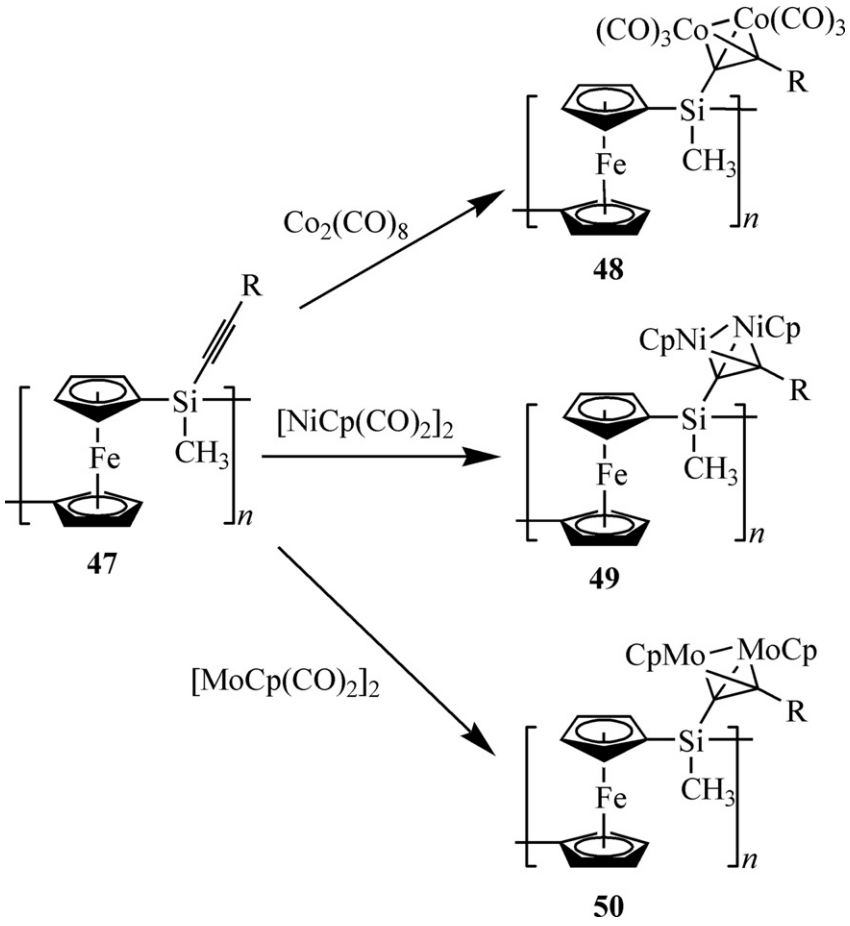

Scheme 9. Synthesis of poly(ferrocenylsilane)s containing metal–metal bonds (**48**–**50**) [87].

containing complexes **51** and **58** were first reacted with 2-butyne-1,4-diol (**52**) to afford organometallic complexes **53** and **59**, respectively. Subsequently, 5-carboxylic-2-norbornene (**54**) was reacted with complexes **53** and **59** to afford, alkyne-based organometallic norbornene derivatives **55** and **60**, respectively. Mixed organocobalt/organoiron norbornene monomers **56** and **61** were subsequently prepared by reacting norbornene monomers **55** and **60**, respectively, with dicobalt octacarbonyl. Lastly, ROMP of heterometallic norbornene monomers **56** and **61** in the presence of Grubbs' 2nd generation catalyst afforded organoiron/organocobalt polynorbornenes **57** and **62a,b** with weight average molecular weights between 55,300 and 69,000 (PDIs between 1.2 and 1.9), respectively. Additionally, thermal analysis of the polymers revealed that the polymer backbone was thermally stable up to 350 °C and that the cobalt carbonyl moiety degraded around 130 °C. Furthermore, a reversible reduction for the dicobalt hexacarbonyl

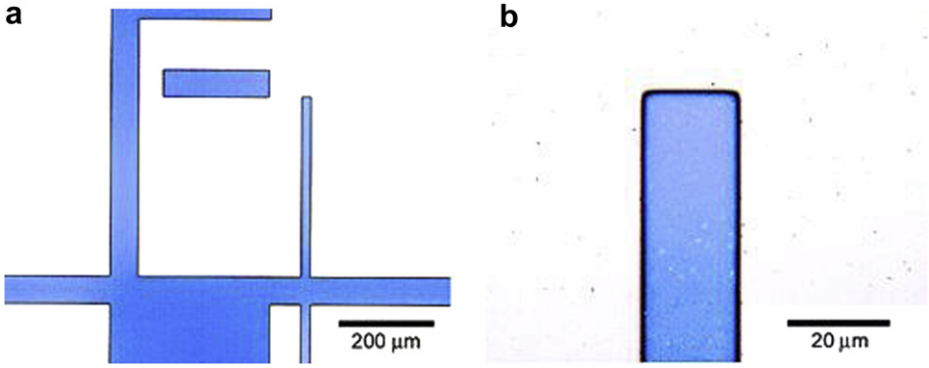

Fig. 20. Bright field optical micrographs of (a) a pattern of polymer **50** fabricated with UV-photolithography through a chrome contact mask; (b) higher magnification of the smallest line in (a) [87]. Reprinted with permission from J Am Chem Soc, 127, Chan WY, Clendenning SB, Berenbaum A, Lough AJ, Aouba S, Ruda HE, Manners I, "Highly metallized polymers: synthesis, characterization, and lithographic patterning of polyferrocenylsilanes with pendant cobalt, molybdenum, and nickel cluster substituents", 1765–1772. Copyright (2005) American Chemical Society.

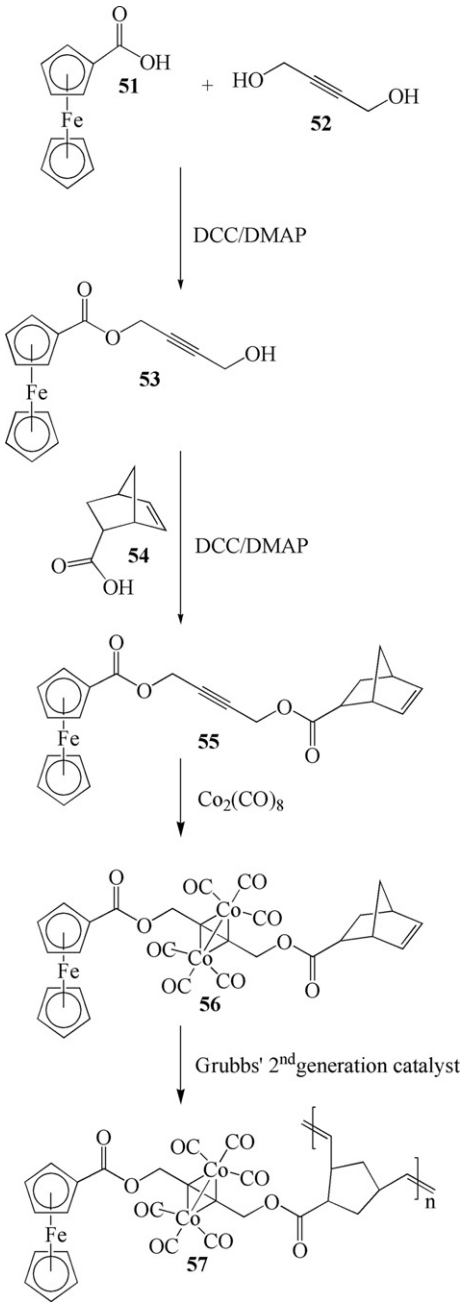

Scheme 10. Synthesis of cobalt/iron-containing polymer **57** [88].

moieties and cationic complexes with η^6-benzene-η^5-cyclopentadienyliron and a reversible oxidation for the ferrocene-containing complexes were observed in the monomers' and polymers' cyclic voltammograms.

Difunctionalized metallic dimers containing cyclopentadienyl (Cp) rings can be used to synthesize polymers with M–M bonds via step polymerization [85]. For example, step polymers containing $Cp_2Mo_2(CO)_6$ groups (**64**) can be prepared from the reaction of difunctional, Cp-substituted metal dimers (**63**) with disubstituted organic monomers, as seen in Scheme 12 [89]. Tyler and coworkers conducted photochemical degradation studies of a number of polymers with crosslinks of $Cp_2Mo_2(CO)_6$ moieties in the backbone, which demonstrated the use of the metal–metal bonds as chromophores [89,90]. Additionally, the studies showed that a decrease in the quantum yields of photochemical degradation of the polymers occurred over thirty days [90].

Similarly, photodegradable organometallic oligomers containing metal–metal bonds were prepared via acyclic diene metathesis polymerization (ADMET) [91]. Scheme 13 shows the reaction between $Cp_2Mo_2(CO)_4$ dimer **65** and a phosphine ligand containing a terminal alkene substituent (**66**). The authors attempted the polymerization of dialkene monomer **67** with Grubbs' 1st and 2nd generation Ru-based catalysts and Schrock's Mo-based catalyst, but were unsuccessful with any of the catalysts. Tyler and coworkers suggest that steric effects as opposed to electronic effects of the alkyne moiety in the phosphine ligand were the most probable cause for polymerization failure.

A number of polymerization methods such as ROMP or click chemistry can be used to prepare polymers containing bimetallic metal carbonyl complexes functionalized with cyclopentadienyl rings in the backbone [85]. For example, Tyler et al. have reported the synthesis of polymers with $Cp_2Mo_2(CO)_6$ moieties in the backbone via click chemistry [92]. Scheme 14 gives an example of a polymerization reaction using bimetallic dialkyne **68** to react with diazide-terminated telechelic polystyrene **69** in the presence of the catalyst $Cp^*Ru(PPh_3)_2Cl$ (Cp^* = pentamethylcyclopentadienyl). The resulting polymerization afforded a high molecular weight polymer (**70**; M_n = 120,000). The incorporation of M–M bonds into the backbone of polymers such as polystyrene can be challenging. Thus, the reported polymerization method employed by Tyler and coworkers allows for the inclusion of M–M bonds in polymer backbones to be more readily available.

Several oligomers containing Mo–Ir clusters that were subsequently incorporated into polymer backbones afforded organometallic polymers with optical limiting properties [93]. Scheme 15 illustrates a sample synthesis of a linear oligomer (**72**) with an estimated molecular weight of 16,200 via the reaction of a Mo–Ir cluster-containing monomer (**71**) and 1,4-diisocyanatobutane with catalytic amounts of dibutyltin diacetate (DBTA). The methyl groups bound to the cyclopentadienyl rings on the metal clusters of oligomer **72** were subsequently removed, followed by cross-polymerization to afford a Mo–Ir cluster-containing cross-linked polymer with a high molecular weight of 2.7×10^7.

The synthesis of polysilanes containing cobalt–cobalt bonds tangent to the polymer backbone was reported by Si and Koo [94]. Copolymerization resulted from the reduction of organosilyl chlorides (**73**) and cobalt-coordinated organosilyl chlorides (**74**) via Wurtz coupling (Scheme 16). Additionally, the structures of polymers **75**–**77** were easily manipulated by altering the monomer ratios. The resulting Co–Co-containing polysilanes had molecular weights between 46,000 and 65,000.

Uemura and coworkers prepared dinuclear paddle-wheel complexes containing platinum and rhodium moieties that linked the subunits to form linear polymers **78**–**80** (Fig. 21) [95]. The study indicates that the rhodium and platinum σ^* orbital interactions enabled the linear chain construction. Furthermore, the electronic structures of the 1-D polymers were potentially modified when the dirhodium bridging units were functionalized with trifluoroacetate, acetamidate, and acetate groups.

Zirconacyclopentadienes can undergo a metallocycle transfer reaction to form germole-containing complexes that can later undergo polymerization [96]. Tomita et al. employed this method to transform titanacyclopentadiene derivatives (**81**) into various organometallic polymers containing germanium [97] or tin [98] metallacycles. Scheme 17 shows the polymerization of titanocene **81** with internal dialkyne **82** to afford titanacyclopentadiene-containing polymer **83**. Subsequent addition of either $GeCl_4$ or $SnCl_4$ gave chlorinated metallocenes **84**, which were further

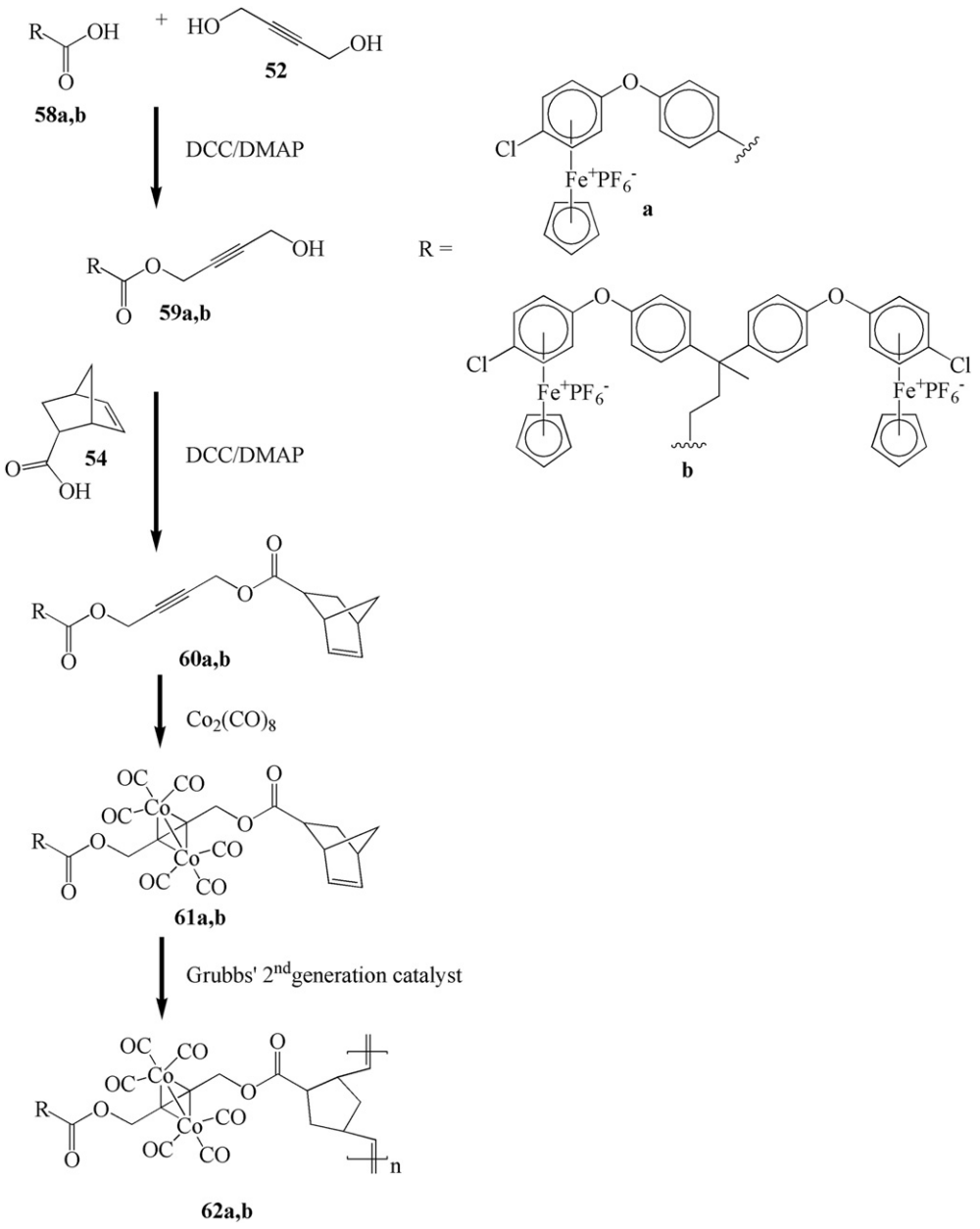

Scheme 11. Synthesis of heterometallic polymers **62a,b** [88].

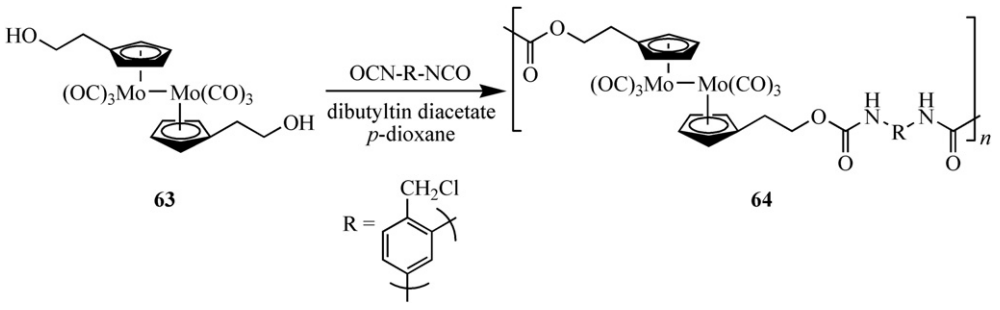

Scheme 12. Synthesis of organometallic polymer **64** containing $Cp_2Mo_2(CO)_6$ [89].

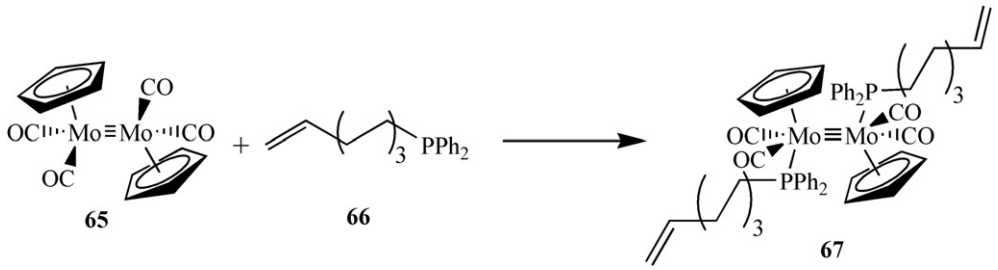

Scheme 13. Reaction of $Cp_2Mo_2(CO)_4$ (**65**) with phosphine ligand **66** with a terminal alkene group to afford bimetallic monomer **67** [91].

reacted with methyl lithium to afford methylated Ge(IV)- or Sn(IV)-containing polymers **85** (Scheme 17). Cyclic voltammetric studies of polymers **85a** and **85b** indicated low-lying LUMO energy levels of −3.95 eV and −3.58 eV, respectively, which is significantly lower than the LUMO energy levels of similar polymers containing thiophene moieties [98].

A number of polygermafluorenes have been prepared by Leclerc et al. which possess low electronic band gaps [99]. Fig. 22 illustrates polygermafluorene **86** as an example. These germanium-based polymers make them suitable candidates for their use as bulk heterojunction solar cells and polymer-based field-effect transistors. Furthermore, differential scanning calorimetry of polymer **86** revealed a glass transition temperature of 95 °C and electrochemical studies revealed one quasi-reversible oxidation and reduction process [99]. The results showed that the HOMO and LUMO energy levels calculated from the oxidation and reduction onsets were −5.58 and −3.91 eV, respectively. Moreover, the *J*–*V* curve of polymer **86** (Fig. 23) displays a fill factor of 0.51, an open-circuit voltage of 0.79 V, and a current density of 6.9 mA cm^{-2}. As a result, a power conversion efficiency of 2.8% was obtained, which indicates that polymer **86** is an excellent candidate for use in photovoltaic applications.

Rhenium diimine units incorporated into poly(*N*-vinylcarbazole) block copolymers were prepared by Chan and coworkers [100]. The study revealed that the Re polymers (**87** is shown as an example in Fig. 24) show intriguing phase separation properties and may be used as photosensitizers. Moreover, their photophysical properties can be altered by substituting the rhenium center for other transition metal ions.

Ferrocene can be linked to the polymer backbone and side chains using various methods [101]. For instance, Tang's research group incorporated ferrocene into the side chains of methacrylate and acrylate polymers using different chain lengths and types of bridging groups between the main chain and the ferrocene units

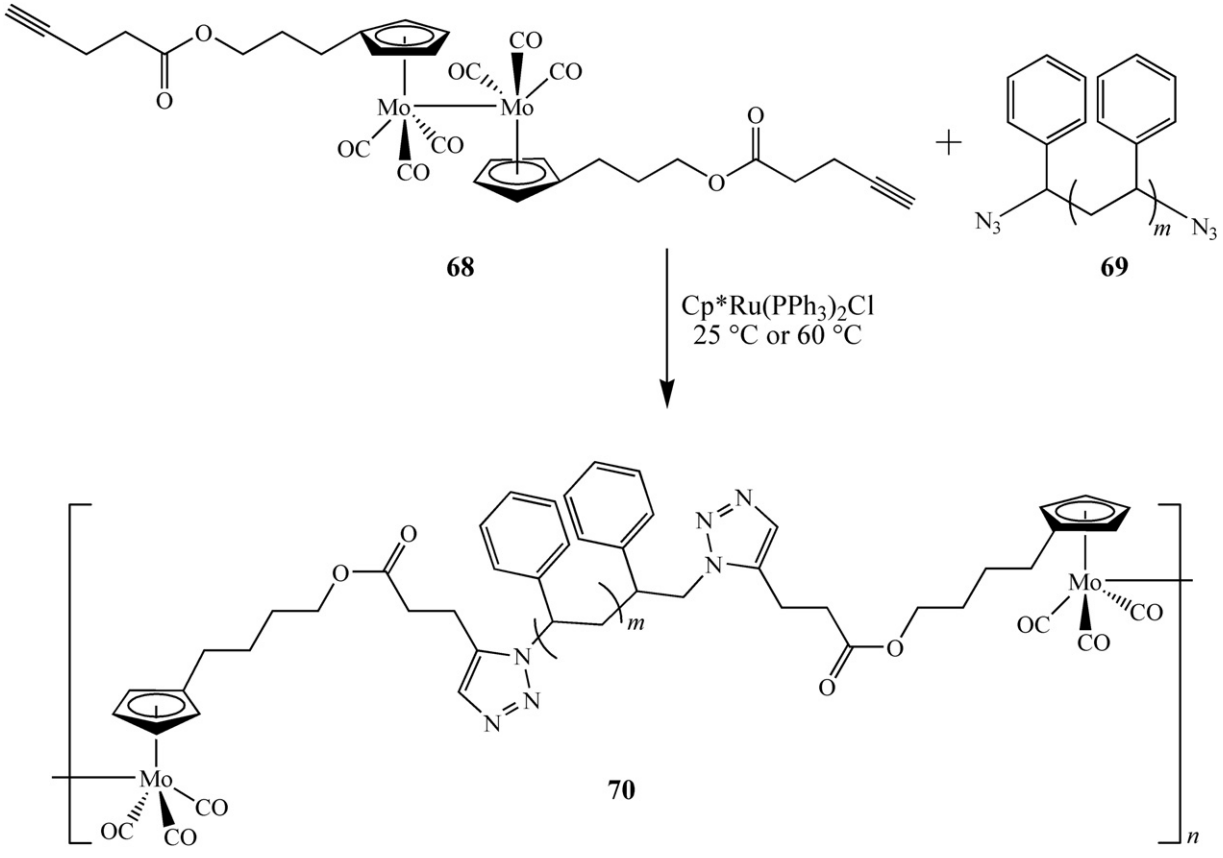

Scheme 14. Polymerization of bimetallic dialkyne **68** via click reaction with azide-terminated telechelic polystyrene **69** [92].

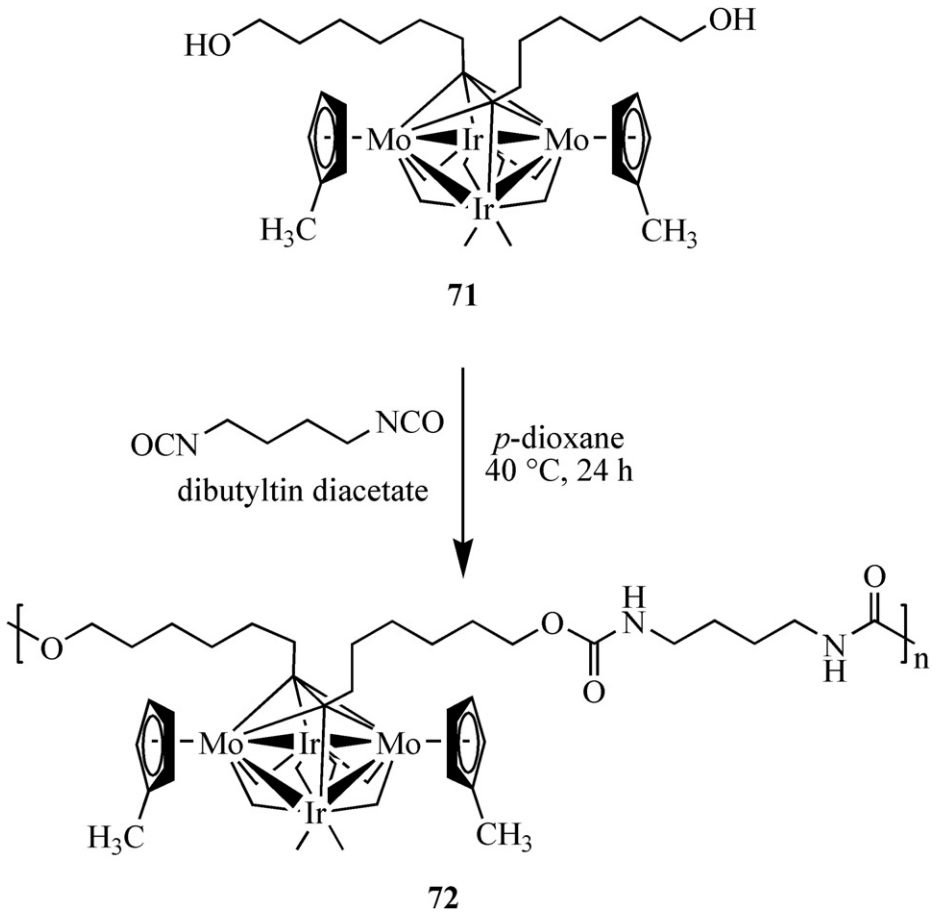

Scheme 15. Synthesis of a linear oligomer containing Mo–Ir clusters (**72**) [93].

[101]. Scheme 18 provides an example synthesis of a ferrocene-containing methacrylate polymer (**90**) which occurred via atom transfer radical polymerization (ATRP) of monomers **88** and **89**. The results indicated relatively controlled polymerizations with PDI values ranging between 1.12 and 1.71.

Poly(hydrosiloxane) was functionalized with planar, chiral ferrocene-based monomers and the resulting polymeric materials (**91**, **92**) (Fig. 25) exhibit optical properties [102]. The study showed that polymers **91** and **92** have molecular weights between 19,000 and 27,000, respectively (PDI = 1.3–1.6).

Polymers containing metallic moieties π-coordinated to varying ring sizes such as arenes coordinated to $Mo(CO)_3$, $Mn(CO)_3$, $Cr(CO)_3$, $CpRu^+$, and $CpFe^+$ are commonly investigated because of their electron-withdrawing properties which can facilitate nucleophilic aromatic substitution and addition reactions [103–112].

As a result of the strong electron withdrawing ability of the iron center, the incorporation of cationic cyclopentadienyliron moieties can enhance solubility and facilitate nucleophilic aromatic substitution and addition reactions [113]. Cationic cyclopentadienyliron-complexed polyaromatic ethers and thioethers containing azo dyes (**95a**–**i**) were prepared [114]. Synthesis took place via condensation reactions between assorted oxygen- and sulfur-containing dinucleophiles (**94**) and iron-coordinated arylazo dye monomers (**93a**–**c**) (Scheme 19). UV–vis studies indicated that these vibrantly coloured macromolecules exhibit wavelength maxima between 417 and 489 nm due to the azo functionalities. In addition, photolysis was used to isolate the corresponding organic polymer

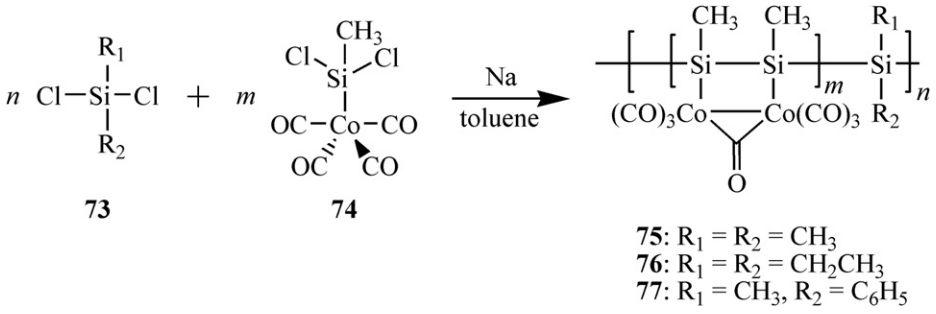

Scheme 16. Synthesis of bimetallic polysilanes **75**–**77** [94].

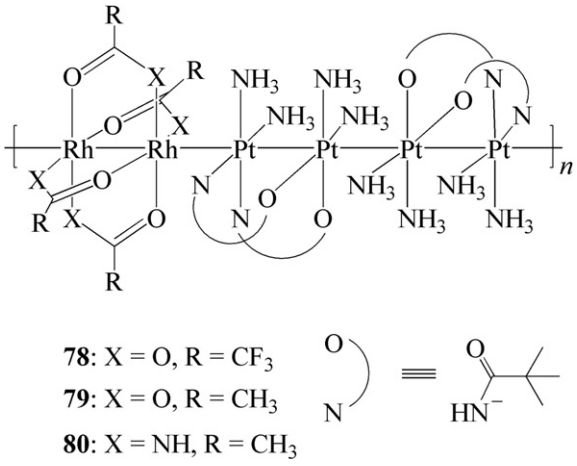

78: X = O, R = CF_3
79: X = O, R = CH_3
80: X = NH, R = CH_3

Fig. 21. Dinuclear paddle-wheel complexes containing platinum and rhodium moieties (**78**–**80**) [95].

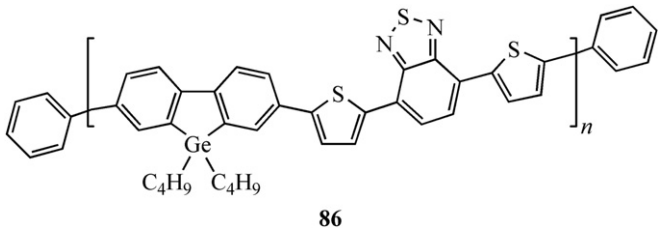

86

Fig. 22. Example structure of polygermafluorene **86** synthesized by Leclerc and coworkers [99].

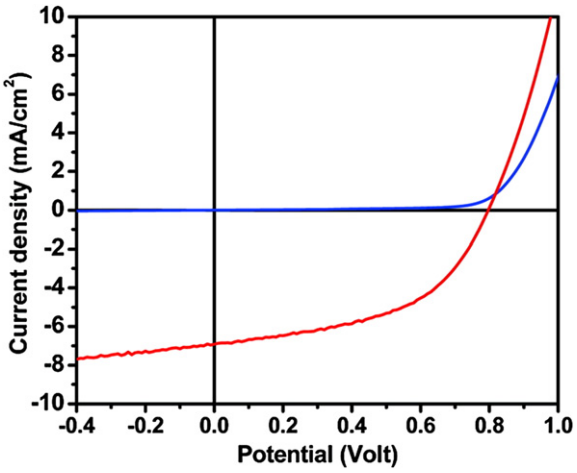

Fig. 23. *J-V* curves of polymer **86** solar cell. Under illumination of AM 1.5 G in red and dark curve in blue [99]. Reprinted with permission from Macromolecules, 43, Allard N, Aïch RB, Gendron D, Boudreault P-LT, Tessier C, Alem S, Tse S-C, Tao Y, Leclerc M, "Germafluorenes: new heterocycles for plastic electronics", 2328–2333. Copyright (2010) American Chemical Society.

analogues **96a**–**i**, and the non-metallic azo-based polymers were photobleached in the presence of hydrogen peroxide [115]. Furthermore, the glass transition temperatures and thermal properties of the organoiron polymers were varied by incorporating different aromatic or aliphatic spacers [115]. Additionally, thermal studies indicated that the loss of the cationic iron groups resulted in an increase in the thermal stabilities of the polymers.

Photolytic discolouration of similar cationic organoiron polymers containing azo chromophores to polymers **95a**–**i** has been investigated [116]. The monomers were synthesized via metal-mediated nucleophilic aromatic substitution and AIBN was used as a radical initiator for polymerization to afford organoiron polymers with pendent azo dyes. Discolouration of the polymers was achieved via irradiation with 300 nm UV light, due to the decomplexation of the organoiron unit and its interaction with the azo dye. To ensure the complete loss of colour, the polymer concentration was less than or equal to 0.025 M.

Incorporating ferrocenyl units into the polymer side chains make it easier to control the polymer structure and increase its molecular weight. Three different organometallic monomers were functionalized with three different diols by Abd-El-Aziz and coworkers in order to investigate mixed-charge organoiron polymers [84]. Scheme 20 illustrates a condensation reaction of the

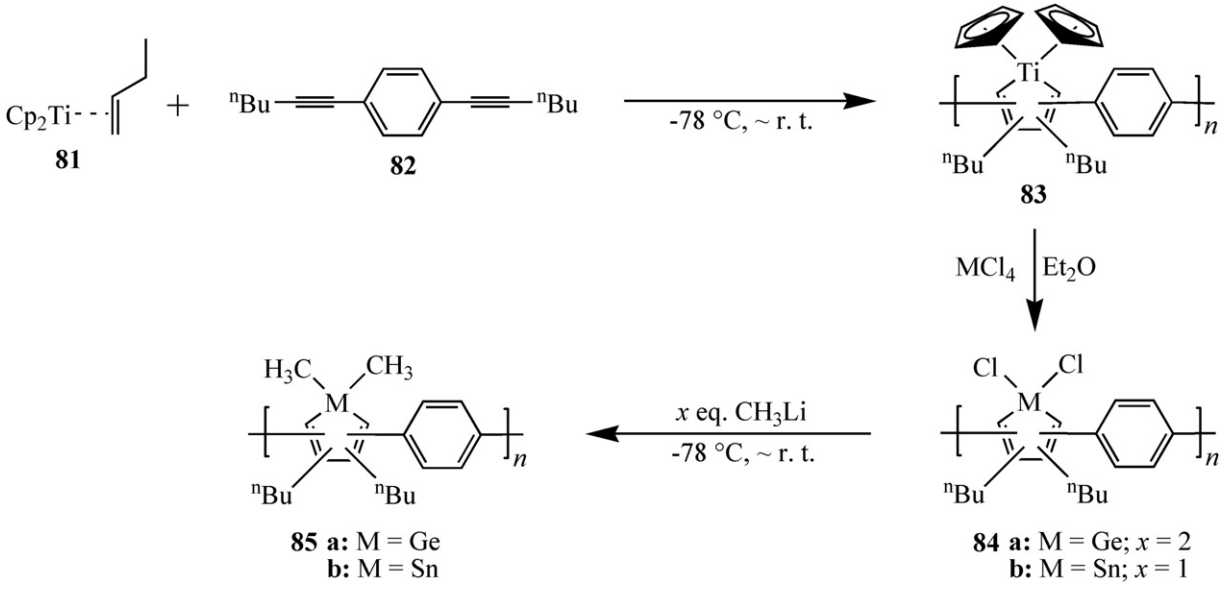

Scheme 17. Synthesis of Ge and Sn organometallic polymers **85a,b**, respectively [98].

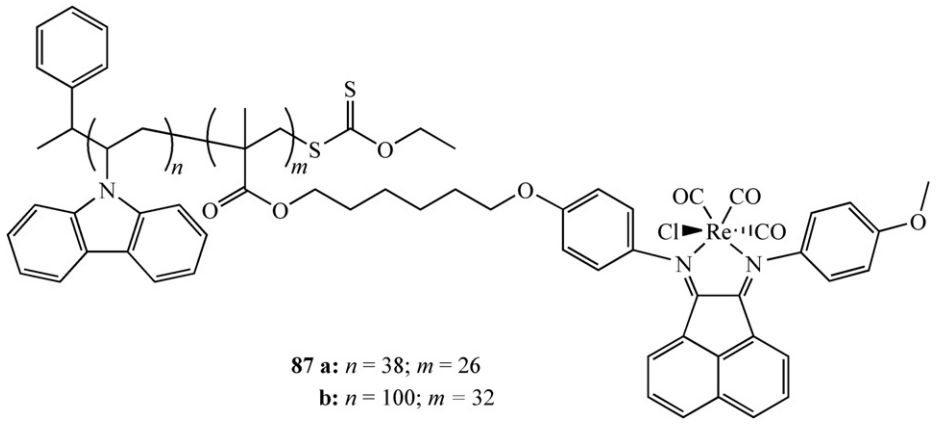

Fig. 24. Structure of photosensitizing rhenium poly(*N*-vinylcarbazole) block copolymers (**87a,b**) [100].

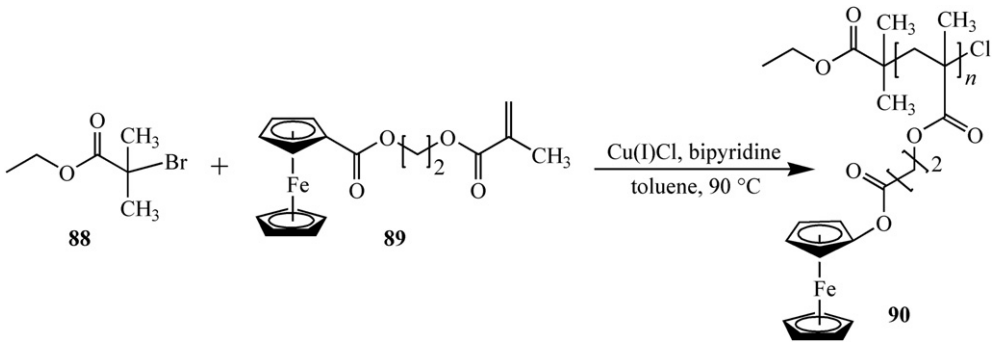

Scheme 18. Synthesis of a methacrylate polymer containing ferrocene unit in the side chain (**90**) [101].

carboxylic acid-functionalized organoiron complex **97** with various diols to afford complexes **98** with terminal alcohol groups. Subsequently, these complexes underwent coupling reactions with ferrocene carboxylic acid to produce monomers **99**. Polymerization of monomer **99** occurred via nucleophilic aromatic substitution of the terminal chloroarene moieties.

Direct electrophilic substitution of cobaltocene-containing materials can be extremely challenging since the 19-electron cobalt center can be readily oxidized to form cationic 18-electron cobaltocenium. Moreover, as a result of the chemical inertness of the cobaltocenium salts, the syntheses of substituted cobaltocene- or cobaltocenium-containing derivatives have not been widely studied [61]. Despite this challenge, Tang and coworkers have recently prepared polymers and block copolymers containing cobaltocenium in the side-chains [61,117]. Side-chain cobaltocenium-containing polymer **100** [117] and block copolymer **101** [61] are shown in Fig. 26 as examples. This research group was the first to report the free radical polymerization of side-chain cobaltocenium-containing polymer **100** using AIBN as a radical initiator [117]. The study showed that polymer **100** is a water-soluble

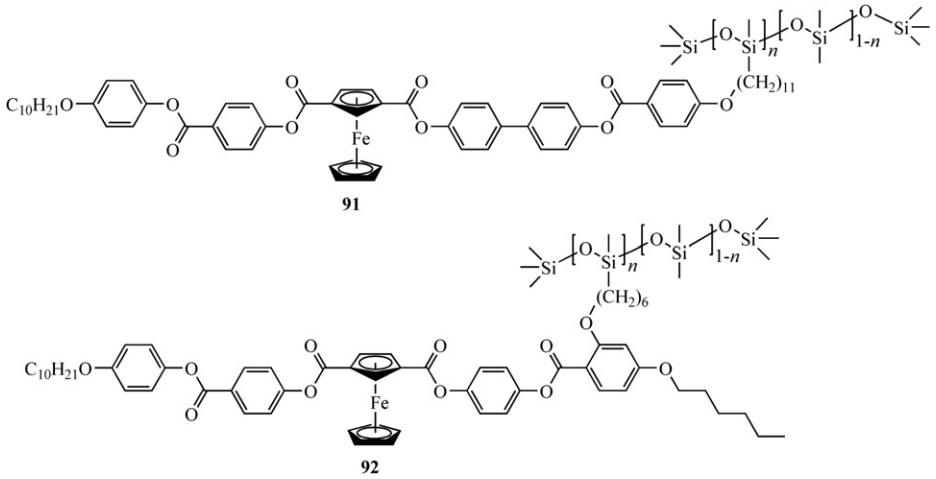

Fig. 25. Structures of polysilanes containing ferrocene units in the side chains (**91** and **92**) [102].

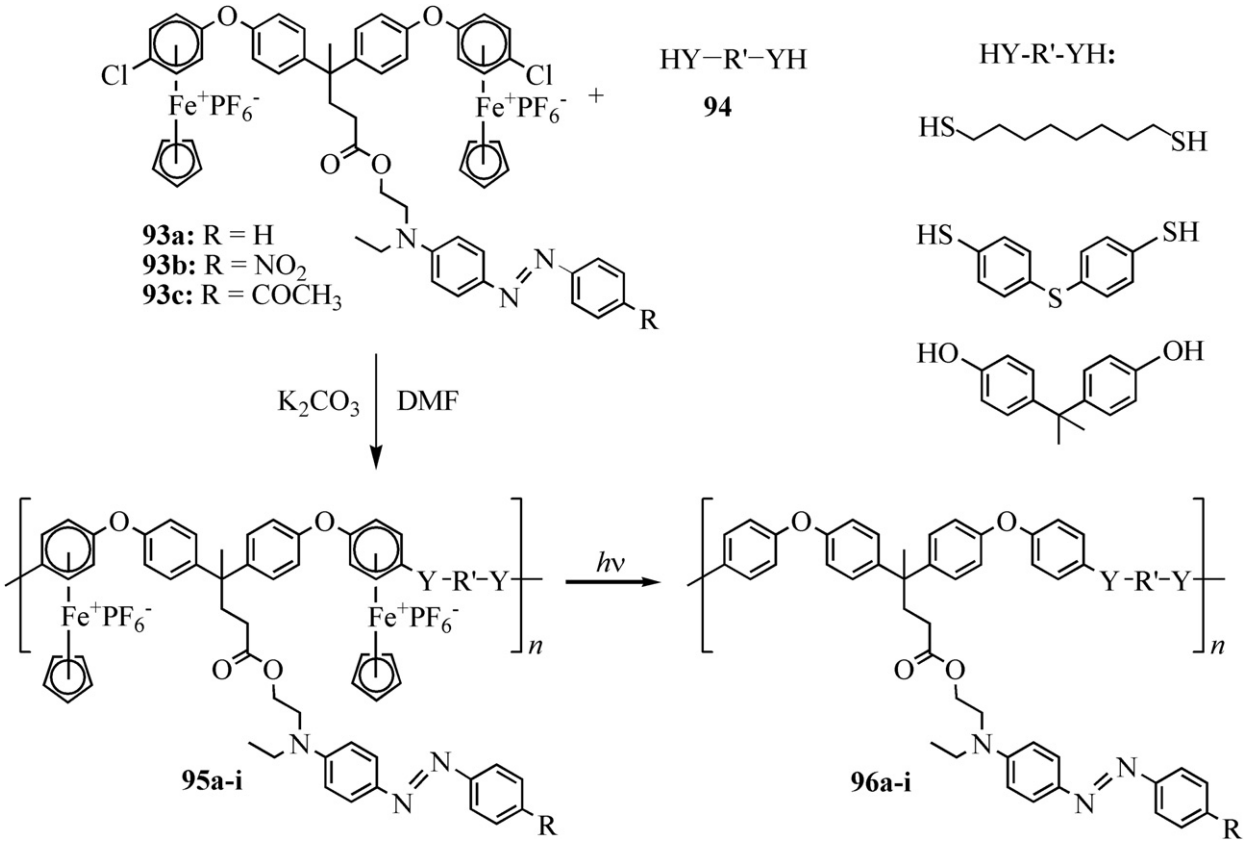

Scheme 19. Synthesis of organoiron polymers containing azo dye side chains (**95a**–**i**) and their subsequent demetallation to afford organic polymers (**96a**–**i**) [114].

polyelectrolyte and has high thermal stability, according to thermogravimetric analysis. In addition, ion-exchange of the hexafluorophosphate counterion with a tetraphenylborate counterion was carried out and resulted in the formation of a hydrophobic polyelectrolyte. According to cyclic voltammetric studies, both hydrophilic and hydrophobic polymers exhibit reversible redox processes.

Tang and coworkers also used postpolymerization modification to prepare block copolymer **101** (Scheme 21), beginning with the synthesis of monosubstituted carboxycobaltocenium (**102**) which was carried out using an established procedure with minor modification to achieve nearly 100% purity [61]. The acyl chloride derivative (**103**) of carboxycobaltocenium **102** was prepared using thionyl chloride and was subsequently reacted with the well-

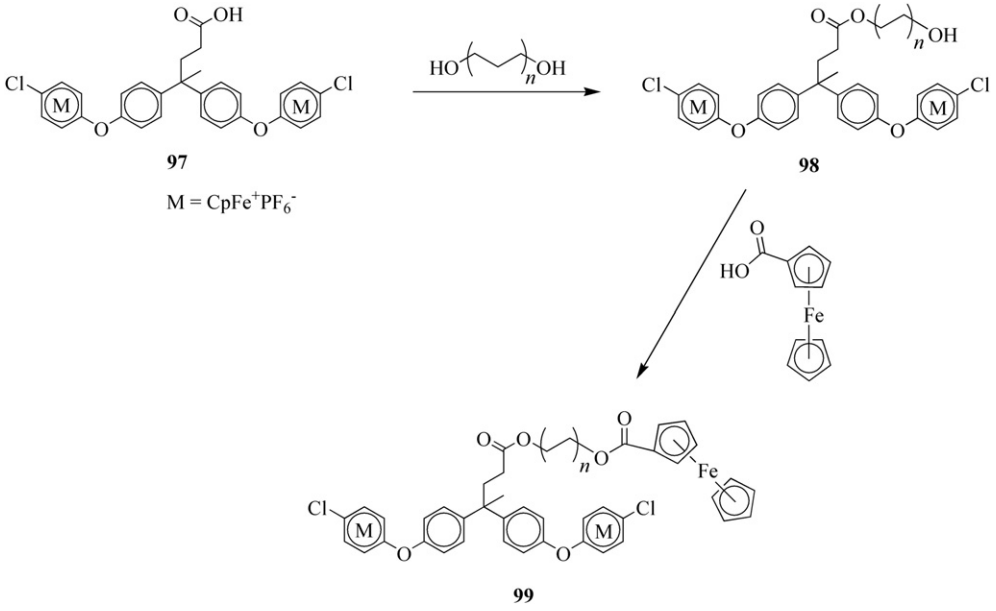

Scheme 20. Synthesis of ferrocene side chain monomer **99** [84].

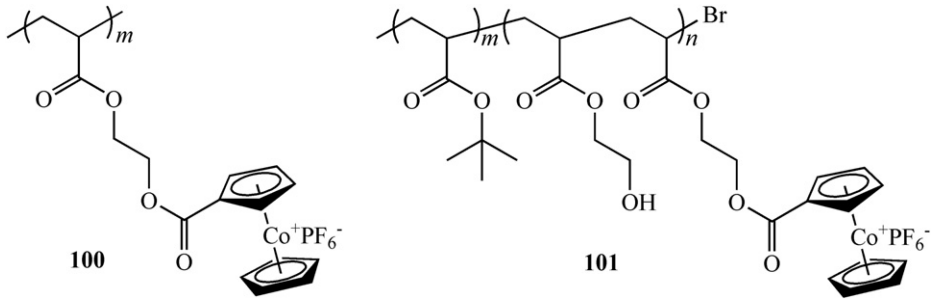

Fig. 26. Example structures of a side-chain cobaltocenium-containing polymer (**100**) [117] and block copolymer (**101**) [61].

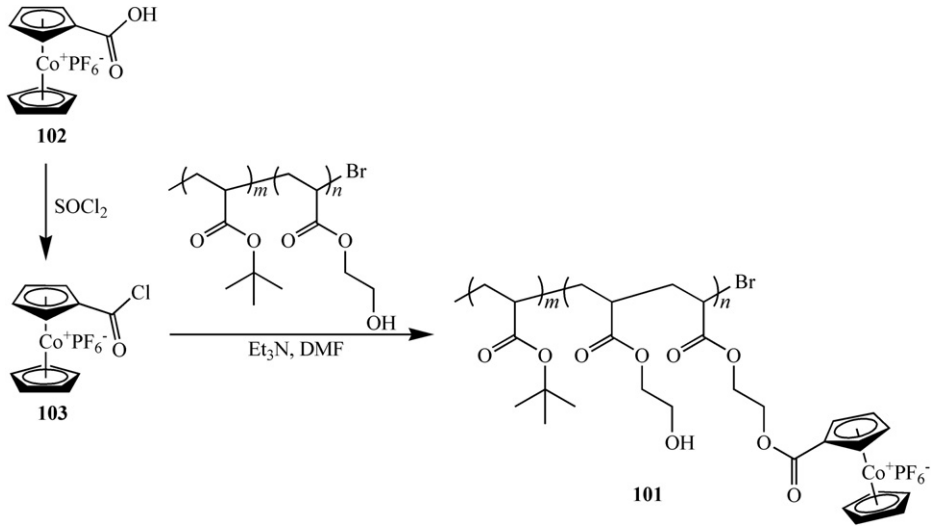

Scheme 21. Preparation of a block copolymer containing cobaltocenium side-chains (**101**) [61].

known block copolymer, poly(*tert*-butyl acrylate)-*block*-poly(2-hydroxyethyl acrylate) to afford the side-chain cobaltocenium-containing block copolymer **101** (Scheme 21). The study showed that these cationic block copolymers exhibit unique solubility and will self-assemble in solution. Furthermore, depending on the solvent mixtures, they demonstrated the ability to form self-assembled nanotube and vesicle structures, as determined by transmission electron microscopy (TEM).

5. Coordination polymers

The use of metal centres with various coordination geometries as well as appropriate spacer ligands allow for unique properties to be obtained in the polymers. For instance, Harvey and coworkers prepared cofacial bismacrocycle dyads (**104**) (Fig. 27) and demonstrated their photophysical properties including intramolecular electron and energy transfers [118]. The singlet–singlet (S_1) and

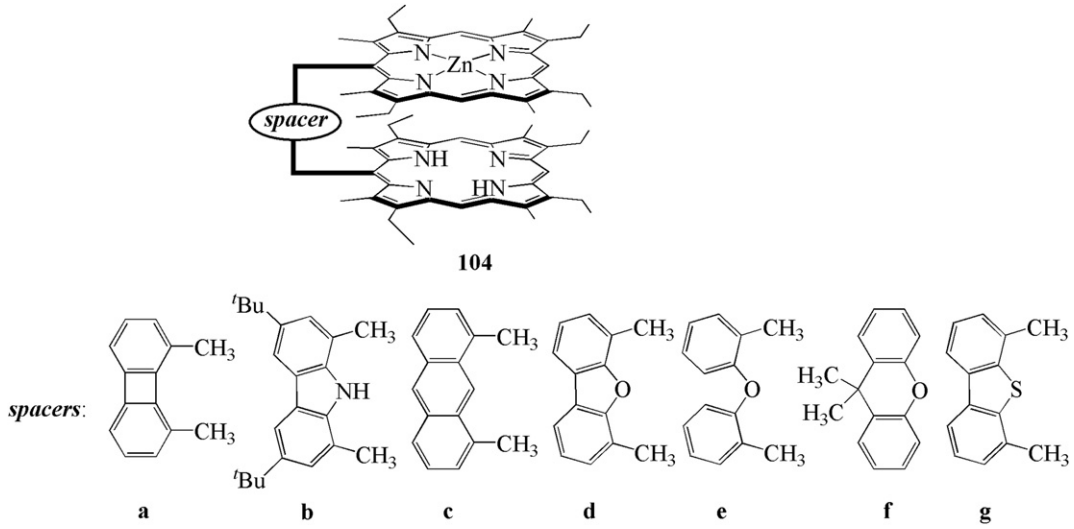

Fig. 27. Examples of bifacial bisporphyrin dyads with various spacers (**104**) [118].

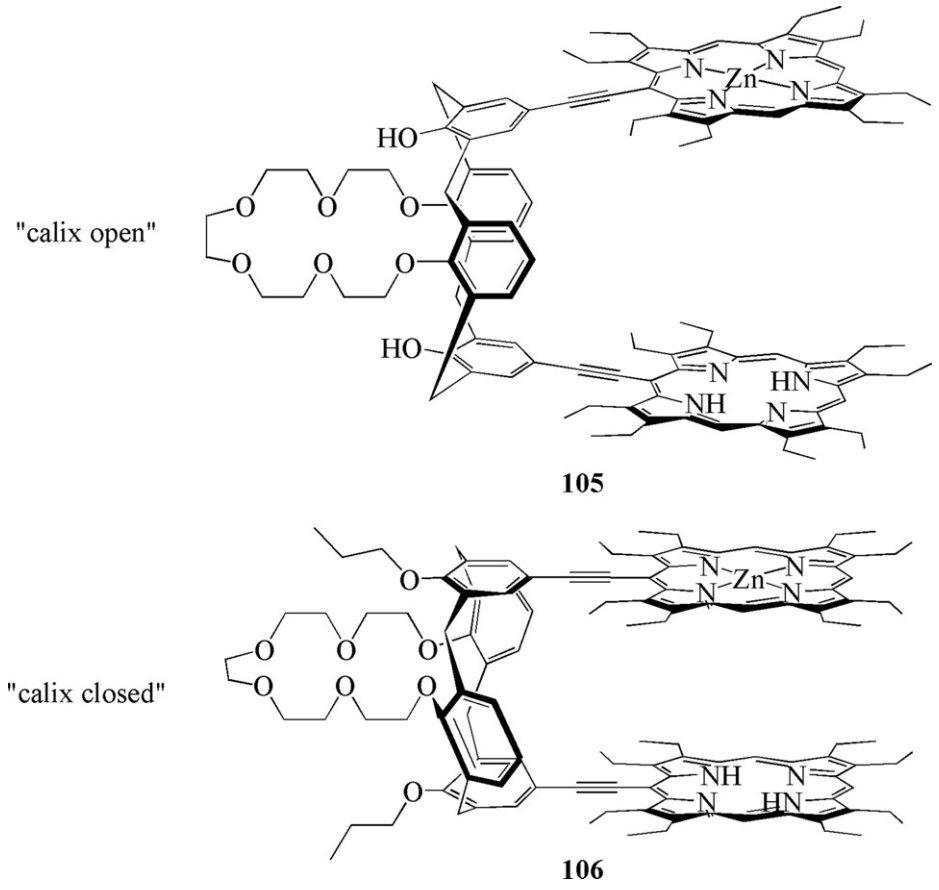

Fig. 28. Structures of "calix open" **105** and "calix closed" **106** conformers [118].

triplet–triplet (T_1) energy transfer rates through space of bifacial bisporphyrin dyads (**104**) were studied. The authors found that these macrocyle dyads have very similar through space S_1 energy transfer rates in light harvesting devices. As a result, these macromolecules may be employed as practical models for further investigation into such applications.

Harvey and coworkers also investigated two semi-flexible calixarene-based models [118]. The "calix open" conformer **105** (Fig. 28) was formed as a result of intramolecular hydrogen bonding between the hydroxyl groups on the lower rim and the oxygen atoms on the crown ether moiety. On the other hand, the "calix closed" conformer **106** (Fig. 28) was produced from the substitution of the hydroxyl groups with ethoxy groups, which prevents any hydrogen bonding. The closed conformer enables fast electron transfer between the two porphyrin chromophores as a consequence of their close proximity.

A number of tin(IV) polymers with polydendate ligand bis(1,2,4-triazoyl)methane (**107**), were reported by Masciocchi and coworkers [119]. The polydentate ligands (**107**) (Fig. 29) used to link the tin(IV) subunits were 9.5–11.2 Å apart in 1-D chains grouped in parallel bundles. Compared to the rigid bis(imidazoyl)methane ligand **107**, the structure of ligand **108** (Fig. 29) has increased flexibility and a higher number of coordination sites. As a result, compound **108** is a more suitable ligand for these tin(IV) 1-D polymers.

Pombiero and coworkers have reported the synthesis and catalytic activity of a coordination polymer containing (triethanolamine)copper(II) moieties connected by pyromellate units (**109**) (Fig. 30) [120,121]. The study has shown that polymer **109** can be employed as a catalyst precursor for the peroxidative oxidation of

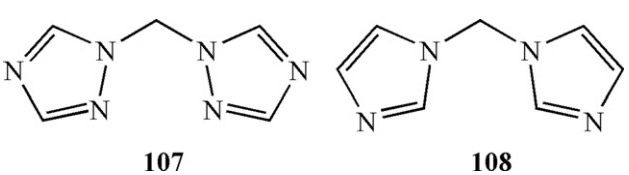

Fig. 29. Structures of polydentate ligands **107** and **108** that have been employed as linkers for a number of tin(IV) polymers [119].

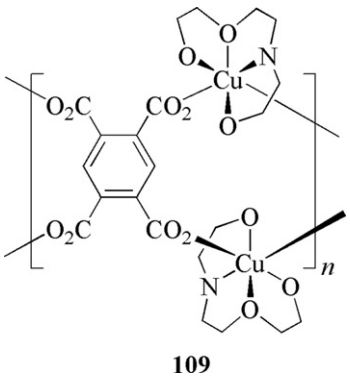

Fig. 30. Coordination polymer **109** with (triethanolamine)copper(II) moieties joined by pyromellate units [120,121].

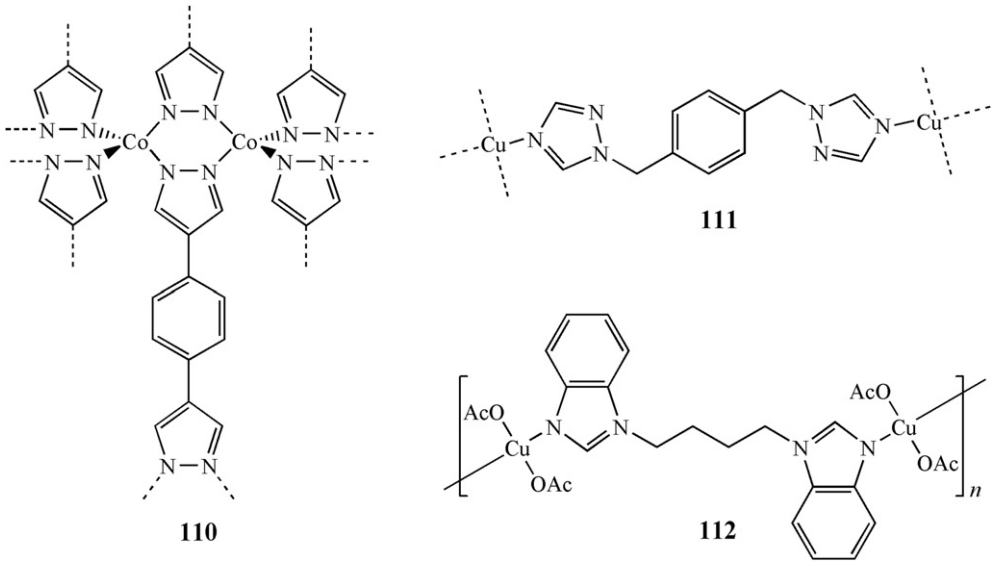

Fig. 31. Example structures of cobalt- or copper-containing coordination polymers (**110**–**112**) [123,124].

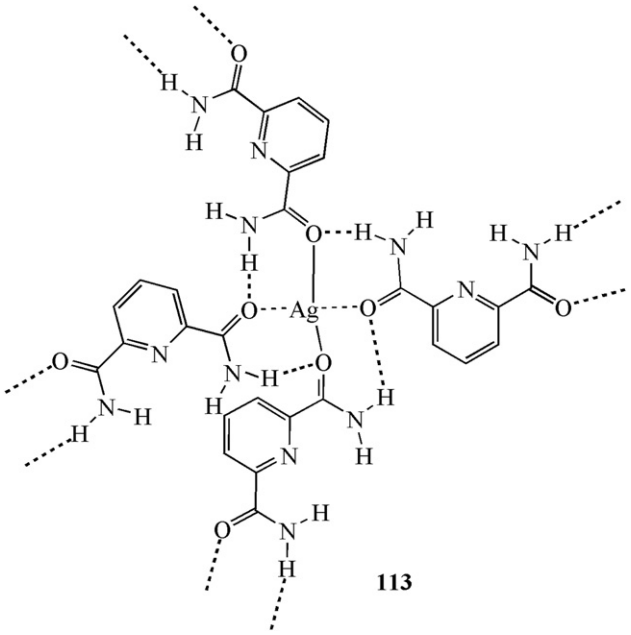

Fig. 32. Perspective view of a square secondary building unit with an Ag(I) metal center from a 2-D square framework (**113**) [126].

cyclohexane into cyclohexanol and cyclohexanone by hydrogen peroxide at room temperature [121].

Llabrés i Xamena et al. synthesized a cobalt(II)- and a copper(II)-containing metal organic framework (MOF) that have phenylimidazolate or 2-hydroxypyrimidinolate linking units [122]. These organometallic macromolecules are used in the conversion of tetralin to a hydroperoxo derivative intermediate via aerobic oxidation and then subsequently oxidized to the ketone. The conversion rate for oxidizing tetralin to the hydroperoxo intermediate occurs at a moderate rate for the Cu(II) MOF, but occurs slowly for the Co(II) MOF. However, the use of the Co(II) system results in increased ketone production compared to the Cu(II) system. Utilizing the Cu(II) and Co(II) MOFs together results in significant selectivity and activity, as opposed to when either of the organometallic systems are used separately.

A cobalt coordination polymer (**110**) containing bis(pyrazolyl) benzene units (Fig. 31) has been previously reported [123] and is used as a catalyst for the oxidation of cyclohexene by *tert*-butylperoxide. Coordination polymers with 1-D chains and 2-D grid topologies have been prepared from the reaction of copper(II) salts with either 1,4-bis(triazolylmethyl)benzene or 1,4-bis(benzimidazolyl) butane as linking units for polymers **111** and **112**, respectively (Fig. 31) [124]. Significant activity and selectivity were observed for the coordination polymers with a 2-D grid framework compared to those with 1-D polymer chains. The authors attribute these results to

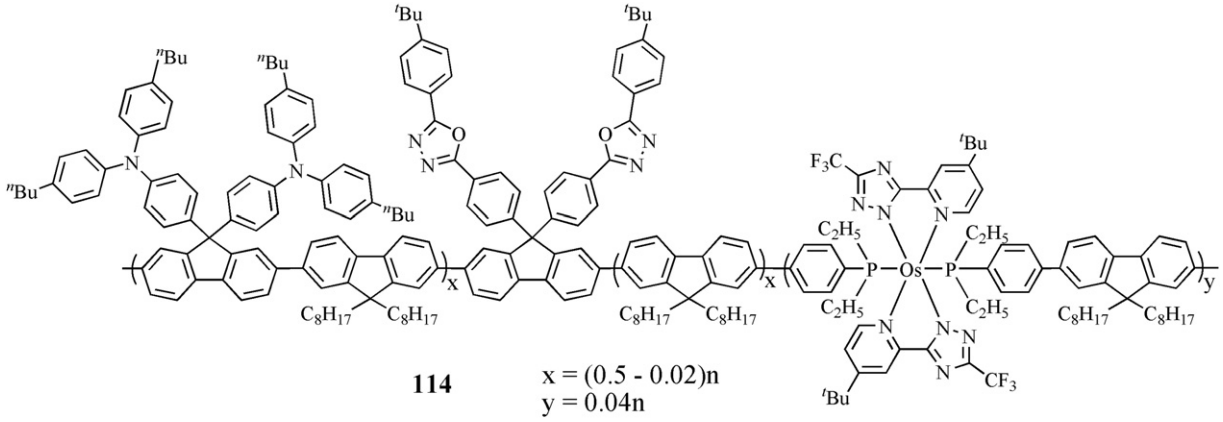

Fig. 33. Structure of electrophosphorescent polyfluorene copolymer **114** [129].

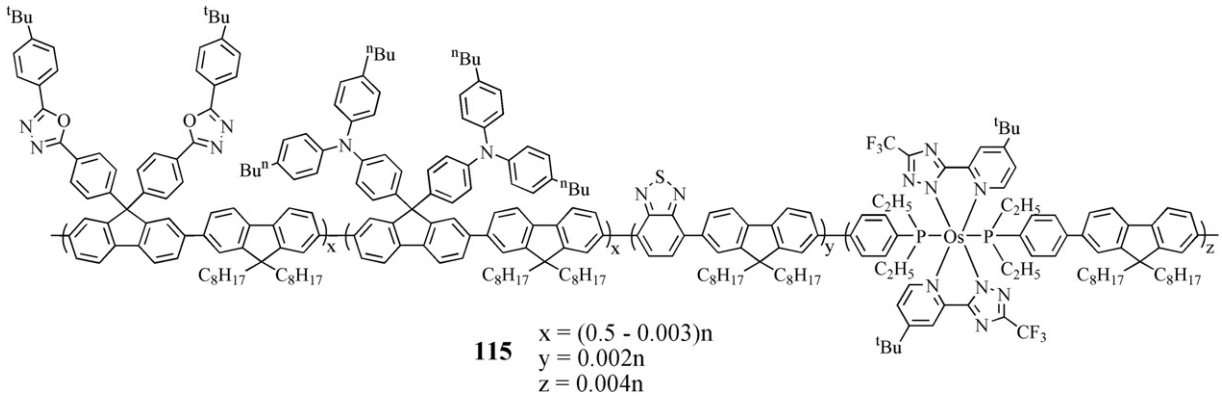

Fig. 34. Structure of white-light emitting polyfluorene copolymer **115** [129].

the variances in the sterics at the metal centers in the various macromolecules.

Pyridine-based coordination polymers can be synthesized by chelating a pyridine monomer to the metal center prior to polymerization. For example, Chen and coworkers have used 2,6-disubstituted pyridyl compounds as bridging ligands for the assembly of 1-, 2-, and 3-D coordination polymers [125,126]. The central pyridyl moiety of 2,6-disubstituted pyridyl compounds enables enhanced π–π stacking interactions, which allows for the formation of a well stabilized macromolecule [127]. Furthermore, 2,6-disubstituted pyridyl ligands can act as hinges [125,128], causing them to be more flexible and allow for the formation of macromolecules of various dimensions as a result of the ligand's flexible nature [125,126]. For instance, 2,6-bis(imidazol-1-yl)pyridine was used as a bridging ligand to assemble multi-dimensional Zn(II) and Ag(I) coordination polymers [125,126]. Fig. 32 illustrates a perspective view of a square secondary building unit containing an Ag(I) metal center from a 2-D square framework (**113**) [126]. Additionally, these macromolecules possess the necessary characteristics for novel functional crystalline materials due to their stable homochiral framework and increased robustness [125].

Chien et al. employ osmium complexes functionalized with two 3-trifluoromethyl-5-(4-tert-butyl-2 pyridyl)triazolate (bpftz) ligands to prepare electrophosphorescent polyfluorene copolymers [129]. Fig. 33 displays an Os-containing polyfluorene copolymer (**114**) as an example. The authors found that the red-emitting Os(bpftz) moiety and blue-emitting polyfluorene used to form a copolymer enabled

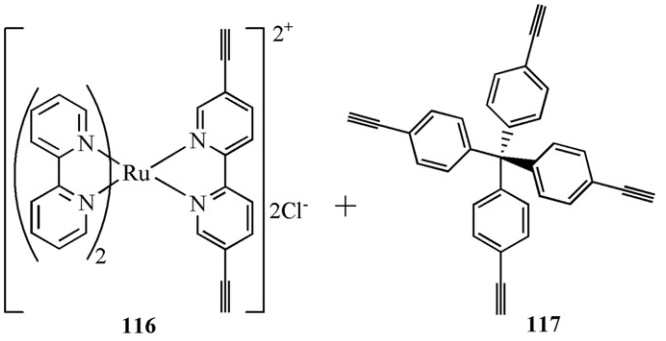

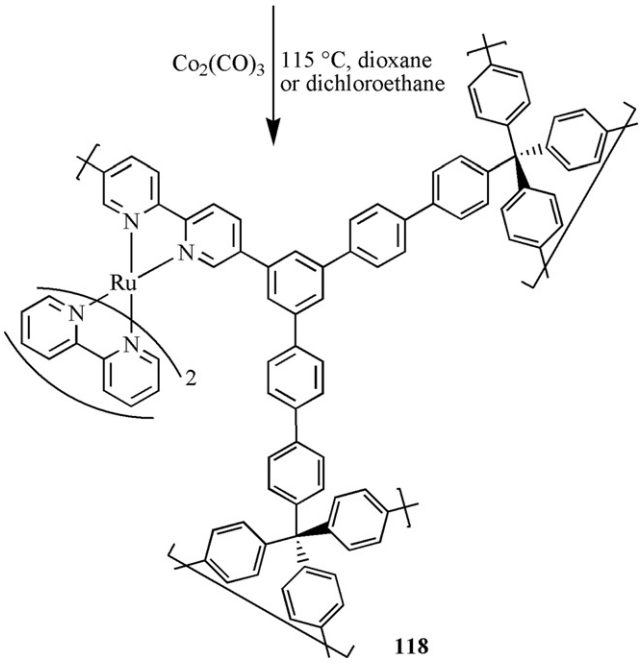

Scheme 22. Synthesis of a ruthenium porous cross-linked polymer functionalized with a 2,2′-bipyridine moiety (**118**) [130].

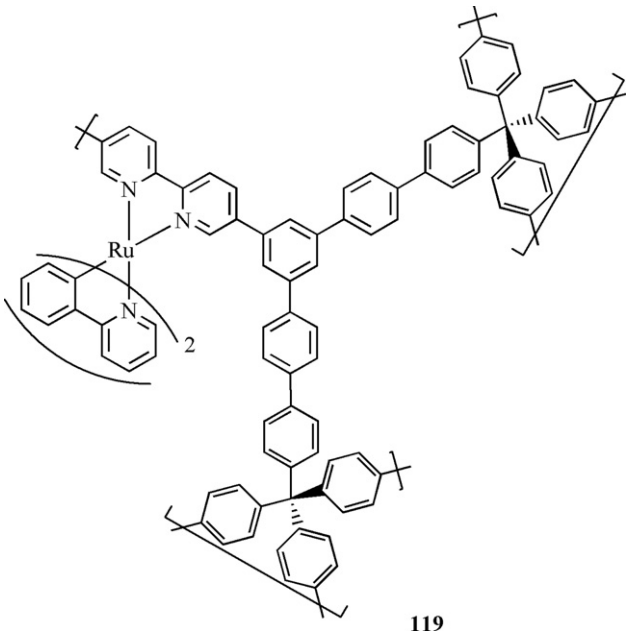

Fig. 35. Structure of iridium monomer containing 2-phenylpyridine moieties (**119**) that was used for the synthesis of an iridium PCP [130].

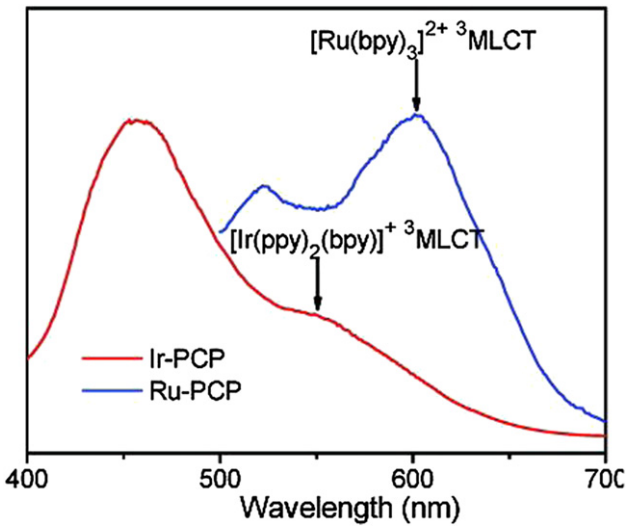

Fig. 36. Uncorrected emission spectra of ruthenium cross-linked polymer **118** (represented in blue as **Ru**–**PCP**) and iridium cross-linked polymer (represented in red as **Ir**–**PCP**) [130]. The emission spectra of Ru **118** and Ir **119** were taken at 450 nm and 380 nm excitation, respectively. Adapted with permission from J Am Chem Soc, 133, Xie Z, Wang C, deKrafft KE, Lin W, "Highly stable and porous cross-linked polymers for efficient photocatalysis", 2056–2059. Copyright (2011) American Chemical Society.

them to be used as a very efficient red polymer light-emitting diode (PLED). The results indicated that the PLED has a maximum brightness of 38,000 cd m^{-2} and an external quantum efficiency of 18%. Additionally, a green-emitting benzothiadiazole group was incorporated into an Os(bpftz)-containing polyfluorene copolymer via Suzuki polycondensation which resulted in the formation of a white-light emitting polymer (**115**) which exhibited all blue, green and red emissions (Fig. 34).

Very recently, the synthesis of phosphorescent ruthenium and iridium bypyridine-containing porous cross-linked polymers (PCPs) via cobalt carbonyl-catalyzed trimerization of the monomers' terminal alkyne moieties has been reported [130]. Scheme 22 shows the synthesis of a ruthenium PCP (**118**) from Ru monomer **116** and tetra(4-ethynylphenyl)methane (**117**).

An analogous iridium PCP (**119**) (Fig. 35) was prepared under the same conditions as ruthenium polymer **118**, but instead of using the Ru monomer **116**, an iridium bipyridine monomer with 2-phenylpyridine units was used [130]. Thermogravimetric analysis revealed that PCPs **118** and **119** were thermally stable up to 350 °C and did not decompose when exposed to a variety of organic solvents. It has been shown in the past that tris(bipyridine)ruthenium(II) derivatives exhibit homogeneous photocatalytic activity [130]. Additionally, an iridium 2-phenylpyridine derivative, $Ir(ppy)_2(dtbbpy)PF_6$ (ppy = 2-phenylpyridine and dtbbpy = 4,4′-di-

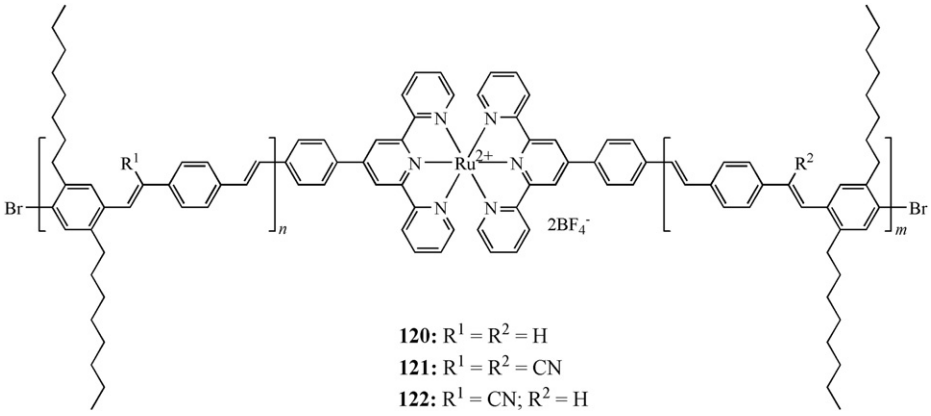

Fig. 37. Structures of terpyridine-containing ruthenium homopolymers **120** and **121** and copolymer **122** [134].

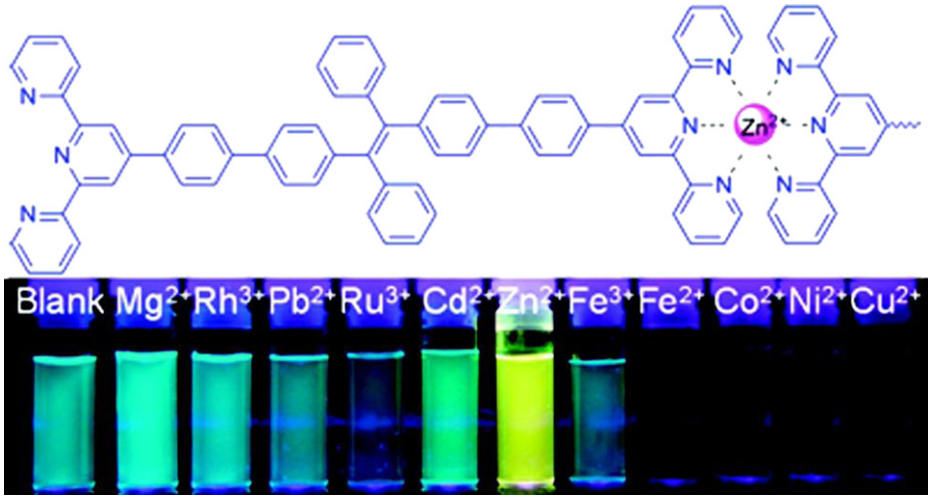

Fig. 38. Structure of terpyridine-containing tetraphenylethene derivative with Zn^{2+} cation (above) and photograph taken under UV light of aqueous solutions of terpyridine-containing TPEs/cation mixtures (below) [137]. Reprinted with permission from ACS Appl Mater Interfaces, 3, Hong YN, Chen SJ, Leung CWT, Lam JWY, Liu JZ, Tseng NW, Kwok RTK, Yu Y, Wang ZK, Tang BZ, "Fluorogenic Zn(II) and chromogenic Fe(II) sensors based on terpyridine-substituted tetraphenylethenes with aggregation-induced emission characteristics", 3411–3418. Copyright (2011) American Chemical Society.

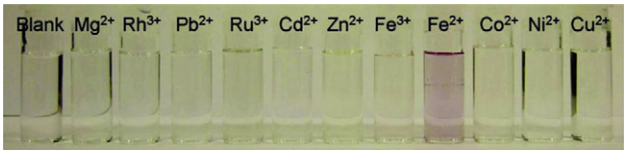

Fig. 39. Photograph taken under natural light of aqueous solutions of terpyridine-containing TPE/cation mixtures [137]. Reprinted with permission from ACS Appl Mater Interfaces, 3, Hong YN, Chen SJ, Leung CWT, Lam JWY, Liu JZ, Tseng NW, Kwok RTK, Yu Y, Wang ZK, Tang BZ, "Fluorogenic Zn(II) and chromogenic Fe(II) sensors based on terpyridine-substituted tetraphenylethenes with aggregation-induced emission characteristics", 3411–3418. Copyright (2011) American Chemical Society.

*t*butyl-2,2′-bipyridine), has also previously been shown to behave as a photo-redox catalyst in reactions such as aza-Henry reactions [130]. Phosphorescence studies revealed metal-to-ligand charge-transfer (MLCT) to ground state transitions at approximately 602 nm and 550 nm for Ru cross-linked polymer **118** and Ir cross-linked polymer **119**, respectively (Fig. 36). The study also indicated that the phosphors were reductively quenched by the amine substrate of ruthenium PCP **118**. The iridium PCP **119** also exhibited this quenching effect; however, due to the framework fluorescence interference, the quenching was unable to be measured spectroscopically. Consequently, the authors suggest that this quenching effect may result in efficient photocatalytic performance of the polymers, since it is the first step in the photocatalytic cycle of homogeneous aza-Henry reactions. This led the authors to test the catalytic activity of the Ru and Ir-based PCPs in aza-Henry reactions. The results indicated that these polymers exhibited high catalytic efficiency and could be recycled and reused as heterogeneous photocatalysts in aza-Henry reactions.

Polymer structure and metal species coordinated to terpyridine-containing coordination polymers can give rise to unique photophysical properties [14,131,132]. As a result, quenching or enhancement of polymer fluorescence can be varied, which has led to their use as luminescent sensors for metal ions and their application in photovoltaics [131,133–136]. For instance, terpyridine-containing ruthenium homopolymers **120** and **121** and copolymer **122** (Fig. 37) were used to prepare polymer solar cells and dye-sensitized solar cells (DSSCs) [134]. Poly(*p*-phenylenevinylene)s (PPVs) functionalized with terminal terpyridine moieties were attached via ruthenium complexation to afford photoactive copolymer **122** and homopolymers **120** and **121** [134]. The study showed that the Ru complexes were able to quench fluorescence which indicated that the polymers could transfer energy to the terpyridine-containing ruthenium complexes. Furthermore, the results revealed that copolymer **122** was the most favourable polymer used to prepare DSSCs and gave efficiencies reaching approximately 0.1%. On the other hand, homopolymer **121** gave superior results when used to prepare organic solar cells with efficiency less than 0.01%.

Tang and coworkers recently prepared tetraphenylethenes (TPEs) functionalized with terpyridine moieties that act as fluorescent chemosensors for metal ions (Fig. 38) [137]. For instance, the incorporation of zinc(II) ions into a solution of terpyridine-containing TPEs, the colour changed from greenish blue to yellow and a shift in the emission spectra by 50 nm was observed. Additionally, when iron(II) ions were added to an aqueous solution of TPEs with terpyridine groups, the solution colour changed from colourless to light magenta. This colour change observation occurred as a result of the metal-to-ligand-charge-transfer process. Overall, these TPE derivatives exhibit different fluorescence responses to a variety of metal cations.

Interestingly, these compounds are only faintly coloured in aqueous solution (Fig. 39), but their nanoaggregates in aqueous media or thin films in the solid state are strongly emissive. Due to the strong emission of the nanoaggregates, these TPE derivatives exhibit a new phenomenon of aggregation-induced emission (AIE), a term coined by Tang and coworkers [138,139]. Moreover, the emission of the nanoaggregates is sensitive to pH changes, as observed when the terpyridine moieties were protonated, causing the quenching of light emission [137].

A number of butadiyne-linked zinc porphyrin oligomers were prepared by Anderson and coworkers [140]. These single-stranded oligomers self-assemble into double-strand ladders (Fig. 40), significantly increasing the conjugation lengths compared to the analogous single-strand chains. As a result of this ladder formation and thus increased conjugation length, the two-photon absorption

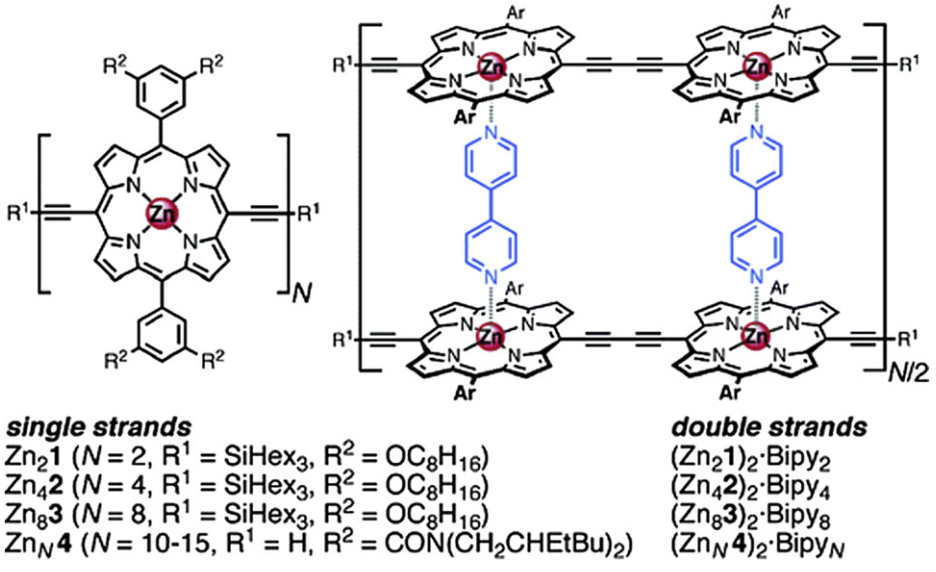

Fig. 40. Structures of various butadiyne-linked zinc porphyrin oligomers [140]. Reprinted with permission from J Am Chem Soc, 128, Drobizhev M, Stepanenko Y, Rebane A, Wilson CJ, Screen TEO, Anderson HL, "Strong cooperative enhancement of two-photon absorption in double-strand conjugated porphyrin ladder arrays", 12,432–12,433. Copyright (2006) American Chemical Society.

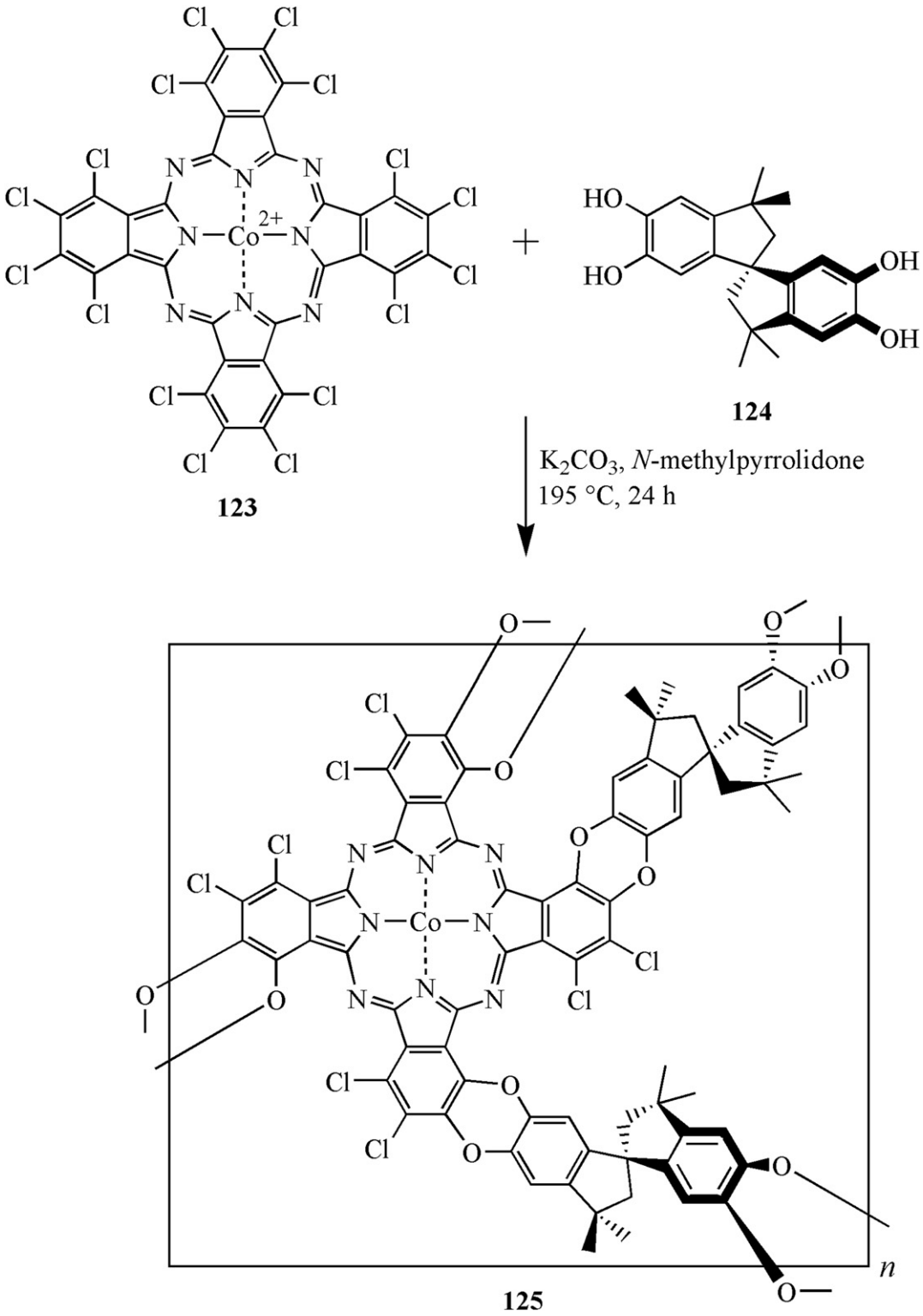

Scheme 23. Synthesis of a spiro-linked cobalt phthalocyanine network polymer (**125**) [141].

is dramatically enhanced. Such macromolecular nanostructures may be used in optical switching and signal processing in fiber-optic communications technologies.

McKeown et al. reported the synthesis of iron porphyrin and cobalt phthalocyanine network polymers and investigated their heterogeneous catalytic performance compared to analogous low molecular weight catalysts [141]. The incorporation of Co phthalocyanine or Fe porphyrin moieties into the polymer networks resulted in polymers of intrinsic microporosity that demonstrated enhanced catalytic activity. For example, a chlorinated phthalocyanine monomer (**123**) and spirobisindane **124** were used to prepare a microporous Co phthalocyanine polymer network (**125**)

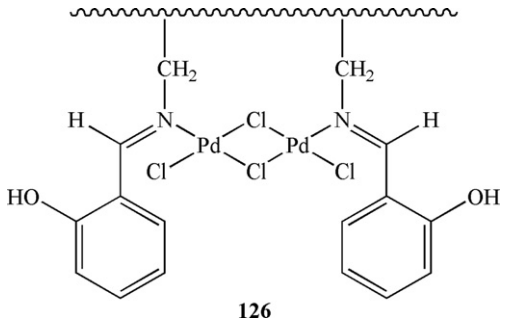

126

Fig. 41. Structure of polymer-bound palladium(II) Schiff base complex **126** [152].

(Scheme 23) [141]. The cobalt phthalocyanine polymer network **125** exhibited increased catalytic activity for hydrogen peroxide decomposition. Additionally, a similar fluorinated iron porphyrin polymer network showed increased catalytic activity for oxidation of hydroquinones [141]. McKeown and coworkers have recently utilized X-ray diffraction to show that single-crystal-single-crystal (SCSC) transformations were used to form a heme homogenous model system derived from a phthalocyanine nanoporous crystal with axial coordination at the iron center [142]. The study revealed that monodentate ligands will selectively add to the axial binding site inside the cubic framework of the nanoporous crystal, as opposed to bidentate ligands which selectively add to the opposite axial binding site to connect the cubic frameworks. Similar differentiation of the ligand binding sites is observed in hemoproteins. Furthermore, the mono- and bi-dentate ligands can rapidly bind to the axial sites as a result of the nanoporous molecular crystal. This phthalocyanine nanoporous crystal is an example model that can be potentially used to design practical industrial catalysts.

Various coordination polymers containing metals such as iron [143], lanthanides [144–147], and manganese [148,149] have been prepared using a variety of multidentate Schiff base ligands. As a result, polymers of various architectures, including 2-D and 3-D networks, interpenetrating structures, square-grid motifs, and molecular square units were formed [150]. Recently, Liu et al. reported a number of coordination polymers with cadmium, zinc, or cobalt moieties prepared from reduced Schiff base multidentate anions and 1,4-bis(1H-imidazol-1-yl)butane [151]. The resulting compounds exhibit 2-D and 3-D frameworks, including one with a 2-D interpenetrating network with both polycatenane and polyrotaxane character. Thermogravimetric analysis of

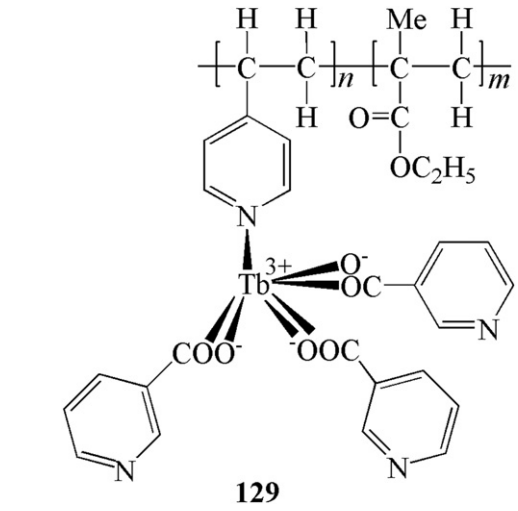

129

Fig. 43. Structure of luminescent terbium copolymer **129** [154].

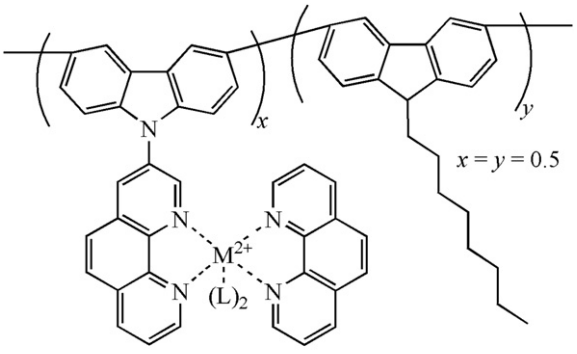

130: M = Zn, L = CH_3COO^-
131: M = Cd, L = Cl^-
132: M = Ni, L = NO_3^-

Fig. 44. Structure of Ni, Cd, and Zn phenanthroline copolymers containing carbazole moieties (**130**–**132**) [155].

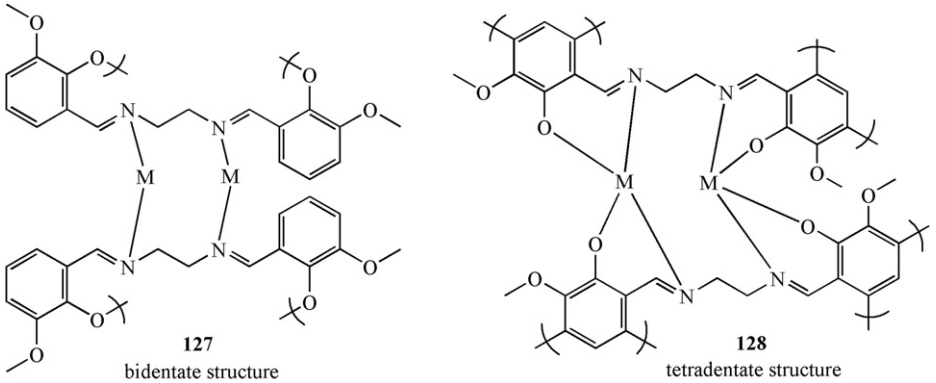

M = Cu(II), Co(II), Ni(II)

Fig. 42. Structures of bidentate (**127**) and tetradentate (**128**) ligand polymeric complexes [153].

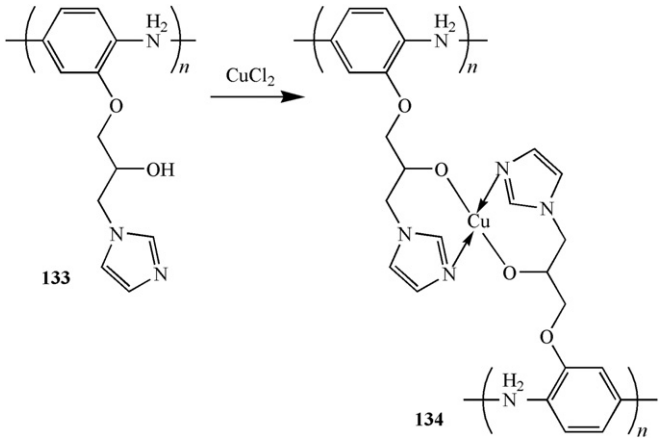

Scheme 24. Synthesis of polyaniline copper coordination polymer **134** [156].

a Cd(II)-coordinated polymer indicated that the removal of the organic moieties occurs between 262 and 646 °C, which is comparable to other Schiff base coordination polymers [143]. Furthermore, solid-state luminescent studies of the coordination polymers revealed emission maxima occurred from 398 to 458 nm. As a result, these macromolecules have potential use in photoactive materials.

Schiff bases are prepared via condensation reactions of aromatic amines with ketone and aldehyde derivatives and can be used to synthesize coordination polymers. For instance, Alexander et al. reported the catalytic activity of a polymer-bound palladium(II) Schiff base complex (**126**) (Fig. 41) towards the hydrogenation of several olefins [152]. The results indicated the effectiveness of the catalyst in the hydrogenation of numerous olefins and can be recycled many times with negligible loss in its activity.

The activity of a given polymeric material highly depends on the coordination site and the type of Schiff base ligand. Moreover, the activity is also dependent on the metal center used in the synthesis of polymer-supported Schiff base complexes. Copper, cobalt, and nickel complexes of Schiff base polymers were synthesized by Tuncel and coworkers [153]. The results indicate the formation of binuclear complexes **127** and **128** containing nitrogen and oxygen donor atoms (Fig. 42) when there is a 1:1 M ratio of Schiff base polymers and metal ions present in the reaction. Additionally, these complexes contain dimeric structures that are bridged by polymeric ligand moieties. As a result of the C–O–C type coupling in the polymers, these complexes may coordinate to Ni^{2+}, Co^{2+} and Cu^{2+} ions to afford various functional materials.

Yan and Wang have reported a number of terbium-containing polymers that exhibit highly efficient luminescence [154]. Three terbium binary complexes with pyridine carboxylic acids were prepared and subsequently incorporated into 4-vinyl pyridine-ethyl methacrylate copolymer matrices. Copolymer **129** is represented as an example in Fig. 43. The study shows that the energy transfer mechanism appears standard through these polymer systems.

Very recently, three nickel-, cadmium-, and zinc-phenanthroline copolymers containing carbazole moieties (**130**–**132**) (Fig. 44) were prepared by Guo and coworkers [155]. The thermal, photovoltaic, and optical properties of copolymers **130**–**132** were also studied. The electrochemical and photophysical properties were adjusted as a result of incorporating the metal units in the branched chain. Thermal studies revealed high thermal stability up to 454, 489, and

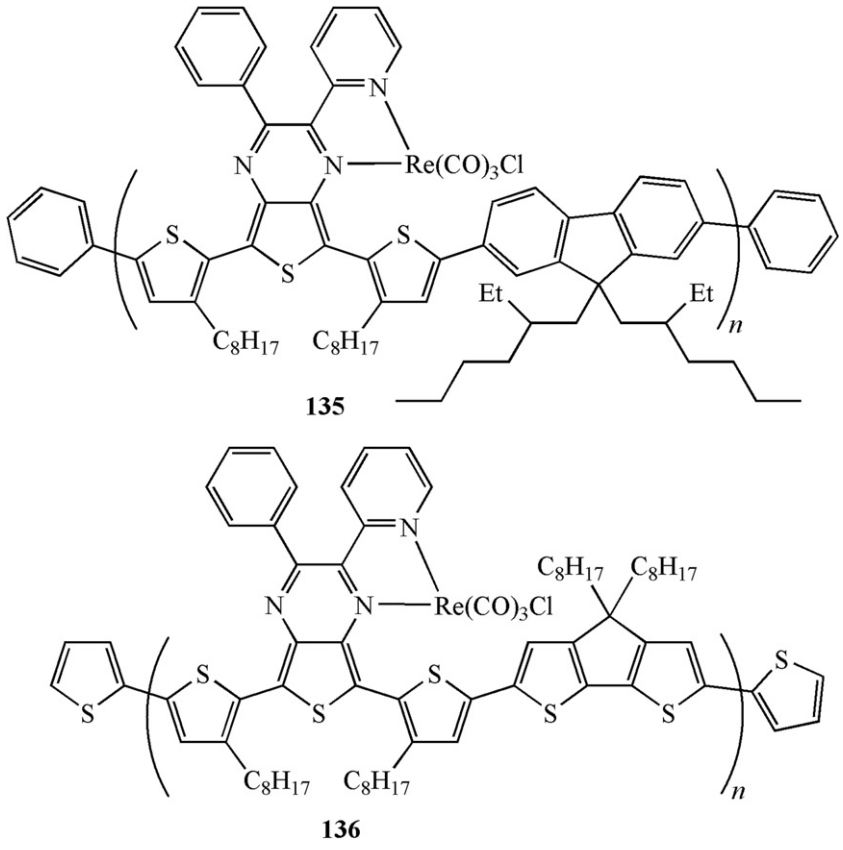

Fig. 45. Structures of light harvesting rhenium polymers **135** and **136** [157,158].

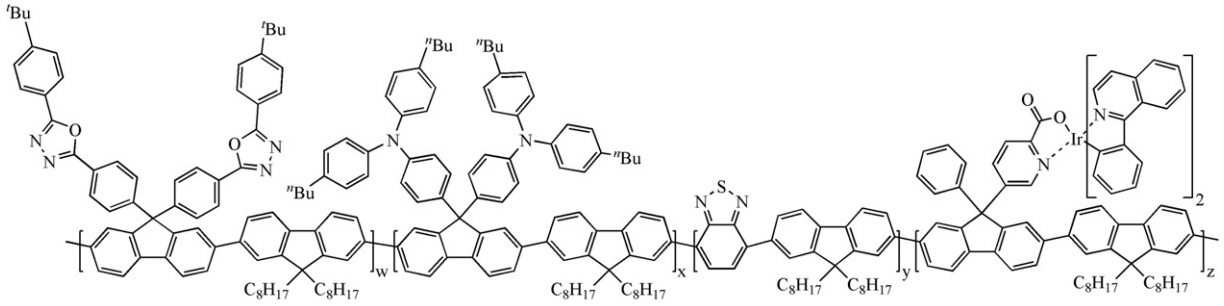

137

Fig. 46. Structure of electroluminescent iridium copolymer **137** [159].

310 °C for polymers **130**, **131**, and **132**, respectively. The study shows that these π-conjugated copolymers show sufficient open-circuit voltages and fill factors with moderate power conversion. However, the authors indicate that further optimization of the power conversion efficiencies of the copolymers is necessary in order for their use in dye-sensitized solar cells.

Joseph et al. very recently used a polyaniline derivative (**133**) to prepare a polyaniline coordination polymer with copper-coordinated imidazole units (**134**) (Scheme 24) [156]. Functionalization of the polyaniline with imidazole enabled the polymer to function as a metal ion receptor. Furthermore, the incorporation of the copper moieties into the coordination polymer enables tuning of the physical and electronic properties. For instance, aggregation occurs as a result in the morphology change when Cu(II) is coordinated. Additionally, increased molecular weight, lower PDI, and changes in crystallinity resulted from copper coordination. Increased conductivity was also observed when Cu(II) was incorporated into the polymer as a result of the formation of hydrochloric acid as secondary ions.

Research studies have shown that low band gap metallopolymers can be used as light harvesting materials [157]. Recently, Chan's research group has synthesized low band gap rhenium-containing conjugated copolymers (**135** and **136** are shown in Fig. 45 as examples) that have potential use in photovoltaic applications [157,158]. Due to the functionalized intramolecular charge transfer linking units in polymers **135** and **136**, a strong, broadened absorption band in the UV–vis region was observed.

Copolymers **137** (Fig. 46) functionalized with iridium in the side chain via Suzuki coupling have been prepared [159,160]. Using an electron-injection cathode enabled the iridium complex to emit one of three primary colours. The colours of these white light electroluminescent materials were changed by varying the concentrations of the emitting species [159].

Shunmugam and Tew have used terpyridine ligands to coordinate europium and terbium into a polymer side chain, **138** and **139**, (Fig. 47) to afford luminescent materials [161]. The results showed that the terbium polymer emitted green light and the europium polymer emitted pink light. Interestingly, when the two Tb(III) and Eu(III) ions were coordinated (1:1 ratio) to the same polymer backbone, the resulting mixed-metal system emitted a yellow light. When the mixed-metal polymer was heated above 50 °C, reversible thermochromism was exhibited, resulting in a colour change from yellow to orange/pink (Fig. 48).

Recently, the synthesis of substituted bipyridine-functionalized phosphazene polymers (**140**) was reported. These polymers were subsequently reacted with either $[Pt(PhCN)_2Cl_2]$ or $[Re(CO)_5Cl]$ to afford analogous metallopolymers **141** or **142**, respectively (Scheme 25) [162]. The study showed that the metal-free polymer, **140**, has a PDI value of 1.97 and a glass transition temperature of

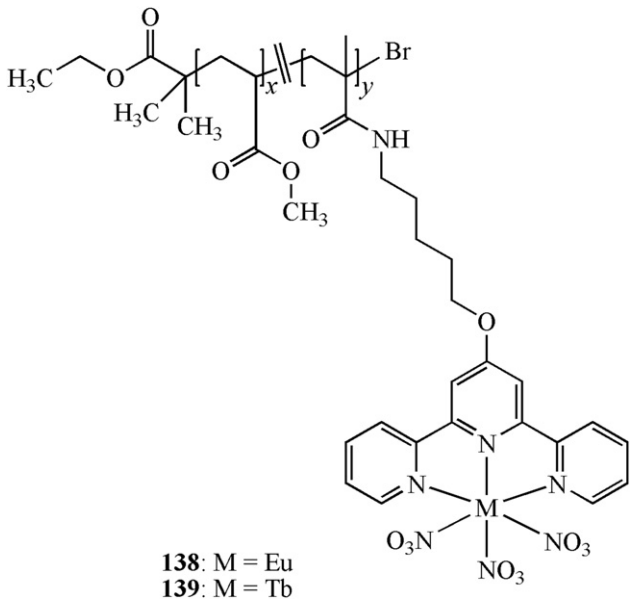

138: M = Eu
139: M = Tb

Fig. 47. Structure of luminescent Eu- and Tb-containing polymers **138** and **139**, respectively [161].

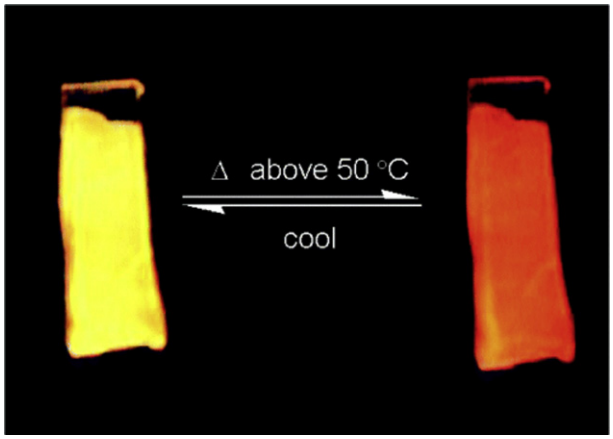

Fig. 48. Reversible thermochromism of mixed-metal polymer. Polymer was heated above 50 °C and thin films were excited with a UV lamp [161]. Reprinted with permission from J Am Chem Soc, 127, Shunmugam R, Tew GN, "Unique emission from polymer based lanthanide alloys", 13,567–13,572. Copyright (2005) American Chemical Society.

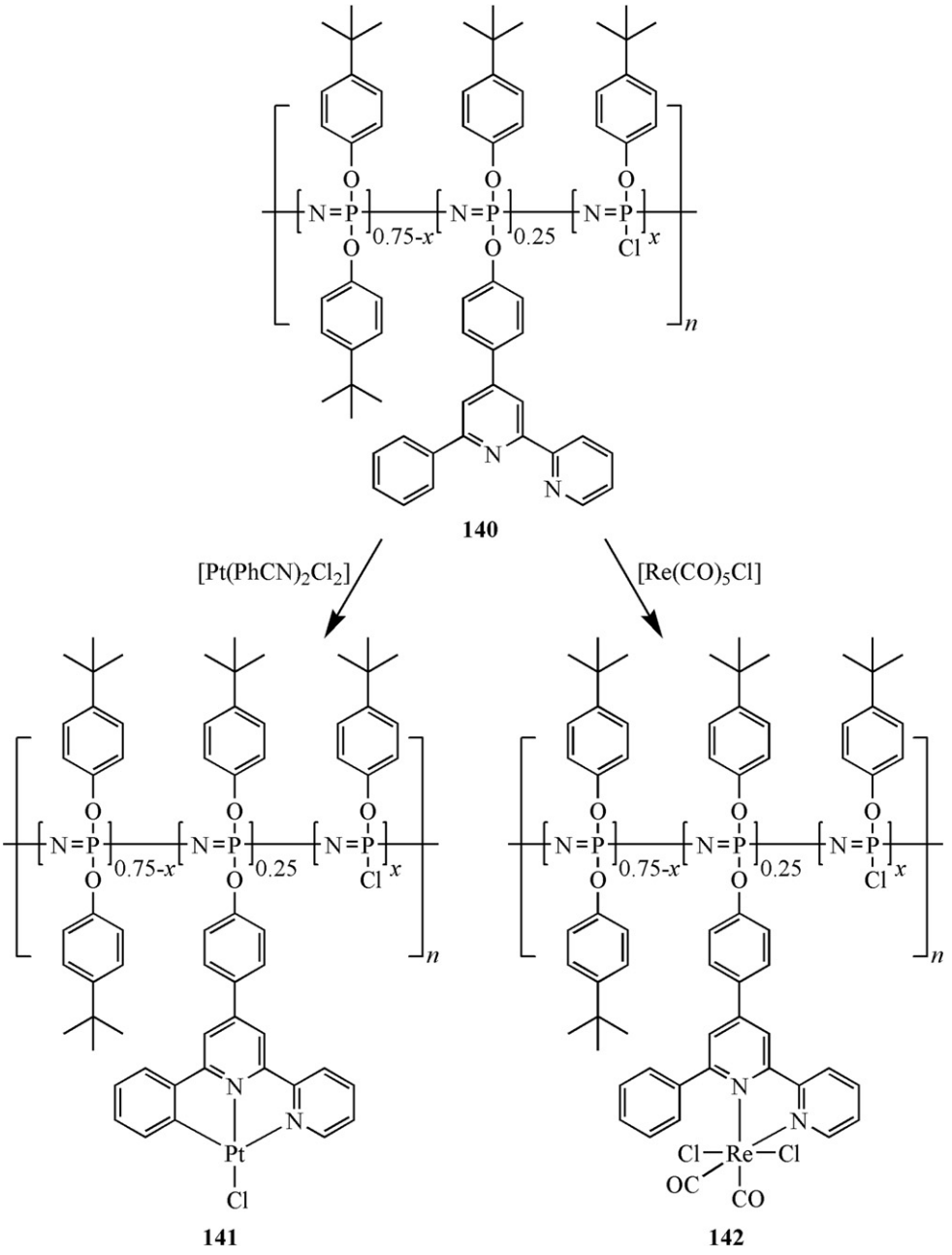

Scheme 25. Synthesis of bipyridine-containing metallopolymers **141** and **142** [162].

83 °C. However, when rhenium or platinum was incorporated into the polymer side chain, the PDI increased above 2.0 as a result of partial thermal degradation of the backbone. The increase in glass transition temperature of the rhenium-containing polymer (**142**) from 83 °C to 120 °C suggests an interaction occurs between the carbonyl ligands on the rhenium center with the hydrogen atoms from the neighbouring O^{t}BuPh groups. In other known small-molecule metal complexes, comparable carbonyl-hydrogen weak interactions have been observed. Photophysical studies of these metallated polymers revealed very little differences in the photophysics of similar, known metal chromophores. As a result, the authors suggest that independent control of their photophysical properties could be obtained, making the introduction of new properties such as catalytic activity while maintaining control over thermal and chemical stability possible.

6. Dendrimers and star polymers

Dendrimers and star-shaped polymers consist of similarly sized polymeric chains that originate from a central multifunctional core [163]. The preparation of star-shaped macromolecules containing diverse multifunctional groups can be highly controlled and is accomplished via divergent or convergent synthesis [163–168]. This versatile construction has led to applications in light-harvesting systems, drug delivery, catalysis, and biomedicine [6,84,169–191]. For instance, a zinc phthalocyanine-containing dendrimer **143** (Fig. 49) has been synthesized and found to absorb light at longer wavelengths compared to analogous porphyrin dendrimers [192]. The carboxylic acid moieties in **143** can be deprotonated to form an anionic dendrimer, and when combined with poly(ethylene glycol)-poly(L-lysine) block

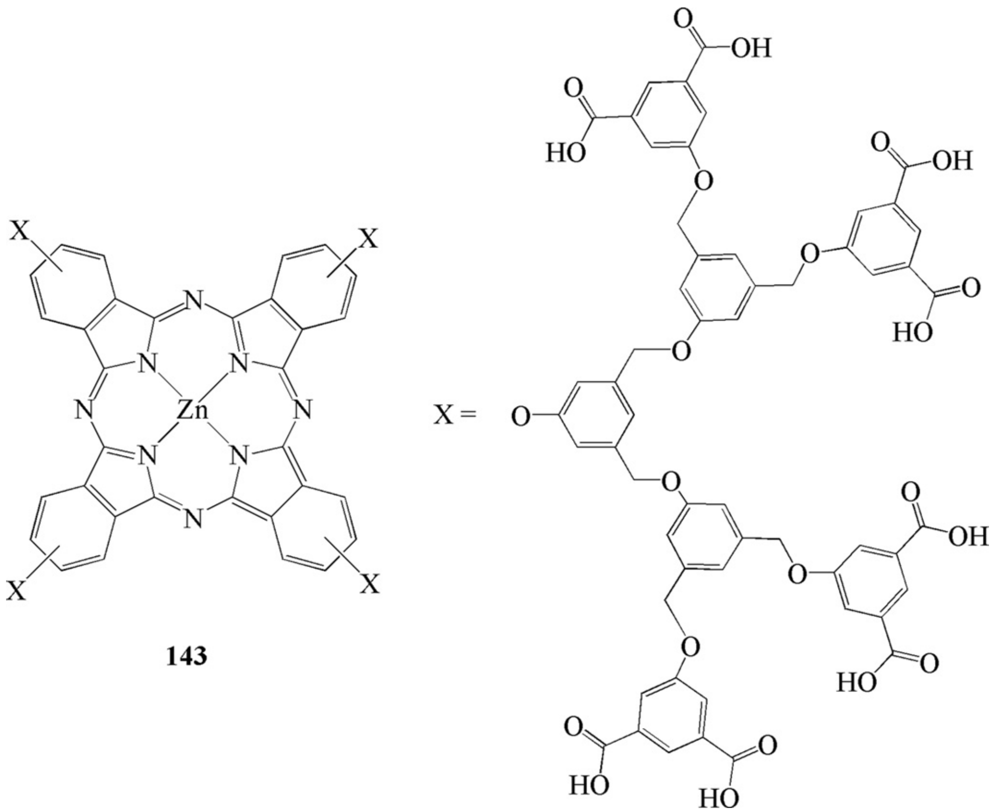

Fig. 49. Structure of phthalocyanine-containing metallodendrimer **143** [192].

copolymers, a micelle is formed. This polymeric micelle may potentially be used as a photosensitizer for photodynamic therapy (PDT), a method used for anti-cancer treatment [192,193].

Additionally, studies devoted to the preparation and analysis of redox-dendrimers have provided example models and greater insight towards electron-transfer metalloproteins due to the dendrons' ability to protect the active site and minimize the ease of its accessibility, which is similar to that of a protein [191]. Metallodendrimers can also be used in guest-host systems. For example, Tsukube and coworkers have prepared a number of unsymmetrical zinc porphyrin-containing dendrimers [194]. Dendrimer **144** is referred to as a pocket dendrimer because it contains dendritic wedges on three sides of the metalloporphyrin complex, leaving the fourth side available for guest molecules to coordinate to the metal center and form a guest-host system (**145**) (Scheme 26) [194,195].

Kimura and coworkers have prepared a number of benzyl ether dendritic azides containing a porphyrin core [196]. For example, a zinc dendritic porphyrin functionalized with benzyl ether dendrons via 1,2,3-triazole links (**146**), displayed in Fig. 50, was

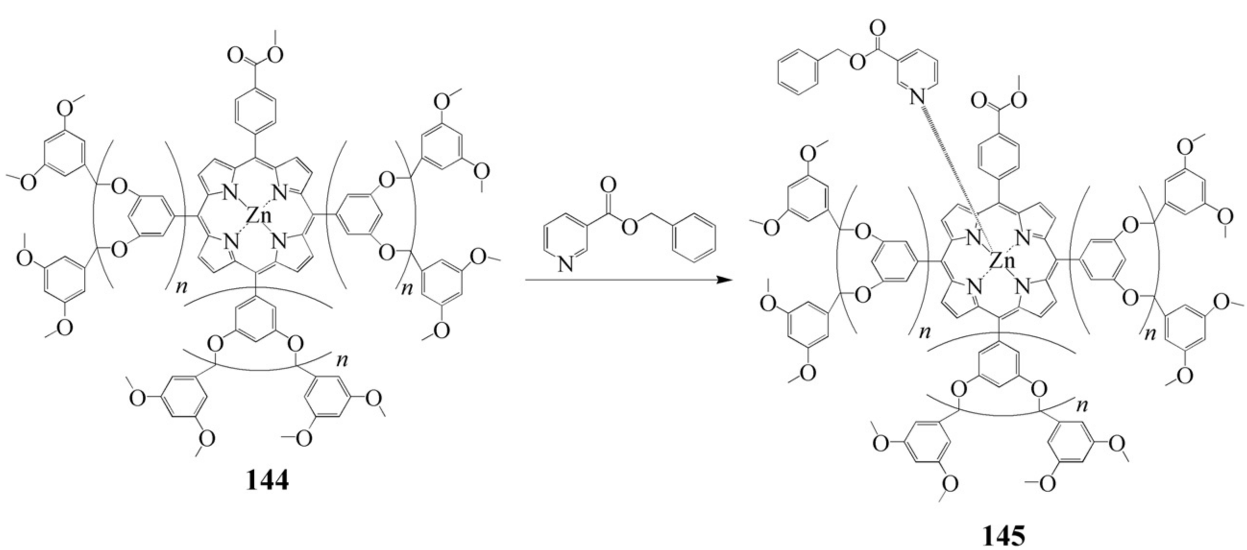

Scheme 26. Coordination of guest molecules in zinc porphyrin-based pocket dendrimers **144** [194].

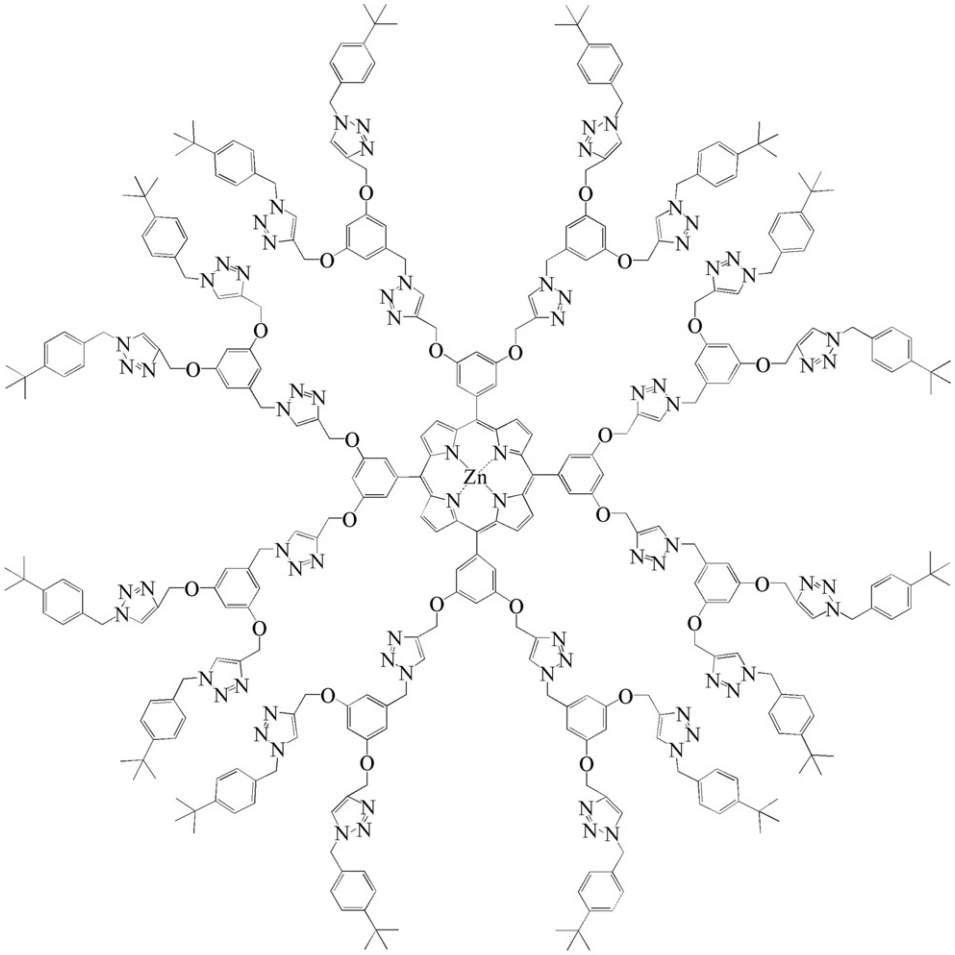

146

Fig. 50. Example of dendritic porphyrin containing benzyl ether dendrons linked via 1,2,3-triazole moieties (**146**) [196].

prepared via copper-catalyzed cycloaddition of dendritic azides and terminal acetylene moieties bound to the porphyrin core. The study showed that a stable axial ligation occurred at the zinc center, and the complex's stability was significantly influenced by the spatial position of the 1,2,3-triazole links in the dendritic porphyrin. Since the functionality of natural bio-systems is improved by three-dimensional interactions, axial ligation at the metal center and strategic design of the dendritic porphyrin may enable it to function similarly to natural biological systems including catalysis and oxygen transportation.

Okada et al. have prepared cross-shaped multiporphyrin dendrimers containing rigid backbones via Sonogashira coupling reactions [197]. This synthetic method was also applied in the preparation of a metallodendrimer containing a free-base porphyrin core, rigid conjugated phenylethynyl backbones and terminal zinc-porphyrin units (**147**) (Fig. 51) [198]. The results revealed that dendritic porphyrin **147** functions as a light-harvesting antenna and has efficient singlet-energy transfer from the terminal metalloporphyrin moieties to the free-base porphyrin core. Furthermore, the authors conclude that dendrimer **147** can serve as a building block in designing a biomimicking light-harvesting system.

Yamamoto's research group have investigated the preparation of poly(phenylazomethine) dendrimers that have the ability to coordinate metal centers based on the presence of imine groups [199–202]. For example, a zinc-tetraphenylporphyrin core has been incorporated into dendritic phenylazomethines (DPAs) [199]. The imine moieties in the fourth generation DPA with Zn-porphyrin core **148** (Fig. 52) were able to coordinate to metal ions. UV–vis titration using Fe^{2+} and Sn^{2+} coordinating ions demonstrated the stepwise radial metal ion complexation from the imines closest to the zinc-porphyrin core. Furthermore, efficient switching of the redox potential of the Zn-tetraphenylporphyrin core was observed as a result of the coordination of the metal ions.

A series of phosphorescent first generation rhenium dendrimers (**149**–**153**) (Fig. 53) were synthesized by Pu and coworkers [203]. A (1,10-phenanthroline)$Re(CO)_3Cl$ complex was used as the core and reacted with dendrons containing biphenyl moieties and terminal 2-ethylhexyloxy groups. The properties of the dendrimers were fine-tuned depending on the area of attachment and number of dendrons. For instance, dendrons bound to the two- and nine-position of the core complex exhibited higher electrochemical stability compared to the other first generation dendrimers and provided control over the electronic interactions that cause solvatochromism. UV–vis absorption studies indicated that dendrimers **152** and **153** exhibited decreased solvatochromism compared to dendrimers **149**–**151** due to the dendrons' ability to shield the metal center. Furthermore, solution processable materials were formed and demonstrated an increased photoluminescence quantum yield as a solid, compared to their dissolution in a solution. As a result of the electrochemical and photophysical properties of these materials, they may potentially be used to prepare dendrimer light-emitting diodes (DLEDs).

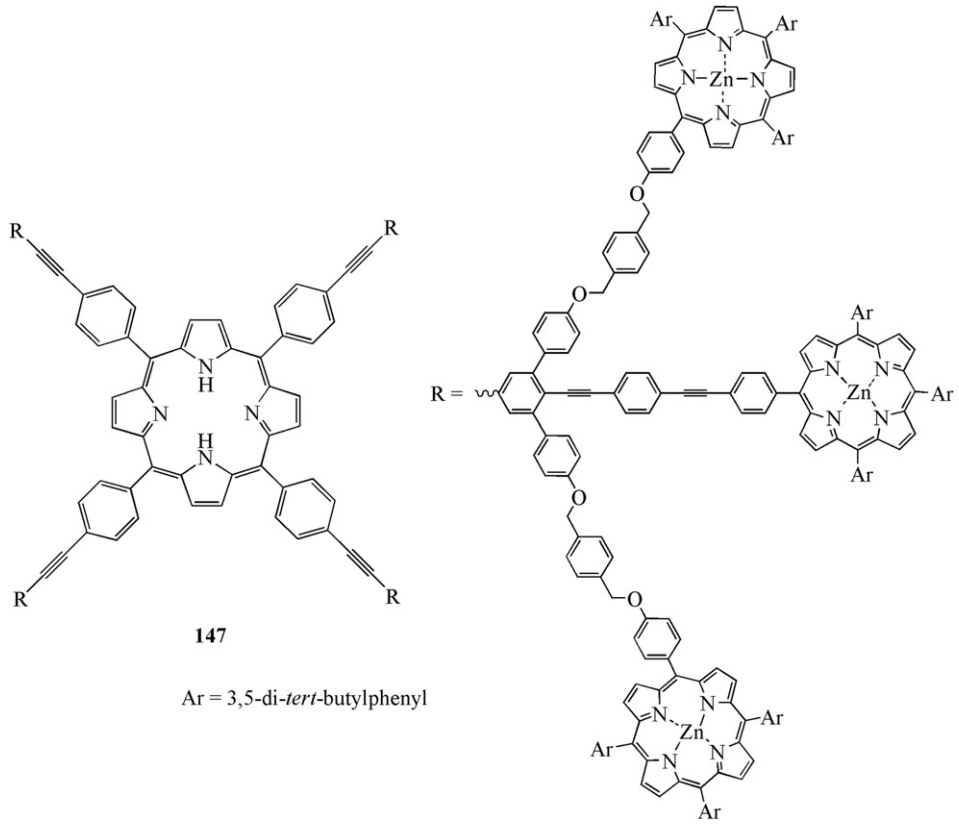

Fig. 51. Structure of a cross-shaped dendritic zinc-porphyrin system (**147**) [198].

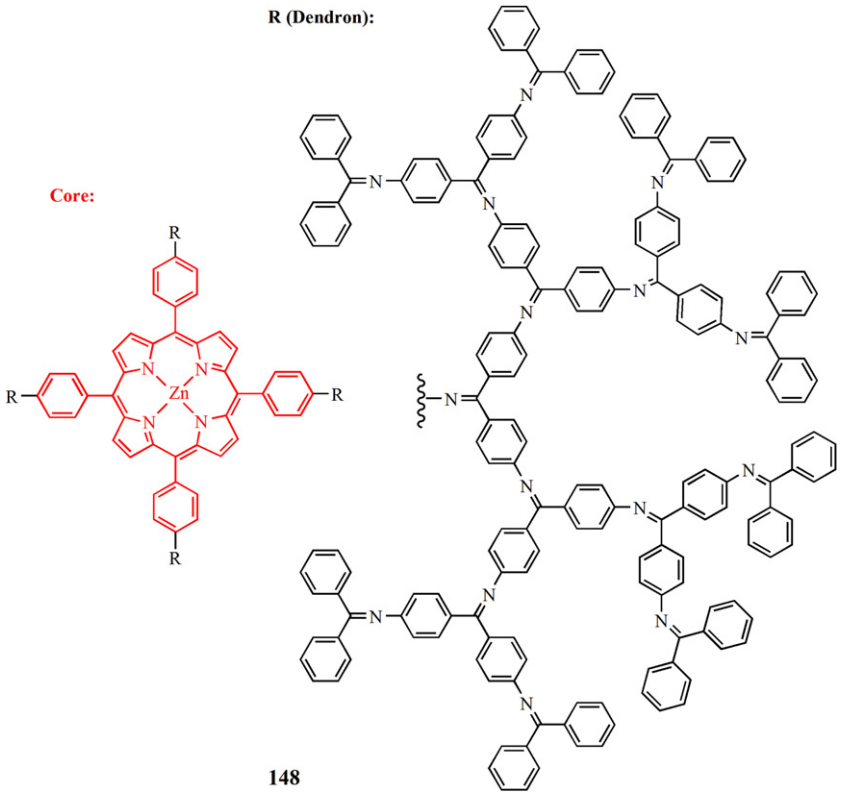

Fig. 52. Structure of fourth generation phenylazomethine dendrimer containing a zinc-tetraphenylporphyrin core **148** [199].

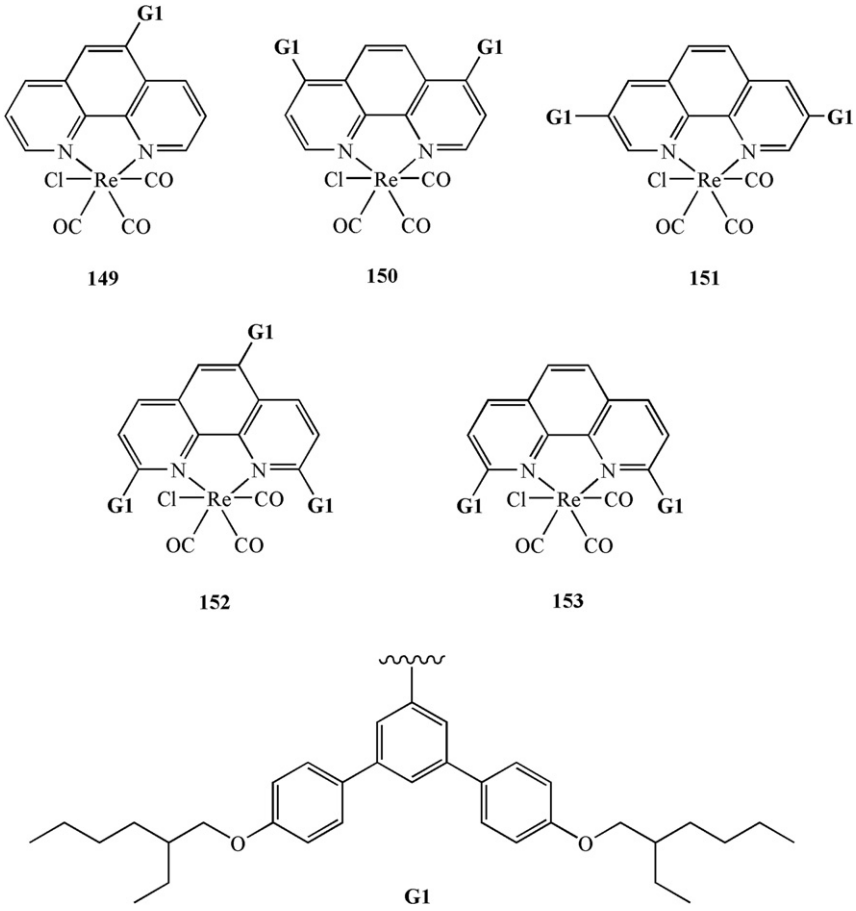

Fig. 53. Structures of phosphorescent first generation rhenium dendrimers **149**–**153** [203].

Light-emitting phosphorescent iridium dendrimers containing carbazole dendrons have been prepared by Jung and coworkers [204]. Scheme 27 illustrates the esterification of an aryl Ir-containing dendrimer core (**154**) with 4-(dimethylamino)-pyridinium-4-toluenesulfonate (DPTS) in the presence of 1,3-dicyclohexylcarbodiimide (DCC) to afford a third generation dendrimer (**155**). Thermal analysis indicated good thermal stability for all of the dendrimers, with dendrimer **155** exhibiting the highest thermal decomposition temperature (T_d = 370 °C) and glass transition temperature (T_g = 72 °C) compared to the other Ir dendrimers. The study showed that the metallodendrimers were very effective solution processable materials and could be used in applications for host-free electrophosphorescent light-emitting diodes.

The number of different studies regarding the development of synthetic routes to heterometallic dendrimers [205–207] is quite low compared to the vast research dedicated to the design of homometallic dendrimers [171,208–211]. The incorporation of two different metal centers into a dendrimer allows for interesting reactivity as well as unique electrochemical and physical properties [191]. For instance, conducting films of electrodeposited dendrimers containing both cobaltocenium and ferrocene moieties were prepared by Alonso and coworkers and used for the dual function of anaerobic and aerobic determination of glucose [212]. A different study conducted by Angurell et al. reported a controlled synthesis for a number of heterometallic carbosilane dendrimers containing two Ru–Au, three Ru–Au–Pd, or four Ru–Au–Au′–Pd metal layers (**156**) (Fig. 54) [213].

Similarly, Zamora and coworkers prepared heterometallic carbosilane-based dendrimers containing bridging silicon links with ferrocenyl and (η^6-aryl)tricarbonylchromium units via the convergent approach (**157**) (Fig. 55) [214]. Electrochemical studies indicated that the dendrimers are redox-active.

Humphrey and coworkers designed and extensively characterized π-delocalizable alkynyl-ruthenium dendritic materials which exhibit quadratic nonlinear optical (NLO) properties [215,216]. The study revealed that the observed reversible metal-centered oxidation processes were accompanied by enhanced linear optical changes. As mentioned previously, numerous studies have been conducted on ferrocenyl-containing complexes because of the advantage that ferrocene offers by combining chemical and electrochemical versatility with high thermal stability. As a result, these ferrocene-based complexes are well-suited for the synthesis of new materials that have applications in organic synthesis, materials science, and catalysis [217–223]. *Trans* configuration dendrons with terminal ferrocene units linked with styryl moieties (**158**) were attached to a free-base porphyrin core (**159**), which afforded dendrimers containing eight (**160**) and sixteen ferrocenyl terminal moieties (Scheme 28) [224].

Since azo dyes are well known for their ability to undergo *trans–cis* isomerization of the N=N moiety in response to photoirradiation [225], the inclusion of metal complexes into azo dyes can provide attractive versatile materials with unique magnetic, optical, and redox properties [225–228]. Over the years, Nishihara's and Astruc's research groups have extensively studied metallated complexes functionalized with azo dyes. For example,

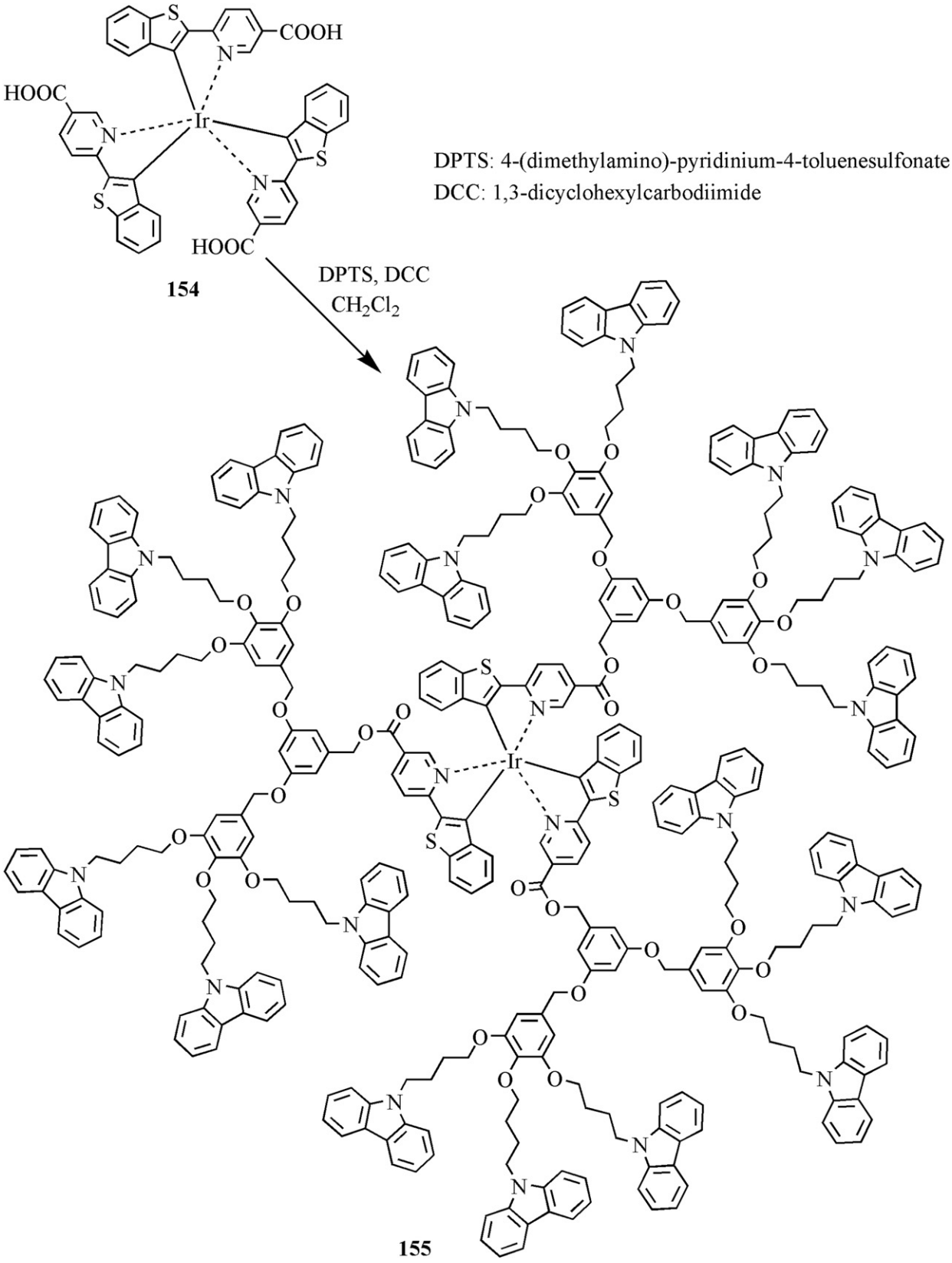

Scheme 27. Synthesis of third generation phosphorescent Ir dendrimer **155** [204].

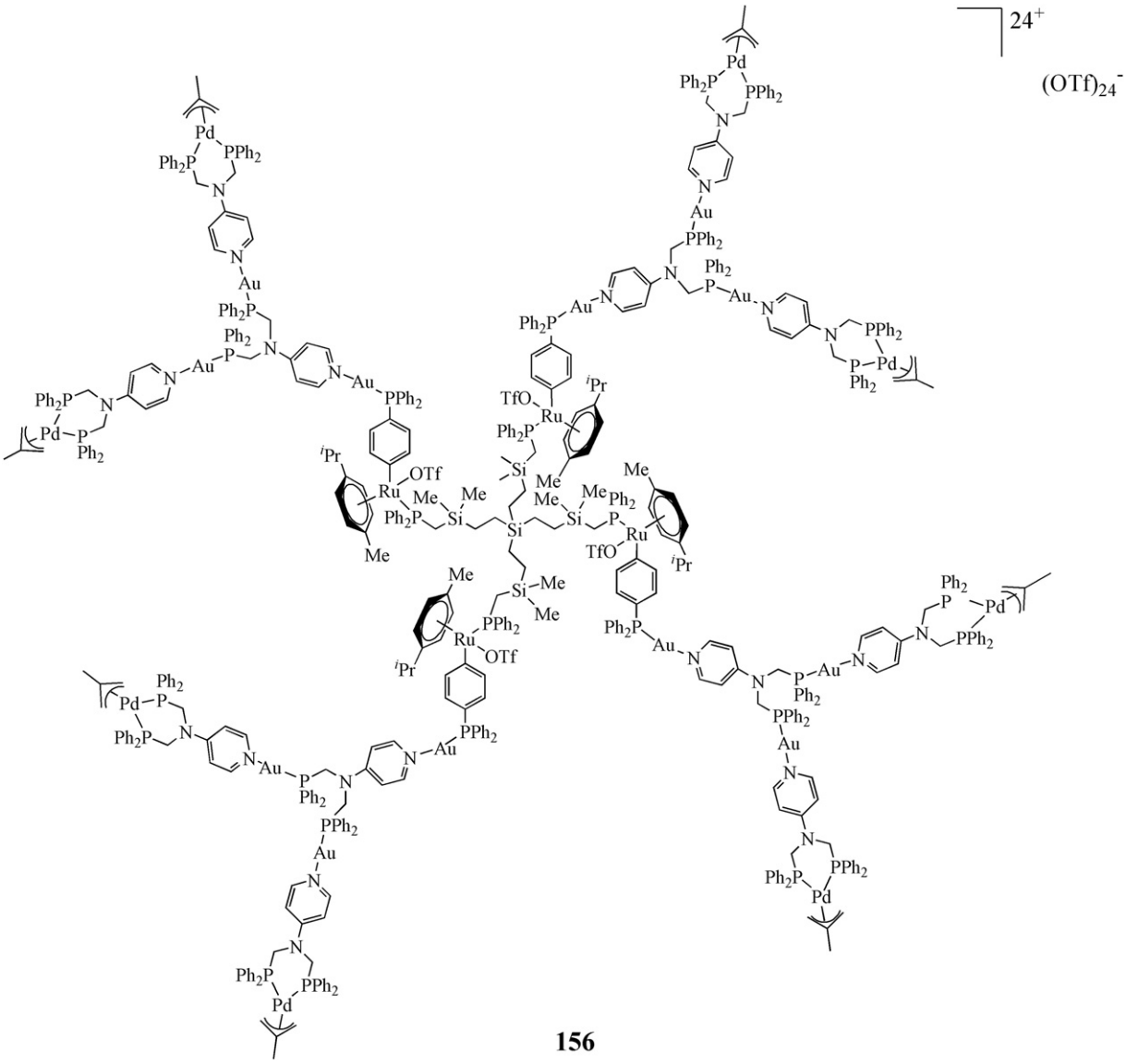

156

Fig. 54. Structure of a dendrimer containing four Ru–Au–Au–Pd metal layers (**156**) [213].

dendrimers (9mer, 27mer and 81mer) containing terminal 3-ferrocenylazobenzene moieties have been prepared [229]. Dendrimer (9mer) **161** is illustrated in Fig. 56 as an example. The study showed that these dendrimers exhibit reversible photoisomerization and photochromism under 365, 436, and 546 nm irradiation. Upon *cis–trans* isomerism of the azobenzene moieties, the size and structure of the dendrimer changes [230]. Moreover, upon photoisomerization, electrochemical studies indicate that as the dendrimer generations increase, the diffusion coefficient decreases. On the contrary, the diffusion coefficient increases for the smaller generation dendrimers and varies in size depending on *cis–trans* isomerization.

Tang and coworkers have prepared and investigated hyperbranched polyphenylenes functionalized with ferrocene units (***hb*-P1**) (Fig. 57) [231]. Synthesis of ***hb*-P1** occurred via polymerization of metallated diyne, *E*-1-[2-(2,5-diethynylphenyl)vinyl]ferrocene, using rhodium- and ruthenium-based catalysts. The resulting high molecular weight (as high as $\sim 1.4 \times 10^5$ g/mol) hyperbranched polyphenylenes ***hb*-P1** exhibited high thermal stability with initial polymer weight loss above 300 °C, according to thermogravimetric analysis. Furthermore, cyclic voltammetry reveals redox activity in the ferrocene-containing polymers ***hb*-P1**, showing a single oxidation wave between −1.0 and 1.0 V, although complete reversibility was not observed. In addition to the incorporation of ferrocene moieties in the polyphenylenes, cobalt carbonyls were complexed to the branched polymers ***hb*-P1** to further metallate them. The homometallic ***hb*-P1** and its heterometallic cobalt complex was pyrolized under nitrogen at 1000 °C in a TGA furnace, resulting in magnetizable ceramics. The study indicated that complexation of the cobalt moieties significantly increased the hyperbranched polymers' magnetizability (M_s up to ~83 emu/g). The authors suggest that these metallopolymers demonstrate excellent potential use as functional materials in high-tech applications.

Star-shaped organoiron macromolecules functionalized with azo chromophores have recently been synthesized [232]. Convergent and divergent methods were employed by reacting a variety of azo dyes and iron-coordinated branches with multifunctional cores. For example, octairon oligomer **162** (Fig. 58) displayed a maximum wavelength at 427 nm and when exposed to an acidic

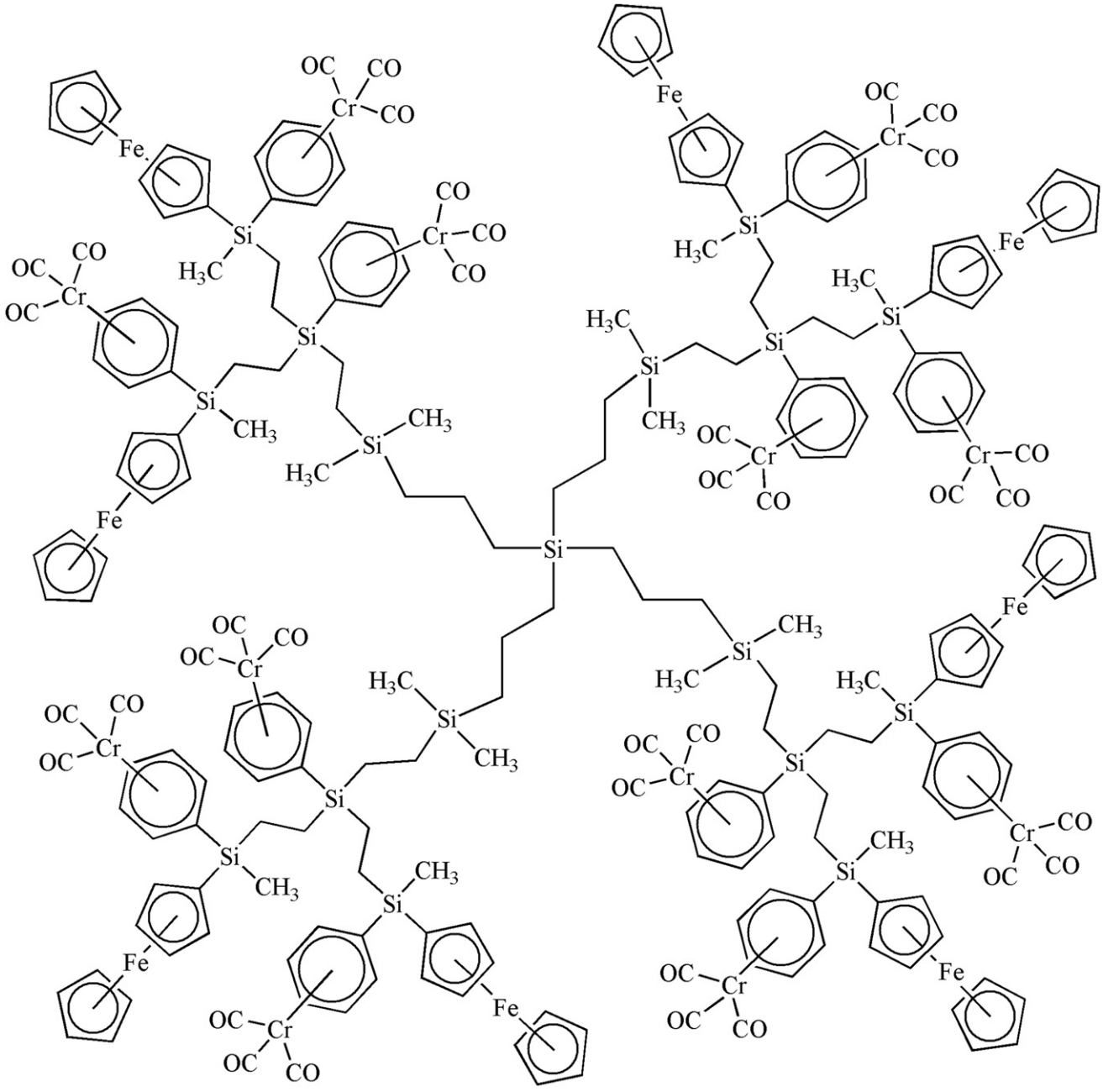

157

Fig. 55. Structure of carbosilane ferrocene-containing dendrimer (**157**) [214].

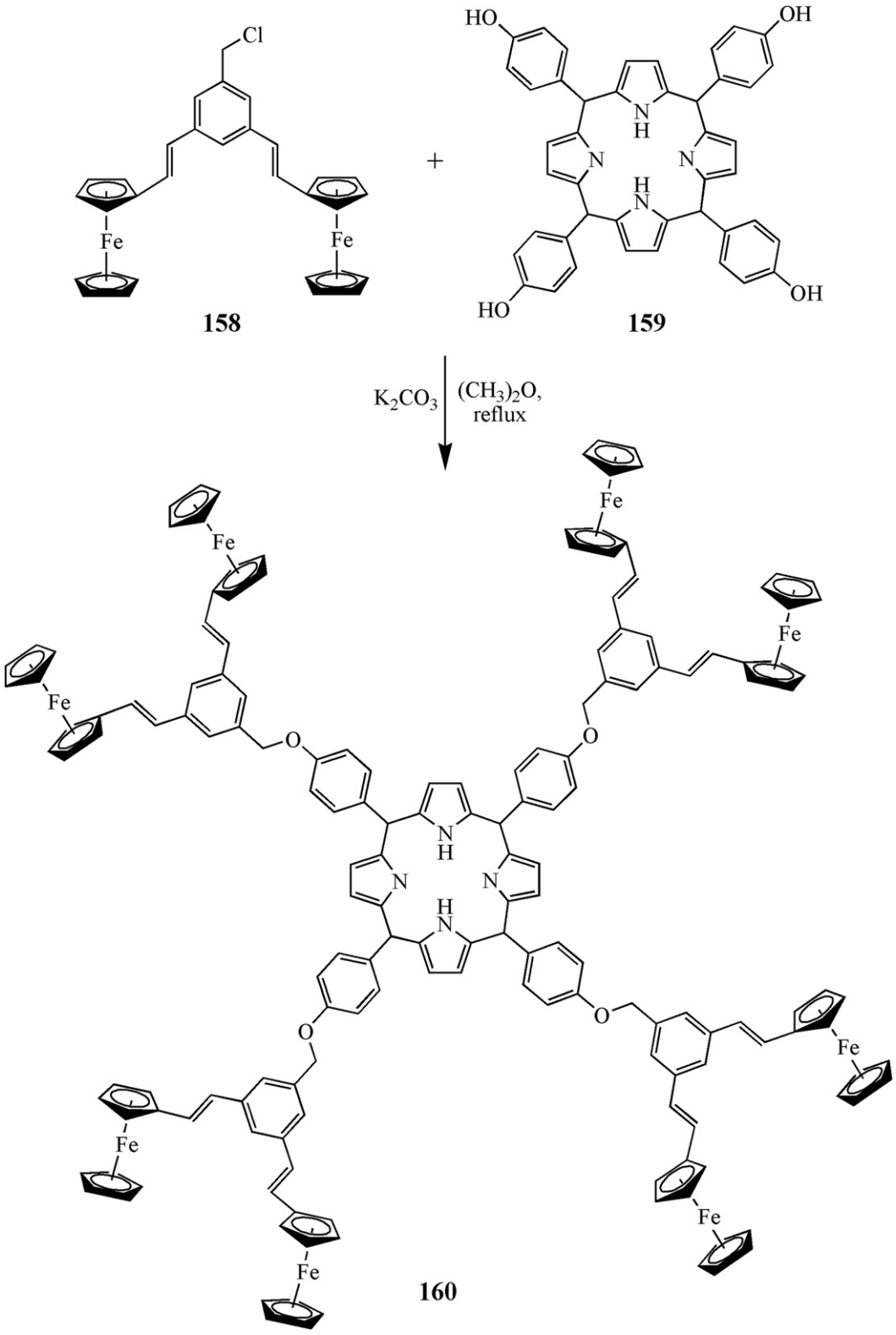

Scheme 28. Synthesis of dendritic porphyrin containing terminal ferrocene moieties **160** [224].

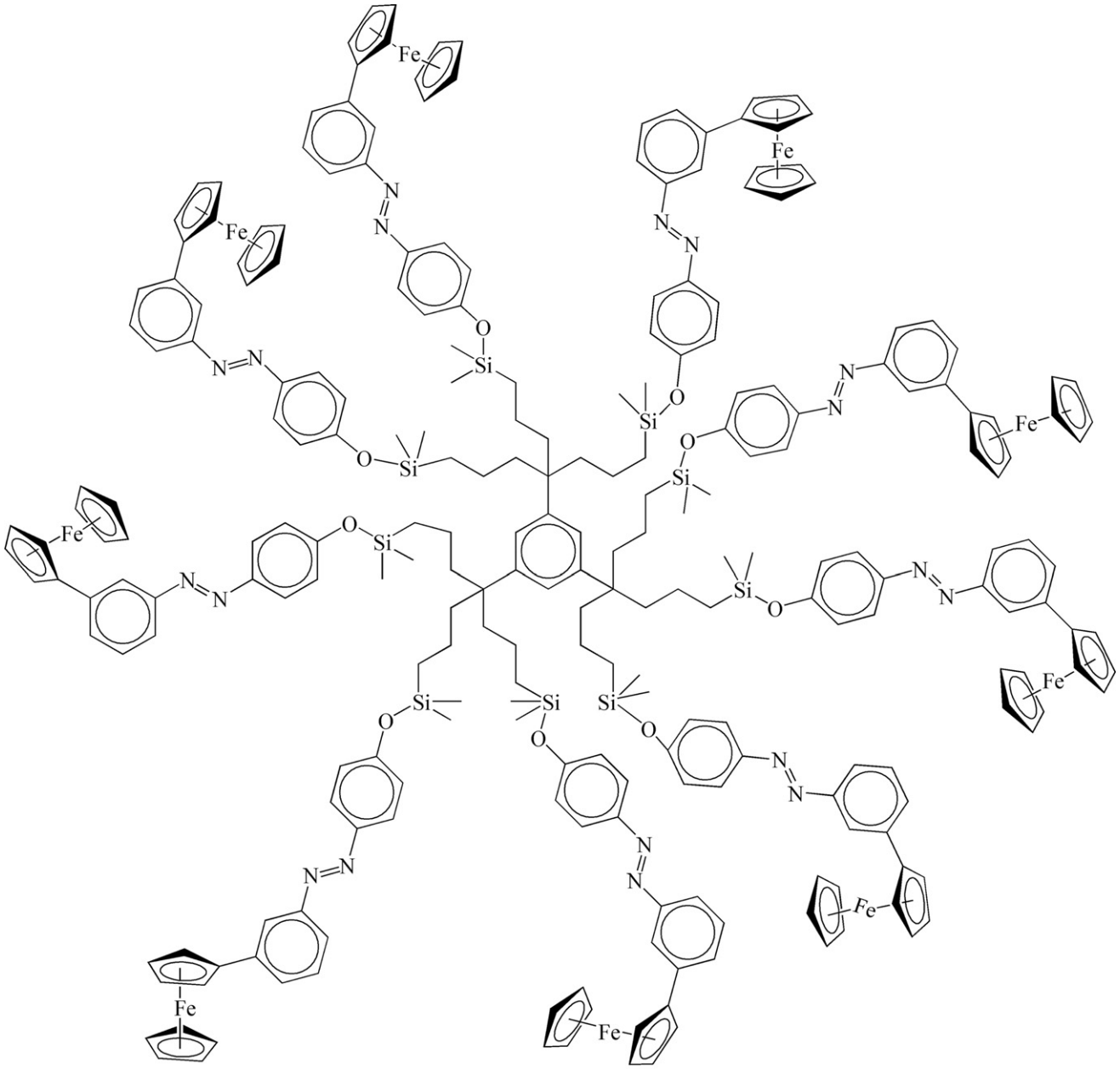

161

Fig. 56. Structure of ferrocene-containing dendrimer (9mer) **161** functionalized with terminal 3-ferrocenylazobenzene moieties [229].

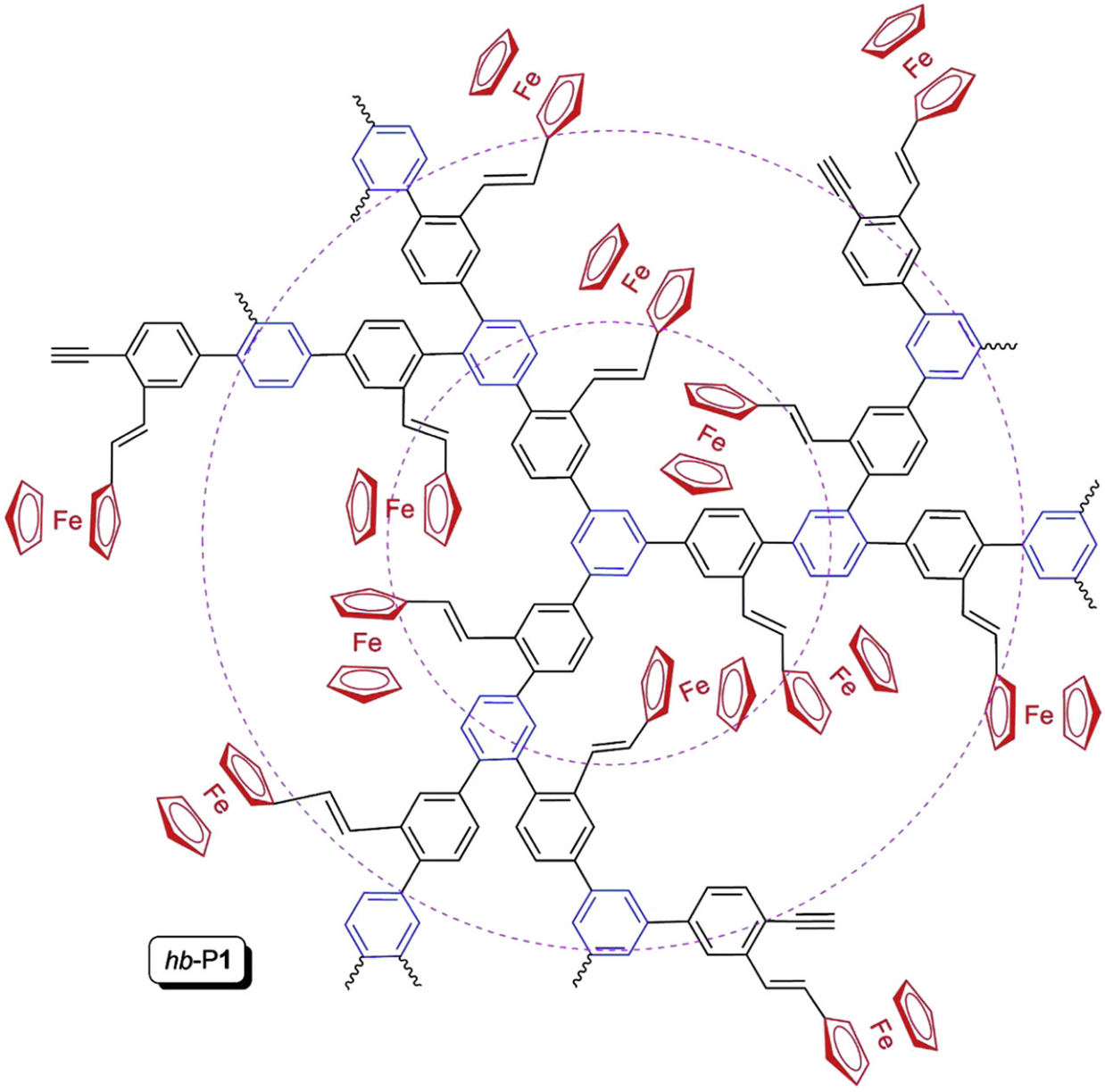

Fig. 57. Structure of hyperbranched polyphenylene (***hb*-P1**) containing ferrocenyl moieties bound to the repeat branches as pendant groups [231]. Adapted with permission from Macromolecules 2010, 43, Shi J, Jim CJW, Mahtab F, Liu J, Lam JWY, Sung HHY, Williams ID, Dong Y, Tang BZ, "Ferrocene-functionalized hyperbranched polyphenylenes: synthesis, redox activity, light refraction, transition-metal complexation, and precursors to magnetic ceramics", 680–90. Copyright (2005) American Chemical Society.

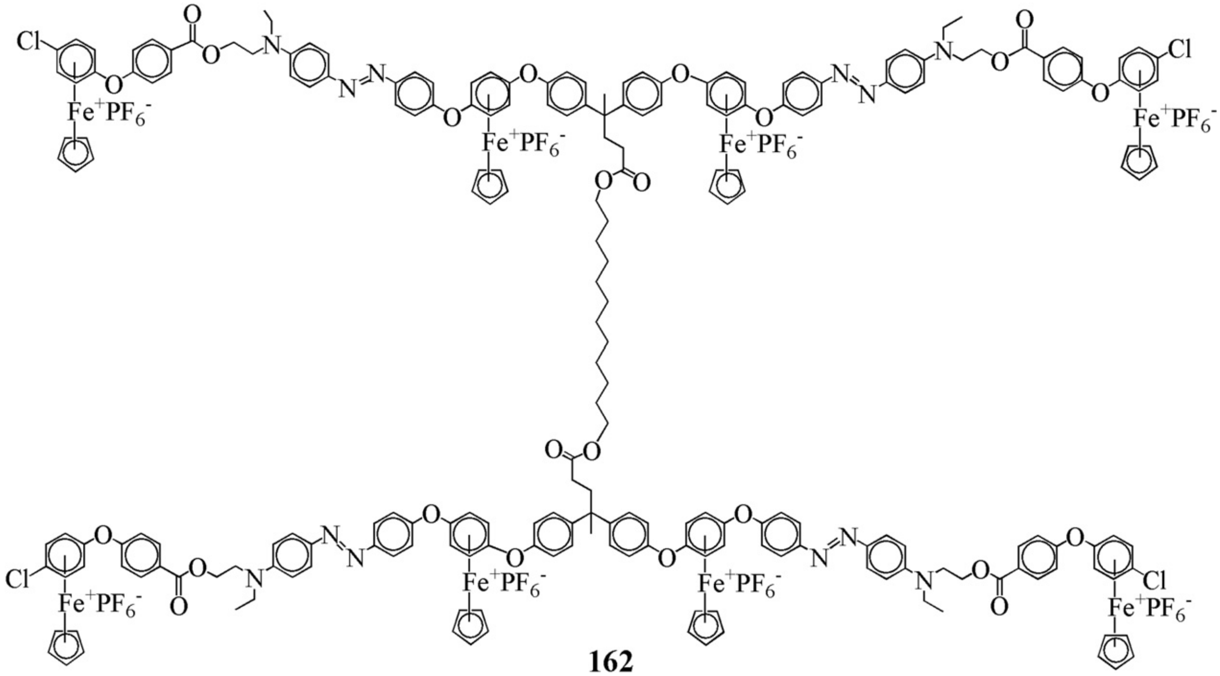

162

Fig. 58. Structure of four-arm organoiron oligomer containing arylazo dyes **162** [232].

media, the wavelength maximum shifted to 558 nm. Additionally, electrochemical studies showed a single reversible redox wave of the octairon oligomer **162** which corresponded to the conversion from 18- to 19-electron iron centers. The cyclic voltammogram of oligomer **162** displayed a redox couple at $E_{1/2} = -1.53$ V (scan rate $\gamma = 0.1$ V s^{-1}) indicating a reduction of the cationic iron center and an oxidation of the azo chromophore, which was displayed at $E_{pa} = 0.7$ V. Furthermore, as the temperature increased, the reversibility of the redox couple of oligomer **162** decreased. The results showed that the reduction process became irreversible at room temperature.

Cationic organoiron-containing hyperbranched star-shaped polymers were prepared by Abd-El-Aziz and coworkers [233]. Synthesis occurred via nucleophilic aromatic substitution of trichloro-substituted organoiron-containing core **163** with aromatic diols or dithols (**164**) (Scheme 29). The resulting hyperbranched polymers containing either sulfur or ether bridges had low viscosities ranging between 0.175 dl/g to 0.300 dl/g. Thermal studies indicate thermal degradation of the cationic cyclopentadienyliron moieties occurs between 230 °C and 280 °C and that the polymeric backbone degrades between 390 °C and 567 °C.

First and second generation rhodium(I) poly(propyleneimine) dendrimers with either chelating bidentate iminophosphine or monodentate iminopyridyl ligands were prepared by Moss and coworkers [234]. The metallodendrimers' catalytic efficiency in the hydroformylation of 1-octene was investigated and demonstrated

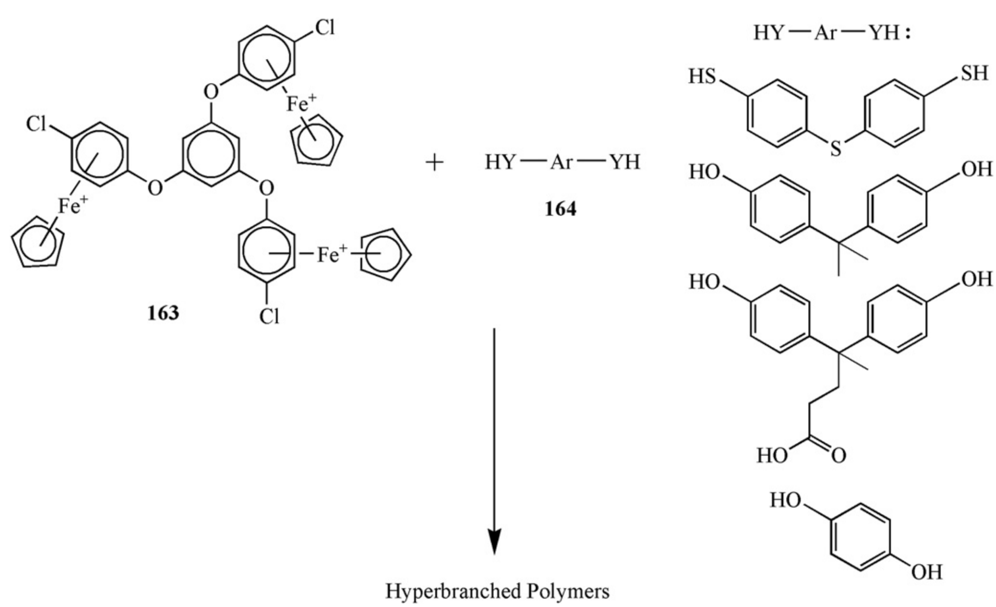

Scheme 29. Synthesis of organoiron-containing hyperbranched polymers [233].

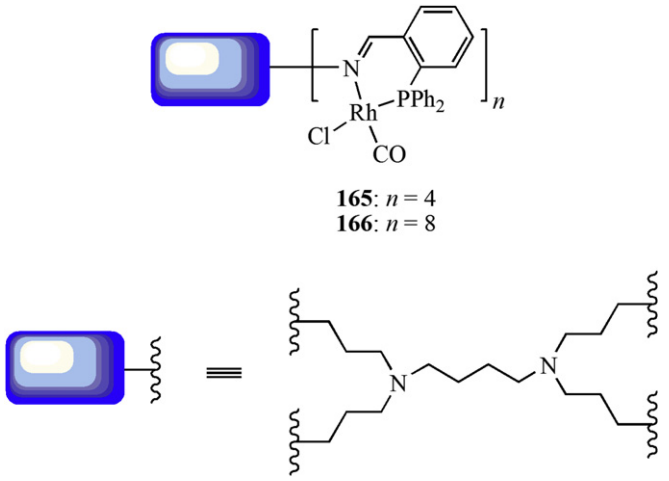

Fig. 59. Structure of rhenium dendrimers containing chelating, bidentate iminophosphine ligands (**165**, **166**) [234].

high substrate conversions with mild reaction conditions. The Rh dendrimers **165** and **166** with bidentate iminophosphine ligands (Fig. 59) exhibited variations in the reaction rate. For the second generation metallodendrimer (**166**), an increased reaction rate was observed compared to the first generation metallodendrimer (**165**), with 80% of the substrate reacting after 2 h. These metallodendrimers show excellent potential for their use in metal-catalyzed hydroformylation of alkenes.

7. Conclusion

This feature article highlights the past five years and surveys the synthesis, properties, and applications of some of these new polymeric materials. Transition metals included into macromolecules continue to be a subject of interest due to their exceptional physical and chemical properties. Interest in new synthetic techniques for these materials and the discovery of their boundless potential applications has led to continuous growth in the fields of chemistry, physics, medicine and engineering. Many of these macromolecules have photoactive, magnetic, and electroactive properties and can also be used for potential drug delivery systems. While there has been an exponential increase in the development of metal-containing macromolecules, especially in the past two decades, there are still tremendous opportunities in the search for new materials with well tailored applications.

Acknowledgements

Financial support provided by the Natural Sciences Engineering and Research Council of Canada (NSERC) is gratefully acknowledged.

References

[1] Rehahn M. Acta Polym 1998;49:201–24.
[2] Nguyen P, Gómez-Elipe P, Manners I. Chem Rev 1999;99:1515–48.
[3] Pickup PG. Mater J Chem 1999;9:1641–53.
[4] Abd-El-Aziz AS, Bernardin S. Coord Chem Rev 2000;203:219–67.
[5] Kulbaba K, Manners I. Macromol Rapid Commun 2001;22:711–24.
[6] Astruc D, Chardac F. Chem Rev 2001;101:2991–3023.
[7] Abd-El-Aziz AS, Todd EK. Polym News 2001;26:5–13.
[8] Eddaoudi M, Moler DB, Li H, Chen B, Reineke TM, O'Keeffe M, et al. Acc Chem Res 2001;34:319–30.
[9] Abd-El-Aziz AS. Coord Chem Rev 2002;233-234:177–91.
[10] James SL. Chem Soc Rev 2003;32:276–88.
[11] Janiak C. Dalton Trans 2003:2781–804.
[12] Long NJ, Williams CK. Angew Chem Int Ed 2003;42:2586–617.
[13] Kitagawa S, Kitaura R, Noro S-I. Angew Chem Int Ed 2004;43:2334–75.
[14] Hofmeier H, Schubert US. Chem Soc Rev 2004;33:373–99.
[15] Andres PR, Schubert US. Adv Mater 2004;16:1043–68.
[16] Rowsell JLC, Yaghi OM. Micropor Mesopor Mat 2004;73:3–14.
[17] Maspoch D, Ruiz-Molina D, Veciana J. J Mater Chem 2004;14:2713–23.
[18] Robin AY, Fromm KM. Coord Chem Rev 2006;250:2127–57.
[19] Férey G. Chem Soc Rev 2008;37:191–214.
[20] Spokoyny AM, Kim D, Sumrein A, Mirkin CA. Chem Soc Rev 2009;38:1218–27.
[21] Whittell GR, Hager MD, Schubert US, Manners I. Nat Mater 2011;10:176–88.
[22] Abd-El-Aziz AS, Shipman PO, Boden BN, McNeil WS. Prog Polym Sci 2010;35:714–836.
[23] Abd-El-Aziz AS, Carraher Jr CE, Pittman Jr CU, Sheets J, Zeldin M. Macromolecules containing metal and metal-like elements. New York: Wiley-Interscience, John Wiley & Sons, Inc; 2003.
[24] Abd-El-Aziz AS. Encyclopedia of polymer science and technology. 3rd ed. New York: Wiley-Interscience, John Wiley & Sons, Inc; 2002.
[25] Abd-El-Aziz AS, Carraher Jr CE. Macromolecules containing metal and metal-like elements. New York: Wiley-Interscience, John Wiley & Sons, Inc; 2006.
[26] Carraher Jr CE, Pittman Jr CU, Abd-El-Aziz AS. Macromolecules containing metal and metal-like elements. New York: Wiley-Interscience, John Wiley & Sons, Inc; 2005.
[27] Abd-El-Aziz AS. Macromol Rapid Commun 2002;23:995–1031.
[28] Manners I. J Polym Sci Part A Polym Chem 2002;40:179–91.
[29] Manners I. Angew Chem Int Ed 1996;35:1602–21.
[30] MacLachlan MJ, Manners I, Ozin GA. J Adv Mater 2000;12:675–81.
[31] Nishihara H, Nalwa HS. Handbook of organic conductive molecules and polymers. New York: Wiley-Interscience, John Wiley & Sons, Inc; 1997.
[32] Allcock HR, Desorcie JL, Riding GH. Polyhedron 1987;6:119–57.
[33] Long NJ, Williams CK. Angew Chem Int Ed 2003;42:2586.
[34] Wong W-Y, Wang X-Z, He Z, Djurišić AB, Yip C-T, Cheung K-Y, et al. Nat Mater 2007;6:521–7.
[35] Whittall IR, McDonagh AM, Humphrey MG, Samoc M. Adv Organomet Chem 1998;42:291–362 [and references therein].
[36] Wong W-Y. J Inorg Organomet Polym Mater 2005;15:197–219.
[37] Zhou GJ, Wong WY, Ye C, Lin Z. Adv Funct Mater 2007;17:963–75.
[38] Wong W-Y, Guo Y, Ho C-L. J Inorg Organomet Polym Mater 2009;19:46–54.
[39] Wong W-Y, Wong C-K, Poon S-Y, Lee AW-M, Mo T, Wei X. Macromol Rapid Commun 2005;26:376–80 [and references therein].
[40] Mei J, Ogawa K, Kim Y-G, Heston NC, Arenas DJ, Nasrollahi Z, et al. ACS Appl Mater Interfaces 2009;1:150–61.
[41] Wu P-T, Bull T, Kim FS, Luscombe CK, Jenekhe SA. Macromolecules 2009;42:671–81.
[42] Qin C, Wong W-Y, Wang L. Macromolecules 2011;44:483–9.
[43] Dong Q, Li G, Ho C-L, Faisal M, Leung C-W, Pong PW-T, et al. Adv Mater 2012;24:1034–40.
[44] Korshak VV, Sosin SL, Alekseeva VP. Dokl Akad Nauk SSSR 1960;132:360–5.
[45] Nesmeyanov AN, Korshak VV, Voevodskii NS, Kochetkova SL, Sosin SL, Materikova RB, et al. Dokl Akad Nauk SSSR 1961;137:1370–5.
[46] Rosenberg H, Neuse EW. J Organomet Chem 1966;6:76–85.
[47] Dzhardimalieva GI, Pomogailo SI, Golubeva ND, Pomogailo AD. Macromol Symp 2011;304:101–8 [and references therein].
[48] Chadha P, Ragogna PJ. Chem Commun 2011;47:5301–3.
[49] Bartole-Scott A, Braunschweig H, Kupfer T, Lutz M, Manners I, Nguyen T-L, et al. Chem Eur J 2006;12:1266–73.
[50] Tamm M, Kunst A, Herdtweck E. Chem Commun 2005:1729–31.

[51] Braunschweig H, Adams CJ, Kupfer T, Manners I, Richardson RM, Whittell GR. Angew Chem Int Ed 2008;47:3826–9.
[52] Chan WY, Lough AJ, Manners I. Organometallics 2007;26:1217–25.
[53] Patra SK, Whittell GR, Nagiah S, Ho C-L, Wong W-Y, Manners I. Chem Eur J 2010;16:3240–50.
[54] Ieong NS, Manners I. Macromol Chem Phys 2009;210:1080–6.
[55] Herbert DE, Mayer UFJ, Gilroy JB, Lopez-Gomez MJ, Lough AJ, Charmant JPH, et al. Chem Eur J 2009;15:12234–46.
[56] Masson G, Lough AJ, Manners I. Macromolecules 2008;41:539–47.
[57] Chandrasekhar V, Thirumoorthi R. Dalton Trans 2010;39:2684–91.
[58] Dong H, Qin A, Jim CKW, Lam JWY, Hussler M, Tang BZ. J Inorg Organomet Polym Mater 2008;18:201–5.
[59] Grubbs RB. J Polym Sci Part A Polym Chem 2005;43:4323–36.
[60] Qin Y, Cui C, Jäkle F. Macromolecules 2008;41:2972–4.
[61] Ren L, Hardy CG, Tang C. J Am Chem Soc 2010;132:8874–5 [and references therein].
[62] Heilmann JB, Schiebitz M, Qin Y, Sundararaman A, Jäkle F, Kretz T, et al. Angew Chem Int Ed 2006;45:920–5 [and references therein].
[63] Chan WK. Coord Chem Rev 2007;251:2104–18 [and references therein].
[64] Wong W-Y, Harvey PD. Macromol Rapid Commun 2010;31:671–713 [and references therein].
[65] Fukumoto H, Yamane K, Kase Y, Yamamoto T. Macromolecules 2010;43:10366–75.
[66] Holliday BJ, Swager TM. Chem Commun 2005:23–36 [and references therein].
[67] Herbert DE, Mayer UFJ, Manners I. Angew Chem Int Ed 2007;46:5060–81 [and references therein].
[68] Bellas V, Rehahn M. Angew Chem Int Ed 2007;46:5082–104 [and references therein].
[69] Williams KA, Boydston AJ, Bielawski CW. Chem Soc Rev 2007;36:729–44.
[70] Vogel U, Lough AJ, Manners I. Angew Chem Int Ed 2004;43:3321–5.
[71] Mayer UFJ, Gilroy JB, O'Hare D, Manners I. J Am Chem Soc 2009;131:10382–3.
[72] Braunschweig H, Kupfer T, Lutz M, Radacki K, Seeler F, Sigritz R. Angew Chem Int Ed 2006;45:8048–51.
[73] Braunschweig H, Kupfer T. Acc Chem Res 2010;43:455–65.
[74] Braunschweig H, Fuß M, Mohapatra SK, Kraft K, Kupfer T, Lang M, et al. Chem Eur J 2010;16:11732–43.
[75] Schachner JA, Lund CL, Quail JW, Müller J. Organometallics 2005;24:4483–8.
[76] Lund CL, Schachner JA, Quail JW, Müller J. Organometallics 2006;25:5817–23.
[77] Bagh B, Gilroy JB, Staubitz A, Müller J. J Am Chem Soc 2010;132:1794–5.
[78] Sharma HK, Cervantes-Lee F, Pannell KH. J Am Chem Soc 2004;126:1326–7.
[79] Tamm M, Kunst A, Bannenberg T, Randoll S, Jones PG. Organometallics 2007;26:417–24.
[80] Chadha P, Dutton JL, Sgro MJ, Ragogna PJ. Organometallics 2007;26:6063–5.
[81] Gilroy JB, Patra SK, Mitchels JM, Winnik MA, Manners I. Angew Chem Int Ed 2011;50:5851–5.
[82] He F, Gädt T, Manners I, Winnik MA. J Am Chem Soc 2011;133:9095–103.
[83] Ahmed R, Priimagi A, Faul CFJ, Manners I. Adv Mater 2012;24:926–31.
[84] Abd-El-Aziz AS, Todd EK, Okasha RM, Shipman PO, Wood TE. Macromolecules 2005;38:9411–9.
[85] Shultz GV, Tyler DR. J Inorg Organomet Polym 2009;19:423–35 [and references therein].
[86] Moran M, Pascual MC, Cuadrado I, Losada J. Organometallics 1993;12:811–22.
[87] Chan WY, Clendenning SB, Berenbaum A, Lough AJ, Aouba S, Ruda HE, et al. J Am Chem Soc 2005;127:1765–72.
[88] Abd-El-Aziz AS, Winram DJ, Shipman PO, Bichler L. Macromol Rapid Commun 2010;31:1992–7.
[89] Daglen BC, Harris JD, Tyler DR. J Inorg Organomet Polym Mater 2007;17:267–74.
[90] Daglen BC, Tyler DR. J Inorg Organomet Polym Mater 2009;19:91–7.
[91] Shultz GV, Berryman OB, Zakharov LN, Tyler DR. J Inorg Organomet Polym Mater 2008;18:149–54.
[92] Brady SE, Shultz GV, Tyler DR. J Inorg Organomet Polym 2010;20:511–8.
[93] Randles MD, Lucas NT, Cifuentes MP, Humphrey MG, Smith MK, Willis AC, et al. Macromolecules 2007;40:7807–18.
[94] Si TS, Koo SM. Polym Int 2005;54:891–6.
[95] Uemura K, Ebihara M. Inorg Chem 2011;50:7919–21.
[96] Lucht BL, Buretea MA, Tilley TD. Organometallics 2000;19:3469–75.
[97] Zhou W-M, Tomita I. Polym Bull 2008;61:603–9.
[98] Zhou W-M, Tomita I. J Inorg Organomet Polym Mater 2009;19:113–7.
[99] Allard N, Aïch RB, Gendron D, Boudreault P-LT, Tessier C, Alem S, et al. Macromolecules 2010;43:2328–33.
[100] Tam WY, Mak CSK, Ng AMC, Djurišić AB. Macromol Rapid Commun 2009;30:622–6.
[101] Hardy CG, Ren L, Tamboue TC, Tang C. J Polym Sci 2011;49:1409–20.
[102] Brettar J, Bürgi T, Donnio B, Guillon D, Klappert R, Scharf T, et al. Adv Funct Mater 2006;16:260–7.
[103] McQuillin FJ, Parker DG, Stephenson GR. Transition metal organometallics for organic synthesis. Cambridge: Cambridge University Press; 1991. p. 429.
[104] McDaniel KF. In: Abel EW, Stone FGA, Wilkinson G, editors. Comprehensive organometallic chemistry, vol. 6. Oxford: Pergamon; 1995. p. 93.
[105] Semmelhack MF. In: Abel EW, Stone FGA, Wilkinson G, editors. Comprehensive organometallic chemistry, vol. 12. Oxford: Pergamon; 1995. p. 979.
[106] Rose-Munch F, Gagliardini V, Renard C, Rose E. Coord Chem Rev 1998;178–180:249–68.
[107] Pike RD, Sweigart DA. Coord Chem Rev 1999;187:183–222.
[108] Astruc D. Chimie Organométallique. Les Ulis, France: EDP Sciences; 2000. p. 111.
[109] Rose-Munch F, Rose E. Eur J Inorg Chem 2002;2002(6):1269–83.
[110] Rose-Munch F, Rose E. In: Astruc D, editor. Modern arene chemistry. Weinheim: Wiley-VCH; 2002. p. 368.
[111] Pape AR, Kaliappan KP, Kündig EP. Chem Rev 2000;100:2917–40.
[112] Bernardinelli G, Gillet S, Kündig EP, Ronggang L, Ripa A, Saudan L. Synthesis 2001;13:2040–54.
[113] Abd-El-Aziz AS, Manners I. J Inorg Organomet Polym Mater 2005;15:157–95.
[114] Abd-El-Aziz AS, Pereira NM, Boraie W, Todd EK, Afifi TH, Budakowski WR, et al. J Inorg Organomet Polym Mater 2006;15:497–509.
[115] Abd-El-Aziz AS, Todd EK. Coord Chem Rev 2003;246:3–52.
[116] Abd-El-Aziz AS, Elmayergi B, Asher B, Afifi TH, Friesen K. Inorg Chim Acta 2006;359:3007–13.
[117] Ren L, Hardy CG, Tang S, Doxie DB, Hamidi N, Tang C. Macromolecules 2010;43:9304–10 [and references therein].
[118] Harvey PD, Stern C, Gros CP, Guilard R. J Inorg Biochem 2008;102:395–405.
[119] Masciocchi N, Pettinari C, Pettinari R, Nicola CD, Albisetti AF. Inorg Chim Acta 2010;363:3733–41.
[120] Karabach YY, Kirillov AM, Guedes da Silva MFC, Kopylovich MN, Pombeiro AJL. Cryst Growth Des 2006;6:2200–3.
[121] Karabach YY, Kirillov AM, Haukka M, Kopylovich MN, Pombeiro AJL. J Inorg Biochem 2008;102:1190–4.
[122] Llabrés i Xamena FX, Casanova O, Galiasso Tailleur R, Garcia H, Corma A. J Catal 2008;255:220–7.
[123] Lu Y, Tonigold M, Bredenkötter B, Volkmer D, Hitzbleck J, Langstein G. Z Anorg Allg Chem 2008;634:2411–7.
[124] Xiao B, Hou H, Fan Y. J Mol Catal A – Chem 2008;288:42–51.
[125] Chen C-Y, Cheng P-Y, Wu H-H, Lee HM. Inorg Chem 2007;46:5691–9.
[126] Cheng P-Y, Chen C-Y, Lee HM. Inorg Chim Acta 2009;362:1840–6.
[127] Roesky HW, Andruh M. Coord Chem Rev 2003;236:91–119.
[128] Zhang J-P, Lin Y-Y, Huang X-C, Chen X-M. Chem Commun 2005:1258–60.
[129] Chien CH, Liao SF, Wu CH, Shu CF, Chang SY, Chi Y, et al. Adv Funct Mater 2008;18:1430–9.
[130] Xie Z, Wang C, deKrafft KE, Lin W. J Am Chem Soc 2011;133:2056–9 [and references therein].
[131] Tang W-S, Lu X-X, Wong KM-C, Yam VW-W. J Mat Chem 2005;15:2714–20.
[132] Wild A, Winter A, Schlütter F, Schubert US. Chem Soc Rev 2011;40:1459–511.
[133] Balzani V, Campagna S, editors. Photochemistry and photophysics of coordination compounds. Berlin: Springer-Verlag; 2007.
[134] Duprez V, Biancardo M, Spanggaard H, Krebs FC. Macromolecules 2005;38:10436–48.
[135] Dobrawa R, Würthner F. J Polym Sci Part A Polym Chem 2005;43:4981–95.
[136] Song P, Sun S-G, Zhou P-W, Liu J-Y, Xu Y-Q, Peng X-J. China J Chem Phys 2010;23:558–64.
[137] Hong YN, Chen SJ, Leung CWT, Lam JWY, Liu JZ, Tseng NW, et al. ACS Appl Mater Interfaces 2011;3:3411–8.
[138] Hong Y, Lam JWY, Tang BZ. Chem Commun 2009:4332–53 [and references therin].
[139] Hong Y, Lam JWY, Tang BZ. Chem Soc Rev 2011;40:5361–88.
[140] Drobizhev M, Stepanenko Y, Rebane A, Wilson CJ, Screen TEO, Anderson HL. J Am Chem Soc 2006;128:12432–3.
[141] Mackintosh HJ, Budd PM, McKeown NB. J Mater Chem 2008;18:573–8.
[142] Bezzu CG, Helliwell M, Warren JE, Allan DR, McKeown NB. Science 2010;327:1627–30.
[143] Li L, Becker JM, Allan LEN, Clarkson GJ, Turner SS, Scott P. Inorg Chem 2011;50:5925–35.
[144] Yin M, Lei X, Li M, Yuan L, Sun J. J Phys Chem Solids 2006;67:1372–8.
[145] Radecka-Paryzek W. Can J Chem 2009;87:1–7.
[146] Patel SH, Pansuriya PB, Chhasatia MR, Parekh HM, Patel MN. J Therm Anal Calorim 2008;91:413–8.
[147] Wang G-L, Tian Y-M, Cao D-X, Yu Y-S, Sun W-B. Z Anorg Allg Chem 2011;637:583–8.
[148] Bermejo MR, Fernández MI, Gómez-Fórneas E, González-Noya A, Maneiro M, Pedrido R, et al. Eur J Inorg Chem 2007;2007(24):3789–97.
[149] Li G-B, Liu J-M, Cai Y-P, Su C-Y. Cryst Growth Des 2011;11:2763–72.
[150] Andruh M, Costes J-P, Diaz C, Gao S. Inorg Chem 2009;48:3342–59.
[151] Liu Y-Y, Wang Z-H, Yang J, Liu B, Liu Y-Y, Ma J-F. CrystEngComm 2011;13:3811–21.
[152] Alexander S, Udayakumar V, Gayathri V. J Mol Catal A Chem 2009;314:21–7.
[153] Tunçel M, Özbülbül A, Serin S. React Funct Polym 2008;68:292–306.
[154] Yan B, Wang Q-M. Opt Mater 2007;30:617–21.
[155] Guo L, Deng J, Zhang L, Xiu Q, Wen G, Zhong C. Dyes Pigm 2012;92:1062–8.
[156] Joseph A, Ramamurthy PC, Subramanian S. J Appl Polym Sci 2012;123:526–34.
[157] Mak CSK, Cheung WK, Leung QY, Chan WK. Macromol Rapid Commun 2010;31:875–82.
[158] Mak CSK, Leung QY, Li CH, Chan WK. J Polym Sci A 2010;48:2311–9.
[159] Wu F-I, Yang X-H, Neher D, Dodda R, Tseng Y-H, Shu C-F. Adv Funct Mater 2007;17:1085–92.
[160] Jiang J, Xu Y, Yang W, Guan R, Liu Z, Zhen H, et al. Adv Mater 2006;18:1769–73.
[161] Shunmugam R, Tew GN. J Am Chem Soc 2005;127:13567–72.
[162] Ainscough EW, Allcock HR, Brodie AM, Gordon KC, Hindenlang MD, Horvath R, et al. Eur J Inorg Chem 2011;25:3691–704.

[163] Fréchet JMJ. Science 1994;263:1710–5.
[164] Tuuttila T, Lipsonen J, Lahtinen M, Huuskonen J, Rissanen K. Tetrahedron 2008;64:10590–7.
[165] Shen X, Liu H, Li Y, Liu S. Macromolecules 2008;41:2421–5.
[166] Rempp P, Herz JE. Encyclopedia of polymer science and engineering. ed. 2. New York: Wiley; 1989. p. 793.
[167] Moughton AO, O'Reilly RK. Macromol Rapid Commun 2010;31:37–52.
[168] Higashihara TH, Sugiyama K, Yoo HS, Hayashi M, Hirao A. Macromol Rapid Commun 2010;31:1031–59.
[169] Wang S, Wang X, Li L, Advincula RC. J Org Chem 2004;69:9073–84.
[170] Onitsuka K, Takahashi S. Top Curr Chem 2003;228:39–63.
[171] Rossell O, Seco M, Angurell I. C R Chim 2003;6:803–17.
[172] Chase PA, Gebbink R, van Koten G. J Organomet Chem 2004;689:4016–54.
[173] Majoral JP, Caminade AM, Laurent R. In: Schubert US, Newkome GR, Manners I, editors. Metal-Containing and metallosupramolecular polymers and materials. Oxford: Oxford University Press; 2006. p. 230–43.
[174] Newkome GR, Moorefield CN, Vögtle F. Dendrimers and dendrons: concepts, syntheses and applications. Weinheim, Germany: Wiley-VCH; 1996.
[175] Fréchet JMJ, Tomalia DA. Dendrimers and other dendritic polymers. Chichester: John Wiley & Sons, Inc; 2002.
[176] Astruc D, Blais J-C, Cloutet E, Djakovitch L, Rigaut S, Ruiz J, et al. Top Curr Chem 2000;210:229–59.
[177] van Manen H-J, van Vergel FCJM, Reinhoudt DN. Top Curr Chem 2001;217:121–62.
[178] Hwang S-H, Shreiner CD, Moorefield CN, Newkome GR. New J Chem 2007;31:1192–217.
[179] Oosterom GE, Reek JNH, Kamer PCJ, van Leeuwen PWNM. Angew Chem Int Ed 2001;40:1828–49.
[180] Kreiter R, Kleij AW, Gebbink RJMK, van Koten G. Top Curr Chem 2001;217:163–99.
[181] Caminade AM, Maraval V, Lauren R, Majoral JP. Curr Org Chem 2002;6:739–74.
[182] Dahan A, Portnoy M. J Polym Sci Part A Polym Chem 2005;43:235–62.
[183] van de Coevering R, Gebbink RJMK, van Koten G. Prog Polym Sci 2005;30:474–90.
[184] Méry D, Astruc D. Coord Chem Rev 2006;250:1965–79.
[185] Reek JNH, Arévalo S, van Heerbeek R, Kamer PCJ, van Leeuwen PWNM. Adv Catal 2006;49:71–151.
[186] Gade LH, editor. Dendrimer catalysis. Berlin: Springer; 2006.
[187] Andrés R, de Jesús E, Flores JC. New J Chem 2007;31:1161–91.
[188] Fréchet JMJ. J Polym Sci Part A Polym Chem 2003;41:3713–25.
[189] Astruc D, Bolsseller E, Ornelas C. Chem Rev 2010;110:1857–959.
[190] Li W, Aida T. Chem Rev 2009;109:6047–76.
[191] Astruc D. Nat Chem 2012;4:255–67.
[192] Jang W-D, Nakagishi Y, Nishiyama N, Kawauchi S, Morimoto Y, Kikuchi M, et al. J Control Release 2006;113:73–9.
[193] Nishiyama N, Nakagishi Y, Morimoto Y, Lai P-S, Miyazaki K, Urano K, et al. J Control Release 2009;133:245–51.
[194] Shinoda S, Ohashi M, Tsukube H. Chem Eur J 2007;13:81–9.
[195] Shinoda S. J Inclusion Phenom Macrocyclic Chem 2007;59:1–9.
[196] Kimura M, Nakano Y, Adachi N, Tatewaki Y, Shirai H, Kobayashi N. Chem Eur J 2009;15:2617–24.
[197] Kozaki M, Tujimura H, Suzuki S, Okada K. Tetrahedron Lett 2008;49:2931–4.
[198] Kozaki M, Uetomo A, Suzuki S, Okada K. Org Lett 2008;10:4477–80.
[199] Imaoka T, Tanaka R, Arimoto S, Sakai M, Fujii M, Yamamoto K. J Am Chem Soc 2005;127:13896–905.
[200] Yamamoto K, Takanashi K. Polymer 2008;49:4033–41.
[201] Higuchi M, Kurth DG, Yamamoto K. Thin Solid Films 2006;499:234–41.
[202] Imaoka T, Tanaka R, Yamamoto K. Chem Eur J 2006;12:7328–36.
[203] Pu Y-J, Harding RE, Stevenson SG, Namdas EB, Tedeschi C, Markham JPJ, et al. J Mater Chem 2007;17:4255–64.
[204] Jung KM, Kim KH, Jin J-I, Cho MJ, Choi DH. J Polym Sci Part A 2008;46:7517–33.
[205] Angurell I, Muller G, Rocamora M, Rossell O, Seco M. Dalton Trans 2003:1194–200.
[206] Angurell I, Muller G, Rocamora M, Rossell O, Seco M. Dalton Trans 2004:2450–7.
[207] Méry D, Plault L, Ornelas C, Ruiz J, Nlate S, Astruc D, et al. Inorg Chem 2006;45:1156–67.
[208] Dasgupta M, Peori MB, Kakkar AK. Coord Chem Rev 2002;233–234:223–35.
[209] Cuadrado I, Morán M, Losada J, Casado CM, Pascual C, Alonso B, et al. In: Newkome GR, editor. Advances in dendritic macromolecules, vol. 3. Greenwich, CT: JAI Press; 1996. p. 151–95.
[210] Arévalo S, de Jesús E, de la Mata FJ, Flores JC, Gómez R. Organometallics 2001;20:2583–92.
[211] Camerano JA, Casado MA, Ciriano MA, Lahoz F, Oro LA. Organometallics 2005;24:5147–56.
[212] Alonso B, García Armada P, Losada J, Cuadrado I, González B, Casado CM. Biosens Bioelectron 2004;19:1617–25.
[213] Angurell I, Rossell O, Seco M. Chem Eur J 2009;15:2932–40.
[214] Zamora M, Alonso B, Pastor C, Cuadrado I. Organometallics 2007;26:5153–64.
[215] Cifuentes MP, Powell CE, Morrall JP, McDonagh AM, Lucas NT, Humphrey MG, et al. J Am Chem Soc 2006;128:10819–32.
[216] Samoc M, Morrall JP, Dalton GT, Cifuentes MP, Humphrey MG. Angew Chem Int Ed 2007;46:731–3.
[217] Kaifer AE. Eur J Inorg Chem 2007;2007(32):5015–27.
[218] Beer PD, Bayly SR. Top Curr Chem 2005;255:125–62.
[219] Wang J. Chem Rev 2008;108:814–25.
[220] Astruc D, Ornelas C, Aranzaes JR. Inorg Organomet Polym 2008;18:4–17.
[221] Ornelas C, Aranzaes JR, Cloutet E, Alves S, Astruc D. Angew Chem Int Ed 2007;46:872–7.
[222] Hwang S-H, Shreiner CD, Moorefield CN, Newkome GR. New J Chem 2007;31:1027–38.
[223] Astruc D, Ornelas C, Ruiz J. Acc Chem Res 2008;1:841–56.
[224] Morales-Espinoza EG, Sanchez-Montes KE, Klimova E, Klimova T, Lijanova IV, Maldonado JL, et al. Molecules 2010;1:2564–75.
[225] Nishihara H. Bull Chem Soc Jpn 2004;77:407–28.
[226] Kurihara M, Nishihara H. Coord Chem Rev 2002;226:125–35.
[227] Nishihara H. Coord Chem Rev 2005;249:1468–75.
[228] Kume S, Nishihara H. Dalton Trans 2008:3260–71.
[229] Daniel M-C, Sakamoto A, Ruiz J, Astruc D, Nishihara H. Chem Lett 2006;35:38–9.
[230] Astruc D, Boisselier E, Ornela C. Chem Rev 2010;110:1857–959.
[231] Shi J, Jim CJW, Mahtab F, Liu J, Lam JWY, Sung HHY, et al. Macromolecules 2010;43:680–90.
[232] Abd-El-Aziz AS, Strohm EA, Ding M, Okasha RM, Afifi TH, Sezgin S, et al. J Inorg Organomet Polym 2010;20:592–603.
[233] Abd-El-Aziz AS, Carruthers SA, Aguiar PM, Kroeker S. J Inorg Organomet Polym Mater 2005;15:349–59.
[234] Antonels NC, Moss JR, Smith GS. J Organomet Chem 2011;696:2003–7.

Dr. Abd-El-Aziz is the President and Vice-Chancellor of University of the Prince Edward Island. Previously he was the Provost and Vice Principal Academic and Research at the University of British Columbia's Okanagan campus in Kelowna, BC. Dr. Abd-El-Aziz received his BSc and MSc degrees from Ain Shams University in Cairo. After receiving his PhD in 1989 from the University of Saskatchewan, he joined the University of Toronto as an NSERC Postdoctoral Fellowship. Dr. Abd-El-Aziz's current research interest is in the synthesis and characterization of metal-containing polymers, which include the development of new synthetic methodologies for organic and organometallic polymers, electrochemical studies of organometallic oligomeric and polymeric materials, investigation of structural variations on the thermal properties of polymers, and the degradation of organic contaminants. Dr. Abd-El-Aziz is a prolific researcher with 144 publications and 138 national and international conference presentations to his credit. He has authored and edited 15 books and has given 49 invited lectures at national and international universities. Dr. Abd-El-Aziz is Co-editor in Chief of the Journal of Inorganic and Organometallic Polymers and Materials and is currently serving on the Editorial Boards of the Royal Society for Chemistry (Polymer Chemistry Series), Macromolecular Rapid Communications as well as Macromolecular Chemistry and Physics.

Elizabeth A. Strohm was born in Vancouver, British Columbia. She completed her BSc (Hon.) degree in chemistry at the University of British Columbia Okanagan campus. In 2010, she joined the polymer research group at the University of British Columbia, supervised by Professor Alaa S. Abd-El-Aziz. Her current research focus is on the synthesis and characterization of polymers containing near infrared dyes. She is in the final stage of completing her MSc degree in polymer science.